Title
Essays in Environmental Economics

Author
Lee, Jaecheol

Publication Date
2023

Peer reviewed|Thesis/dissertation

Essays in Environmental Economics

by

Jaecheol Lee

A dissertation submitted in partial satisfaction of the

requirements for the degree of

Doctor of Philosophy

in

Agricultural and Resource Economics

in the

Graduate Division

of the

University of California, Berkeley

Committee in charge:

Associate Professor Marco Gonzalez-Navarro, Chair
Professor Michael Anderson
Thomas and Alison Schneider Professor of Public Policy Solomon Hsiang

Summer 2023

Essays in Environmental Economics

Abstract

Essays in Environmental Economics
by
Jaecheol Lee

Doctor of Philosophy in Agricultural and Resource Economics
University of California, Berkeley

Associate Professor Marco Gonzalez-Navarro, Chair

How can we effectively mitigate the public health damages associated with air pollution, particularly particulate matter (PM)? While the government can initiate efforts by reducing PM emissions, a critical question emerges: do the public health responses to PM vary depending on its originating locations? If that is the case, the most effective approach would involve prioritizing the abatement of emissions from the origin with the most significant impacts on deteriorating public health outcomes due to PM exposure. This dissertation addresses this question head-on in its first chapter, investigating whether PM impacts exhibit heterogeneity across origins, encompassing transboundary anthropogenic emissions from different countries, non-anthropogenic emissions from desert dust and wildfires, and domestic anthropogenic sources. The second chapter delves into the implications of these findings, exploring the disparities in estimated PM impacts when utilizing different types of transboundary PM contributions as instrumental variables, which have been traditionally considered valid exogenous variations for identifying the impacts of PM. Returning to the core objective of alleviating public health burdens, the third chapter of this dissertation delves into the role of information disclosure. By inducing public awareness of air pollution levels and promoting avoidance behavior through advisories or warnings, governments seek to reduce the health burdens. This chapter examines the efficacy of air quality alert systems in achieving this goal, weighing the potential reduction of healthcare costs against the operating expenses of warnings.

More detailed abstracts of the three chapters are as follows. The first chapter starts by recognizing that a large portion of emitted PM crosses borders, damaging health outside of its originating jurisdiction. As a result, there is substantial interest in determining the origins of imported PM and measuring its impact(ApSimon and Warren 1996; Jazil and Brown 2012; Crawford et al. 2021; Du, Guo, et al. 2020; Du, Jin, et al. 2020a; Jordan et al. 2020; National Research Council 2010). Current

approaches to estimating health damages from PM assume that pollution originating in different jurisdictions causes the same per-unit harm(Dedoussi et al. 2020; Lim et al. 2020; Chen, Li, et al. 2021; Sergi et al. 2020; Chen, Lin, et al. 2022; Diao et al. 2021; Heo, Ito, and Kotamarthi 2023; S.-B. Han et al. 2021; Liu et al. 2020; Gu and Yim 2016). However, because the chemical and physical features of PM originating from different locations vary dramatically,(Harrison and Yin 2000; Kelly and Fussell 2012; Strak et al. 2012; Schmid and Stoeger 2016) it is widely hypothesized that PM from distinct origins may generate differing health effects.(Gilmour et al. 2007; Li et al. 2019; Seagrave et al. 2006; Chen, Hoek, et al. 2022; Strak et al. 2011; Wu et al. 2021; Achilleos et al. 2017; Thurston, Chen, and Campen 2022). It has remained challenging to test this theory because only total PM (i.e., transboundary PM + domestic PM) is measured by the observational network, preventing analyses from disentangling harms that originate from different jurisdictions but impact a single population concurrently. Thus, PM originating domestically has confounded the measurement of harm from transboundary PM, and vice versa. Here, we provide the first direct and unconfounded evidence that the health impacts of PM depend on its origin. We simultaneously measure harm over time from both transboundary and domestic PM within a single population located at the nexus of the world's most contentious transboundary air pollution disputes(Jia and Ku 2019; Shapiro and Yarime 2021; Lim et al. 2020; Jung, Choi, and Yoon 2022). We use an atmospheric model to decompose the origins of PM individuals are exposed to at each location in South Korea every day during 2005–2016. We then link these data to universal healthcare records in an econometric analysis that simultaneously measures and accounts for harms from seven types of PM, each from a distinct origin. We discover that the toxicities of transboundary PM from North Korea and China are approximately 5× and 2.6× greater, respectively, than PM originating domestically in South Korea, and that the health response to natural dust differs from anthropogenic sources. Because toxicity differs by origin, we compute that transboundary sources contribute only 43% of South Korea's anthropogenic PM load but generate over 70% of its associated respiratory health costs. Our results directly validate the longstanding hypothesis(Gilmour et al. 2007; Li et al. 2019; Seagrave et al. 2006; Strak et al. 2011; Wu et al. 2021; Thurston, Chen, and Campen 2022) that PM should not be treated as if it is a single pollutant, but instead should be considered a mixture of pollutants of distinct origin, each with a unique measurable impact on human health.

The second chapter investigates the implications of the results of the first chapter from the perspective of the applied econometrics. When using instrumental variables (IV), many studies in applied econometrics have focused on the conventional requirements for the use of IVs–the first-stage condition and the exclusion restriction–to get

estimates of the causal impacts and extrapolate those coefficients to counterfactual policy settings. An issue is that the results of IV regressions could differ considerably depending on which sets of IVs are in use, even if these IVs are deemed appropriate in terms of those two conventional requirements. Identifying variations induced by a particular set of IVs can be associated with certain groups of people or channels that determine the influence of the endogenous variable on the dependent variable. These groups and channels may have different characteristics compared to those associated with other IV sets, thus leading to heterogeneous responses. (Angrist and Krueger 2001; Mogstad and Torgovitsky 2018; Mogstad, Santos, and Torgovitsky 2018; Dunning 2008) As a result, it is possible that the IV or two-stage least-square (2SLS) estimates may diverge, even though these estimates are assumed to represent one 'causal impact,' and only depict a part of the impacts associated with target variations (or policy-relevant variations (PRV)) one aims to analyze in a counterfactual analysis. However, it is still unknown to what extent the different sets of identifying variations can result in 2SLS estimates which are not qualitatively similar to those produced when other sets of IVs are used, in real-world empirical settings.

The last chapter investigates the welfare impacts of disclosing information on extreme levels of air pollution. Though air-quality alert systems (AQAS) cover more than 1.7 billion people worldwide, there has been little welfare analysis of these systems. This chapter presents a theoretical framework for deriving lower bounds on the net benefits of an AQAS and applies it to a South Korean system currently covering over 51 million people. Estimating a regression discontinuity design, we find that an alert issuance reduced youth respiratory expenditures by 30% and adult cardiovascular expenditures by 23%. The overall system reduced externalized health expenditures by 28.6 million dollars during 2016−2017, with a minimum benefit-cost ratio of 7.1:1. Including dynamic impacts of alerts increases the minimum benefits (benefit-cost ratio) to 36.7 million dollars (9.2:1). Our findings imply that the AQAS generates significant net benefits and suggests that manipulation of air quality data, which has been observed in other contexts, may negatively impact social welfare.

For my mother, Wonmee Kim,
and love of my life, Jieun Kim

Contents

List of Figures

List of Tables

Acknowledgments

Completing my dissertation would not have been possible without the unwavering support of my advisors, colleagues, friends, and family. At the forefront, my deepest gratitude goes to my dissertation committee for their invaluable guidance and counsel. I consider myself exceptionally fortunate to have had the chance to collaborate on projects with each committee member, which allowed me me to immerse myself in the intricacies of academia. These collaborative experiences have been an enlightening journey, where I have absorbed and continue to absorb a wealth of knowledge from the ground up.

Creating an exhaustive list of my learnings would overwhelm this acknowledgment section, but highlighting a few is essential. Solomon Hsiang's advocacy for interdisciplinary research expanded my project horizons beyond imagination. His adept management of a vibrant research community, fostering both collaboration and a sense of community, proved invaluable during the challenging times of COVID-19. Michael Anderson instilled the rigorous ethos essential for applied econometricians, a mindset I carry whenever running regressions. His exceptional teaching resonates in my ongoing referencing of his econometrics and environment courses. Marco Gonzalez-Navarro introduced me to urban economics, equipping me with theoretical tools to evaluate welfare implications, a lens that has been essential for my project ideation process and policy analyses.

Undoubtedly, my co-authoring colleagues serve as the bedrock of this dissertation. I am profoundly grateful to Andrew Wilson and Minwoo Hyun for granting permission to incorporate our collaborative work into this thesis. The co-authored endeavors within this dissertation owe their completion to the indispensable contributions of Andrew and Minwoo. I have also gained immense knowledge and humility from Andrew's remarkable versatility spanning atmospheric models, econometrics, visualization skills, and writing. Minwoo's unwavering dedication, scholarly rigor, and embodiment of Christian values have consistently been a wellspring of inspiration, infusing me with the vigor needed to navigate the challenging path of my Ph.D. journey.

I have received significant support from various members of the Agricultural and Resource Economics department at Berkeley. I am particularly grateful to Sofia Villas-Boas for her invaluable assistance, especially when I was navigating the challenges of the job market. Meredith Fowlie's guidance and support were instrumental during the mid-years of my Ph.D., for which I am deeply thankful. Having Reed Walker as a part of my oral exam committee was truly fortunate, as his insights and

suggestions greatly enhanced my preparation. Joseph Shapiro played a crucial role in helping me prepare my second-year paper, offering invaluable feedback and sharing his extensive knowledge of environmental economics. Ethan Ligon's care and support during my first year were truly appreciated. I would also like to acknowledge Carman Karahalios, who consistently checked in on each of us, including me, ensuring our financial and mental well-being. Her dedication to student well-being is sincerely appreciated.

I had the immense privilege of being surrounded by an exceptional group of peers throughout my Ph.D. journey. Marshall Blundell and Matthew Tarduno's extraordinary kindness became evident when they orchestrated a trip to Death Valley, allowing me to fulfill my dream of gazing upon a night sky adorned with stars. The nostalgia for that journey already overwhelms me. Wenjun Wang and Yuya Takagi were unwavering wellsprings of inspiration, their diligence and composed personalities serving as a constant motivation. Sharing living quarters with Alejandro Favela Nava and Sebastien Annan-Phan fostered a strong sense of community, profoundly enriching my experience. Byoungchan Lee has stood as a prominent role model for me, exemplifying both kindness and excellence within the field of economics. I hold deep appreciation for Chaewon Baek, whose generosity extended to newcomers like myself, and who also played a pivotal role in connecting me to my wife, Jieun Kim.

My enduring friendships with Seungwoo Lee and Jihyeok Lim have remained steadfast over time. I found great comfort in heartfelt communications with Tay Shin, Seungryong Shin, and Hyunwoo Jung, all of whom embarked on their Ph.D. journeys ahead of me. Jaeho Park, Sujee An, and Jongchan Park consistently made me feel welcome whenever I visited South Korea and connected with them. Additionally, Junho Lee has offered unwavering support and invaluable suggestions since 2001. I am grateful for our shared commitment to delve into the pressing issue of climate change, a paramount concern on a global scale.

I also extend my profound gratitude to the exceptional members of the Global Policy Laboratory (GPL) for their unwavering support and collaboration. The enriching environment of GPL fostered open communication and vibrant brainstorming sessions, which were instrumental in shaping the direction of my research. Especially during the challenging times of the COVID-19 pandemic, GPL provided a sense of community that transcended physical distances, reminding me of the collective strength of dedicated individuals. The diverse insights, rigorous discussions, and shared commitment to advancing knowledge have profoundly impacted my academic journey. I am particularly grateful for Ian Bolliger and Andy Hultgren, who served as invaluable mentors during my time as a graduate student researcher at GPL and

Climate Impact Lab, guiding me with remarkable patience and support.

Above all, my journey to this point would not have been possible without the unwavering love and steadfast support of my family. My mother, Wonmee Kim, has consistently believed in me and offered her encouragement regardless of the paths I have chosen. My wife, Jieun Kim, has been an extraordinary source of energy, providing unyielding love that has illuminated my way. I also wish to honor the memory of my father, You June Lee, who himself earned a Ph.D. degree.

Chapter 1

Simultaneous Measurement of Health Damage from Transboundary and Domestic Air Pollution in Mixture

1.1 Introduction

Particulate matter (PM) pollution has significant negative effects on health and well-being, altering risks of many outcomes, including cardiovascular and respiratory illnesses, dementia, suicide, and even crime.(Organization 2021; Peters et al. 2019; Shehab and Pope 2019; Braithwaite et al. 2019; Burkhardt et al. 2019) Thus, to inform the public, support research, and provide a basis for regulation, PM is now widely measured worldwide. These measurements typically classify PM by particle diameter and are reported as a size-specific mass density for all particulates in a sample of air. However, this aggregation obscures differences in PM constituents, which include disparate species like oxidized volatile organic compounds from industrial complexes and mineral dust from desert erosion. Prior research has shown that differences in physical and chemical characteristics can affect the toxicity of PM in a laboratory setting.(Harrison and Yin 2000; Kelly and Fussell 2012; Strak et al. 2012; Schmid and Stoeger 2016; Li et al. 2019; M. Park et al. 2018) Further, observational studies have shown that health outcomes are correlated with the average physical and chemical attributes of PM that groups are exposed to,(Achilleos et al. 2017; Chen, Hoek, et al. 2022; Seagrave et al. 2006; Strak et al. 2011; Wu et al. 2021; Thurston, Chen, and Campen 2022) although it is unknown if those

associations are causal. Other papers have assessed the causal effects of pulses of PM from significant natural sources, including wildfire(Aguilera et al. 2021; Xue et al. 2021) and dust storms,(Heft-Neal et al. 2018; Heft-Neal et al. 2020) but have not conclusively distinguished these effects from those of background PM.[1] Nonetheless, taken together, this collection of facts has led researchers to hypothesize that the same measured quantities of PM from different jurisdictions may have distinct population-level health consequences.(Gilmour et al. 2007; Li et al. 2019; Seagrave et al. 2006; Strak et al. 2011; Wu et al. 2021; Thurston, Chen, and Campen 2022) We provide the first direct and unconfounded test of this hypothesis.

Distinguishing origin-specific health impacts can dramatically influence air quality management, since pollution is managed at its origin but reflects the scale of impacts in downstream locations. Currently, state-of-the-art studies link emitters to recipient locations using atmospheric models(Dedoussi et al. 2020; Lim et al. 2020; Chen, Li, et al. 2021; Sergi et al. 2020; Chen, Lin, et al. 2022; Diao et al. 2021; Heo, Ito, and Kotamarthi 2023; S.-B. Han et al. 2021; Liu et al. 2020; Gu and Yim 2016) and then assume PM has uniform toxicity, leading to an allocation of responsibility for damage that reflects only the quantity of exposure to PM from each origin. However, if toxicity varies by jurisdiction, this approach will misallocate responsibility for health damages, possibly to a large degree. In an impossible and unethical "ideal experiment," a researcher would distinguish the health effects of PM from different emitters by experimentally exposing a fixed set of subjects to different, known mixtures of PM from multiple origins and observing the resulting health outcomes. Our quasi-experimental analysis approximates this approach using observational data.

Specifically, we simultaneously measure the health impacts of PM from multiple origins on the population of South Korea, which is at the nexus of the world's largest and most contentious transboundary air pollution disputes.(Jia and Ku 2019; Jung, Choi, and Yoon 2022; Lim et al. 2020; Crawford et al. 2021; Jordan et al. 2020; Choi et al. 2019) We decompose the daily mixture of total PM_{10} (particulates less than

[1] We note that Aguilera et al. (2021) ("Wildfire smoke impacts respiratory health more than fine particles from other sources") asserts that they have shown the impact of wildfire-specific PM is higher than that of background PM. However, their empirical results are not consistent with this claim. In their reported results (Table 1 of Aguilera et al. (2021)), increases in wildfire and non-wildfire PM are associated with relative risks of hospitalization of 1.00061 [0.10−1.0015] and 1.00068 [1.00049−1.00087], respectively. These effects are not statistically nor meaningfully different (i.e., differences in these estimates are indistinguishable from statistical noise), and the central estimate for the impact of wildfire PM is actually reported to be lower than that for background PM, in contrast to the stated results of the analysis. The inconsistencies between these results and the stated conclusions of that analysis were not resolved in Aguilera et al. (2021), and thus we are submitting a technical comment to the publisher for clarification.

10 micrometers in diameter, which includes $PM_{2.5}$; henceforth "PM") observed at a location into contributions from prominent emitters and measure how changes in PM from each origin independently influence daily health costs. Crucially, by measuring the impact of each type of PM simultaneously, health costs are not "double counted" (i.e., a new hospital visit cannot be attributed to domestic pollution and then again to transboundary pollution), and each estimate of origin-specific toxicity accounts for the impacts related to doses of incident PM from all other origins. To do this, we first use an atmospheric transport model to decompose the provenance of local PM every 3 hours into seven sources: nonanthropogenic sources (including sea salt, nonanthropogenic aeolian dust [which we refer to as "dust"], and forest wildfire), anthropogenic activity (which we group by originating jurisdiction: South Korea, China, and North Korea), and "other sources." Collectively, we call this set of nonanthropogenic sources and anthropogenic jurisdictions "origins." We then combine these probabilistic estimates with high-resolution data on medical spending from South Korea's universal healthcare system, which tracks the public and private medical spending of 97% of South Korea's 52 million residents. The data allow us to deconvolve daily fluctuations of respiratory health costs within each locality into contributions from random variation in origin-specific PM doses over time. To the best of our knowledge, this study is the first to directly and separately measure the simultaneous health effects of both domestic and transboundary PM.

1.2 Empirical Analysis

Partitioning observed PM by origin We create a mapping that assigns PM monitor readings on individual days and locations (i.e., one of South Korea's 147 districts with PM monitoring; see Extended Data Figure A1) to a probability distribution over seven origins—China, South Korea, North Korea, wildfire, mineral dust, sea salt, and "other sources." To do this, we first isolate the influence of dust and sea salt on PM levels using the Copernicus Atmosphere Monitoring Service Global Reanalysis 4 (see Methods).(Inness et al. 2019) To apportion the remaining PM, we then generate a 240-hour backward trajectory starting every three hours at eight altitudes from each PM monitor ($N = 264$) on each day during 2005–2016 (4383 days) using an atmospheric transport model.(Draxler and Hess 1998; Stunder 2004) This results in 67.9 million air parcel trajectories, each defined by 241 points (10 days of hourly observations; see Figure 1.1A for an example month at a single PM monitor). These trajectories enable us to estimate the contribution of various locations to the air arriving at a South Korean district on a given day. We combine these trajectories with information on the spatiotemporal distribution of emissions from anthropogenic

sources(European Commission, Joint Research Centre (JRC)/Netherlands Environmental Assessment Agency (PBL) 2019) and fires(Werf et al. 2017; Randerson et al. 2012; Giglio, Randerson, and Werf 2013) (applying an adjustment for chemical scavenging and deposition over time) to estimate the probability that a unit of PM arriving at location "i" originated at location "j." Figures 1.1B–C depict examples of the distribution of these probabilities across space (all j's) for the district of Busan (i) on two days in April 2016. We integrate these probability distributions over hours, altitudes, and originating jurisdictions to construct district-specific time series of PM contributions, which are then re-scaled to partition station-measured PM into contributions from all seven origins (e.g., Figure 1.1D). The resulting origin-specific PM time series (e.g., Figure 1.1E) thus encapsulate what is known about the emissions, transport, and ground measurement of all PM arriving in South Korea during this period. See Methods for more details.

Measuring impacts of exposure on health outcomes We jointly resolve the effects of all seven origins of PM on spending for respiratory illnesses for the entire population of South Korea. These district-specific data are from a representative sample of individuals covered by South Korea's universal healthcare system (N = 4.87 million) and include expenses for outpatient and emergency visits due to respiratory illness at all healthcare facilities in South Korea (e.g., see Figure 1.1F; for more details on this data, see "Data Collection" in Methods). We empirically estimate the health effects observed for a given district's population when it is exposed to different mixtures of PM (see Methods). Our approach accounts for complex, nonlinear time trends in medical expenditures (i.e., seasonal patterns, secular trends, variations across days of the week, and the impacts of holidays), differences in time-invariant subnational characteristics that may affect health spending (e.g., levels of wealth, the quality of local public health provision, or differences in data quality), non-PM pollutants (nitrogen dioxide, carbon monoxide, ozone, and sulfur dioxide), and changes in weather previously shown to impact human health.(Carleton et al. 2022) We account for cumulative effects over a period sufficiently long (4 weeks) that we capture delayed changes in health expenditure associated with PM exposure (see Methods). In this context, delays can result from many factors: for example, respiratory symptoms may unfold over several days or weeks after pollution exposure, or South Korea's medical appointment referral system may lead to a gap between the initial and final visit for a given health issue. Finally, our empirical specification allows us to flexibly account for the possibility of avoidance behavior that individuals undertake autonomously to limit their total PM exposure (e.g., staying indoors or using masks) while still preserving our ability to distinguish between the effects of subcomponents of over-

all PM (see Methods). Finally, we assess the robustness of our results to different methods for calculating uncertainty, alternative functional forms for how we model avoidance and health responses, and whether we account for air quality alerts; we also assess the consistency of our results over space, time, and seasons (for a detailed explanation of these tests, see Extended Data Figure A4).

1.3 Results

Exposure by PM origin

During the period of our analysis, we estimate that three anthropogenic source regions—China, South Korea, and North Korea—account for roughly 80.9% of total population-weighted PM exposure in South Korea; mineral dust accounts for an additional 11.7%; and wildfire, sea salt, and all other sources together account for the remaining <8% of total exposure (Figure 1.1G). We also estimate that seasonal and spatial differences in exposure across South Korea are large. For example, while sea salt is on average a small component of PM (about 3%), it is a large portion of total PM in less industrial, coastal districts during summer (we estimate that sea salt accounts for over 50% of PM on 0.2% of district–day observations). Likewise, PM from China is highest across all districts in the winter and the spring, when prevailing winds are westerly. During this period, some regions occasionally experience "Yellow Dust" events; when concentrations of PM in South Korea from soil erosion in the deserts of China, Mongolia, and Kazakhstan can rise above 1000 $\mu g/m^3$. These events account for a large portion of total dust exposure, as contributions of dust are generally <5 $\mu g/m^3$. Because most PM (and most of the resulting health damage) originates from South Korea, China, and North Korea—and because these emissions can be modified by human activities—we focus our analysis primarily on anthropogenic PM from these three origins, but note that all analyses account for PM from all seven origins.

Effects of origin on properties of PM mixtures

We analyze the observed chemical and physical properties of PM to validate that our decomposition of PM origin identifies distinct components of the PM mixture incident on South Korean locations. We use the Hybrid Single-Particle Lagrangian Integrated Trajectory (HYSPLIT) atmospheric transport model(Draxler and Hess 1998) because it was designed for backtrajectory calculation, and its computational efficiency is crucial for handling the large number of trajectories we analyze. This

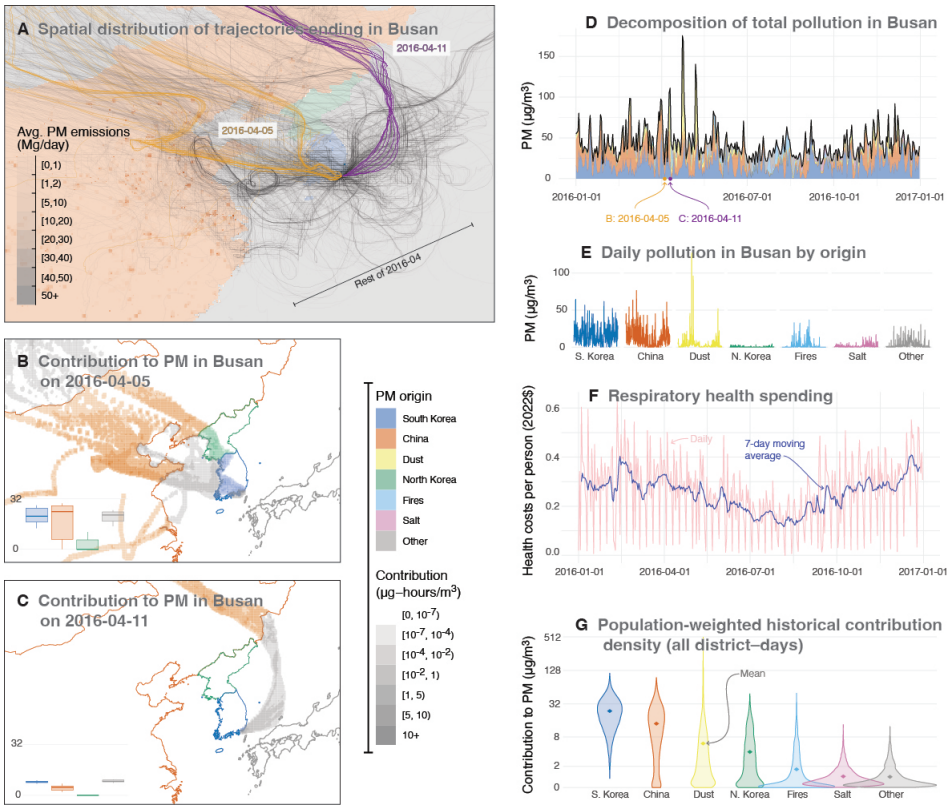

Figure 1.1: **Decomposition of PM by Origin**

Notes: (A) Example set of backtrajectories from a single district in Busan, South Korea, during April 2016. The full analysis includes all districts shown in Extended Data Figure A1. Trajectories for April 5 and April 11 are shown in orange and purple, respectively. Anthropogenic PM emissions during this month are shown as changes in the opacity of the background map, with colors differing by originating jurisdiction. (B) The estimated contribution of each location's emissions to anthropogenic PM exposure experienced in Busan on April 5, 2016 and the distribution of estimates contributions of different origins across the set of backtrajectories (lower left box and whisker plot). (C) Same as (B), but for April 11, 2016. (D) Time series of total PM (black line) measured in Busan throughout 2016, with the two dates in (B)–(C) labeled. Stacked color areas indicate the decomposition of this measured PM by origin based on backtrajectory calculations illustrated in (A)–(C). (E) Time series for each component of total PM by origin for 2016. (F) Daily (pink) and seven-day moving average (blue) time series for respiratory health spending per capita in Busan throughout 2016. (G) Distributions of nationwide population-weighted PM exposure over each of the seven PM origins we investigate. Distributions include all districts and days in our sample, with the mean exposure for each PM origin shown with a diamond shape (note nonlinear y-axis).

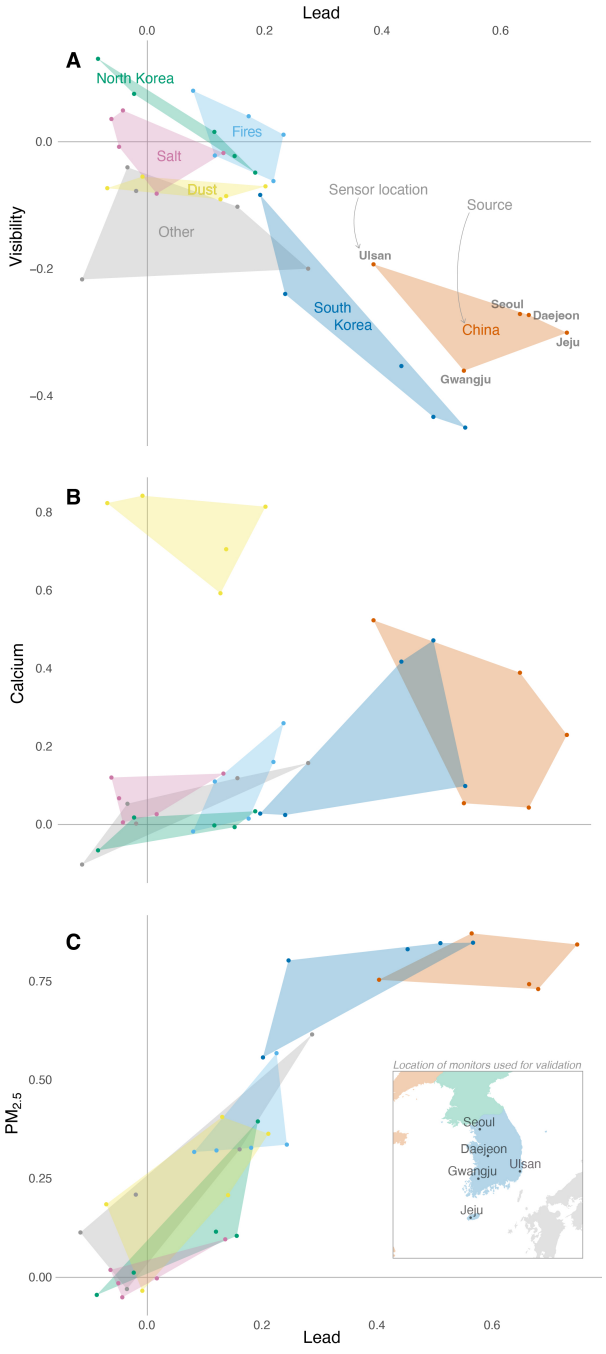

Figure 1.2: **Estimating the Chemical and Physical Signature of PM from Each Origin at Five Locations in South Korea**

Notes: The partial correlations between the quantity of PM from different origins and concentrations of either lead, calcium, fine particulate matter ($PM_{2.5}$), or visibility across five monitors (see inset). Monitor locations are labeled in Panel A. In each panel, marker positions depict partial correlations between aggregate properties (for both x- and y-axes) measured at a given monitor and PM from each origin. Correlations for all origins are estimated simultaneously for each property at each sensor, but colored to group measurements across sensors based on PM origin. Colored regions depict the convex hull of these partial correlations for a single origin across the set of five monitors, indicating the chemical and physical "fingerprint" for each origin. Further explanation of this figure is shown in Extended Data Figure A2.

model has been widely validated for many applications,(Du, Jin, et al. 2020b; Cheng et al. 2013; Sapkota et al. 2005; S. Lee et al. 2021; Escudero et al. 2006; Alam, Qureshi, and Blaschke 2011) although it is possible, in principle, that the absence of active chemistry calculations(Binkowski and Roselle 2003; Wagstrom et al. 2008; X. Han et al. 2021; D. Chen et al. 2007; Liu, Li, and Yao 2022) or other aspects of the model could impact our estimates. We cannot directly test that hourly backtrajectories are correctly modeled; however, we validate that PM contributions from a specific origin appear (i) chemically and physically consistent across South Korea and (ii) chemically and physically distinct from PM attributed to other origins. We do this by identifying the chemical and physical "fingerprint" of PM from each origin, comparing it across sensors, and contrasting it with the "fingerprint" from other origins.

Aggregate chemical characteristics (lead and calcium levels) and physical properties (visibility and $PM_{2.5}$ concentration) of PM are monitored daily at five locations (see Figure 1.2 inset) and for limited periods of time (see Methods). This quantity of data is insufficient for population-scale epidemiological analysis and does not quantify many important physical and chemical aspects of PM, but it can nonetheless validate our calculation of origin-specific contributions. If PM from different origins has distinct chemical and physical characteristics and we have correctly decomposed PM contributions by origin, then the observed aggregate properties of the PM mixture should be an approximately linear combination of properties for components in the mixture—with weights that reflect the fractional contribution from each origin (see Methods). For example, on days when we compute that the PM mixture over Seoul is 90% from China, based on backtrajectories, then we would expect the chemical properties of PM on those days to be dominated by the properties of emissions from China. Based on this idea, we estimate how an influx of PM from each origin alters the observed aggregate chemical and physical properties of the PM mixture, accounting for the estimated contribution and properties of all other origins simultaneously. Specifically, we use multiple regression to decompose how PM from all origins simultaneously impacts aggregate chemical and physical properties at each measurement site (see Methods).

We find that our estimates of PM origin are associated with consistent and distinct changes in lead, calcium, visibility, and the concentration of $PM_{2.5}$ (Figure 1.2). Three features of this result are notable. First, patterns across monitors are relatively consistent for each PM origin. For example, the chemical/physical signature of domestic-origin or Chinese PM is broadly consistent across all sensors in South Korea (high lead, low visibility, moderate calcium, and high $PM_{2.5}$). Second, the four-dimensional chemical/physical signature of each origin is well-separated from the signatures of other origins (note that overlap in Figure 1.2 primarily results from

display in only two dimensions at a time), implying that our approach to isolating PM by origin identifies collections of PM exposures that are physically and chemically distinct from one another.

Third, the patterns we recover are consistent with what is previously known about PM source characteristics. For example, we find that PM contributions from China and South Korea are associated with higher concentrations of lead (partial correlations of 0.39 to 0.73 for China and 0.25 to 0.69 for South Korea), which originates from industrial processes,(Harrison 2012; Del Rio-Salas et al. 2012; Bellis et al. 2001; Roy et al. 2019) and that PM attributed to mineral dust is strongly associated with the level of airborne calcium, consistent with prior analysis.(Heim et al. 2020; W.-H. Kim et al. 2012; S. Park et al. 2004) We observe similarly consistent and distinct patterns for visibility, which both is affected by ambient PM particle characteristics(Yuan et al. 2006; K. W. Kim et al. 2015; Y. J. Kim et al. 2006) and affects avoidance behavior.(He, Luo, and Zhang 2022). We also find that PM attributable to our two main anthropogenic sources, China and South Korea, is more strongly associated with smaller particle sizes, compared to PM originating from dust and sea salt, also consistent with prior research.(Kar and Takeuchi 2004; Perrino et al. 2009; Pérez et al. 2008; Gobbi, Barnaba, and Ammannato 2007) We hypothesize that North Korean PM may appear different from PM from China and South Korea because of its distinct industrial structure and energy system.(Koen and Beom 2020; Kim, Lee, and Kim 2011; Lee, Kim, and Yeo 2021; Kim and Kim 2019; N. K. Kim et al. 2014) Taken together, these results indicate that our decomposition of PM by origin consistently identifies distinct sources of pollution that are normally indistinguishable.

Distinguishing health impacts by PM origin

Dose–response by PM origin We simultaneously estimate the effect of PM from all seven origins on health outcomes in each district over time, discovering that comparably sized exposures to PM of different origins cause significantly different changes in health. To demonstrate these differences, we first replicate the standard approach of pooling all PM, estimating an average health response that is undifferentiated by PM origin (Figure 1.3A). Ignoring origins, we find that a 1 $\mu g/m^3$ increase in overall PM is associated with a nearly linear \$0.002 ($\pm$0.0005) per day increase in respiratory medical cost per person (noting that the model allows for non-linear relationships; see Methods). However, this undifferentiated model masks variation in health responses across origins. Figure 1.3B presents the response of health costs from exposure to PM from different origins. PM from North Korea (green) is the most harmful per unit

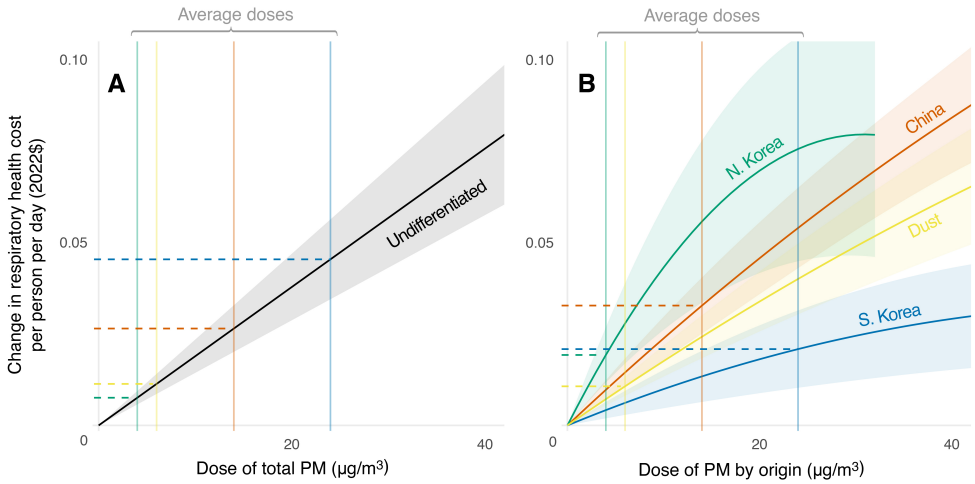

Figure 1.3: **Health-response to PM by Origin**

Notes: (A) The cumulative respiratory health cost for the South Korean population from a single day of exposure to undifferentiated PM, aggregated across all origins. The relationship appears linear but is estimated allowing for a potentially nonlinear relationship. (B) Estimated effects of PM from four major origins: South Korea, North Korea, China, and dust (effects from seven sources are estimated simultaneously following the specification in Methods). Each curve is plotted assuming the levels of other sources are zero. Panel A is shown only for comparison and is not used in our calculations for the attribution of respiratory health costs to PM origins. Vertical lines indicate the population-weighted mean dose for each PM origin across all district–days in the sample; horizontal lines indicate the predicted change in respiratory health costs per person. Dose–response relationships are shown only to the 99^{th} percentile dose for each PM origin if that value falls in the plotted range.

at all common doses (\$0.0048 per µg/m^3 per person per day), with an average effect per unit at the mean dose around 4× larger than the per-unit effect of the mean dose of PM from South Korea ("domestic-origin" PM, whose dose–response function is shown in blue; \$0.0009 per µg/m^3 per person per day). The average per-unit effects of PM from China (red-orange) and dust (yellow) are around 2.6× and 2× larger, respectively, than domestic-origin PM (\$0.0024 and \$0.0018 per µg/m^3 per person per day).

We note that the high harm per unit of PM originating in North Korea is not explained by the chemical and physical properties that we were able to analyze above (recall Figure 1.2). On dimensions we can observe, including particle size and lead concentrations, PM from North Korea appears less threatening to human health. This indicates that the qualities of North Korean PM that we do not observe are likely mediating this relationship, a topic that we believe merits further study.

Total harm from average PM by origin Health costs (horizontal dashed lines in Figure 1.3A–B) result from the combination of dose–response relationships and dose from each origin (solid vertical lines). If the health burden from PM is computed using the undifferentiated dose-response, then the average dose of total PM (52 µg/m^3) would be estimated to generate average costs of \$0.10 ($\pm$0.026) per person per day (roughly \$5 million per day for the entire country), resulting from origin-specific harms that are proportional to the PM load attributed to each origin (Figure 1.3A). However, the estimated contribution of harm from each origin changes dramatically if origin-specific health responses are considered (Panel B). For example, we estimate that the small average dose of transboundary PM from North Korea (4.3 µg/m^3) is so harmful per unit that its impact is comparable to the impact of domestic-origin PM from South Korea, which has a mean dose almost six times higher (23.6 µg/m^3). Similarly, transboundary PM from China exhibits an intermediate mean dose (14 µg/m^3) that we estimate would generate health costs almost twice as large as domestic-origin PM. We estimate that average doses of PM from dust are small (6 µg/m^3), generating half the cost of domestic-origin PM, although Yellow Dust events, which lead to doses above 1000 µg/m^3, can generate substantial harm.

Temporal structure of health impacts by PM origin We find that cumulative respiratory medical expenditures emerge similarly across PM origins, rising gradually until leveling out after roughly three weeks, regardless of whether our model accounts for PM origin (Extended Data Figure A3). The cumulative health response stabilizes after 21 days. Further, we find no evidence that indicates substantial temporal displacement of health costs ("harvesting", see Methods).

Computing damages by PM origin in mixtures

Analyzing the health effects of PM by each origin in isolation provides a clear measure of relative impacts but is an incomplete picture of total PM impacts because PM is experienced as a mixture, and the presence of PM from one origin can affect the health impact of PM from other origins. In particular, prior studies(Anderson, Hyun, and Lee 2022; Hahm and Yoon 2021) and our results suggest that individuals in South Korea engage in avoidance behavior (e.g., staying indoors) to protect themselves from the health effects of the entire PM mixture incident on their community. This implies that a unit of PM from origin j may have a health impact that depends on whether PM from origin k is high or low since higher PM from k may induce greater avoidance, mitigating the effect of PM from j (see Methods). Stated another way, because individuals engaged in avoidance of PM from all origins, PM from each origin mediates the health impact of PM from all other origins. Figure 1.3 depicts

only the *partial* effect of exposure to PM of each origin, holding PM from all origins at zero, thereby abstracting away from these interactions. However, computing the actual health impact of PM from any single origin requires accounting for the entire mixture of PM when exposure occurs.

We compute the total health impact of different PM mixtures, accounting for empirically estimated interactions between PM from different origins (see Methods). Figure 1.4 presents a surface that describes the expected excess nationwide respiratory health spending that would result from exposing every person in South Korea to different mixtures of PM from South Korea, China, and North Korea for a single day (more complex combinations are possible to compute, but difficult to display). "Iso-damage" curves trace out mixtures of PM from the pairs of jurisdictions that generate the same health cost. Here, a slope of -1 would indicate a mixture where a one-unit increase in PM from either of the two originating jurisdictions would have the same incremental health impact (i.e., there would be no change in total spending for a one-to-one exchange of the two pollutants). However, we do not observe this for any observed mixtures (shading indicates historical frequency). Instead, iso-damage curves in both panels are steeper than -1, implying that incremental damages of anthropogenic PM from transboundary sources are always greater than those of domestic PM in our setting.

The mixture-damage surface in Figure 1.4 can be differentiated to compute the incremental harm caused by a unit of PM from a single origin that is contained within a mixture. Based on the average PM mixture from China and South Korea in our sample, assuming zero exposure to PM from other origins, we estimate that the incremental nationwide health costs of exposure to $+1$ $\mu g/m^3$ PM from China and South Korea—relative to historical levels–are \$108,808 ($\pm\$10,896$) and \$32,131 ($\pm\$7,943$), respectively. For North Korea and South Korea, these values are \$182,358 ($\pm\$45,842$) and \$26,665 ($\pm\$8,575$), respectively. In terms of health costs, one additional $\mu g/m^3$ of PM from North Korea is equivalent to an increase of 6.84 $\mu g/m^3$ of PM from South Korea, and one $\mu g/m^3$ of PM from China is equivalent to 3.39 $\mu g/m^3$ of South Korean PM.

We also note that the curvature of this surface is concave, such that (i) overall harm increases with higher PM levels from any origin, but at a declining rate, and (ii) higher PM levels from each origin reduce the incremental harm from other origins (see Methods).

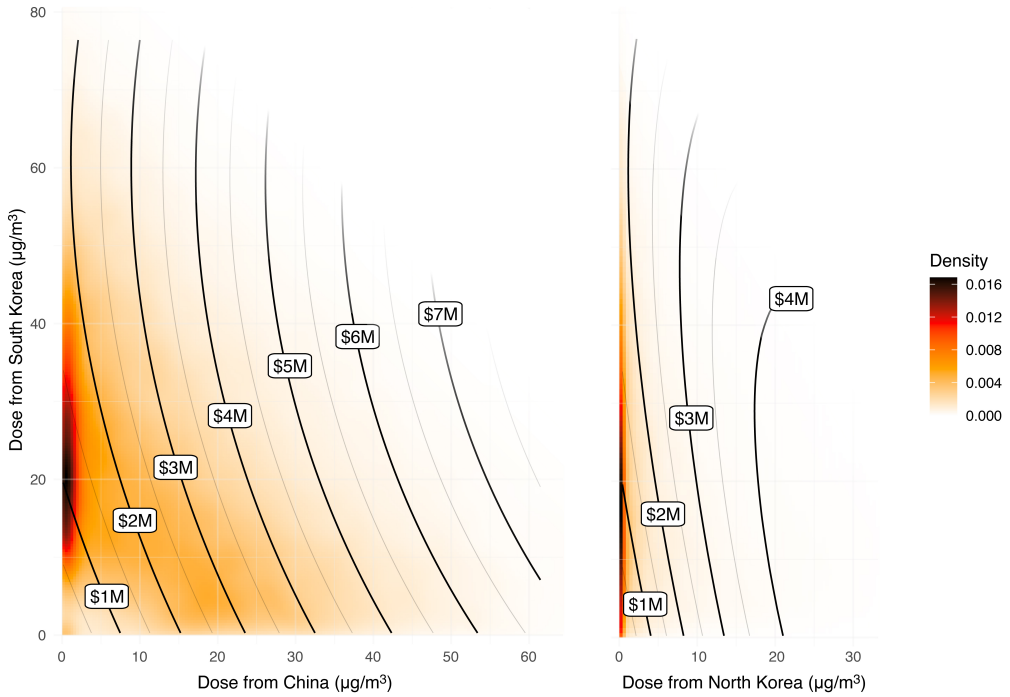

Figure 1.4: **Health Costs from Mixtures of Domestic and Transboundary PM**

Notes: Change in single-day total respiratory health spending (2022$) associated with nationwide exposure to mixtures of PM from combinations of domestic and transboundary PM from China (left) and North Korea (right). Estimates assume exposure to PM from all other origins are zero. Total spending is shown by black contour lines. Bivariate densities of exposure during our data period are shown as colored shading. Relationships are shown to the joint 99^{th}-percentile of population-weighted historical exposures.

Total damages from domestic and transboundary PM

We compute total nationwide damages traceable to each origin during our study period and find that accounting for differences in the per-unit harm by PM origin is critical for estimating the relative harms from domestic and transboundary PM (Table 1.1). We compute total harm from j by estimating the difference in health outcomes that would have been expected to occur in two different scenarios: one where PM emissions reflect actual historical emissions versus a scenario where j unilaterally reduces its emissions to zero (and the emissions of other countries are unchanged; see Methods). Accounting for differences in harm per unit of PM, we

	Fraction of population exposure to anthropogenic PM in South Korea, % total	Estimated annual health cost, million 2022$ ± SE (% total, anthropogenic)	
		This study	Assuming undifferentiated dose–response
South Korea	56.6	305 ± 92 (27.6)	615 ± 70 (58.4)
North Korea	9.9	223 ± 66 (20.1)	97 ± 11 (9.2)
China	33.5	579 ± 66 (52.0)	341 ± 38 (32.3)

Table 1.1: Average Annual Contributions to Anthropogenic PM Exposure and Associated Change in Respiratory Health Spending by Origin

estimate that PM originating in South Korea causes roughly $300 million in health costs in South Korea per year ($0.07 per person per day), while transboundary PM from China and North Korea generate roughly $580 and $220 million per year ($0.14 and $0.05 per person per day), respectively. (Note that health costs in South Korea reflect the low cost of medical care in a national healthcare system where costs for comparable treatments are roughly $6-10\times$ lower than in the United States.(RIHP 2021))

Prior state-of-the-art practice does not differentiate per-unit harms by origin. (Dedoussi et al. 2020; Du, Guo, et al. 2020; Lim et al. 2020; Chen, Li, et al. 2021; Sergi et al. 2020) Had we used the standard undifferentiated approach, we would have estimated that transboundary PM generated 41% of the costs from anthropogenic sources, rather than the 72% that we estimate here (Table 1.1). We estimate that 57% of anthropogenic PM that the South Korean population is exposed to originates domestically, but it generates only 28% of the damage from anthropogenic PM because it is relatively less harmful than transboundary PM.

Damages by origin over time We estimate that PM exposure and damages for major PM origins have exhibited different trends during our study period (see Figures 1.5A–C). We compute that exposure to PM from North Korea declined by roughly 12.5% per year, an effect that could be attributed to falling emissions, changes in meteorology, or other factors; over the same time, PM from South Korea remained essentially unchanged (+0.1% per year) and PM from China declined modestly (−1.6% per year). We estimate that the trends in estimated costs resulting from these exposures largely mirror these trends in exposure, although the overall baseline level of costs is relatively higher for PM from North Korea and China, reflecting the higher impact per unit of PM. Respiratory health costs attributable to PM from North Korea fell to about half of their 2005 level and costs related to PM

from China declined slightly from 2013, reflecting emissions reductions associated with China's "war on pollution."(Heo, Ito, and Kotamarthi 2023; Greenstone, He, Li, et al. 2021; Zheng and Kahn 2017) In contrast, we estimate that health costs traceable to domestic PM emissions have increased steadily by 3.6% per year, an effect that can be explained by avoidance behavior: throughout our study period, domestic PM concentrations remained stable while transboundary PM concentrations declined, which on net increases the per-unit harms of domestic PM due to reductions in avoidance.

Damages by origin across space We find that the source of PM health damages varies substantially across space, with provinces nearer to emission sources generally experiencing relatively more damage from those sources (Figures 1.5D–F). In South Korea's southern and western provinces, we find that the largest portion of PM health damage results from emissions originating in China. PM from China accounts for as much as 80% of the costs in Jeju (the island province in the far southwest) and roughly 60% of the costs in other nearby provinces. PM from North Korea is responsible for relatively more damages in the north of South Korea—accounting for as much as 25% of the costs in the Seoul Metropolitan Area. Domestic emissions are responsible for around 28% of damages nationwide, but costs are relatively larger in South Korea's southeastern areas, rising to 40% of PM damage, where domestic heavy industry is concentrated.

1.4 Discussion

Our findings show that distinguishing the health impacts of PM by its origin qualitatively changes our assessment of where health damage from PM originates. To the best of our knowledge, this study is the first to empirically demonstrate real-world differences in the health impacts of origin-specific contributions to a PM mixture incident on a single population. This is achieved by distinguishing pollutants from different origins and jointly estimating differences in their associated health impacts. Although we apply this approach to transboundary PM in Northeast Asia, it can be generalized to a broader class of pollution problems. For example, different water pollutants may similarly affect common metrics used to assess contamination, such as biochemical oxygen demand,(Jouanneau et al. 2014) but may have distinct per-unit impacts on a population or ecosystem; likewise, summary indices used for soil pollution(Kowalska et al. 2018) may exhibit similar patterns. In settings like these, a key challenge for governance is identifying the linkages between multiple polluters and associated damages over large distances and long time horizons. The techniques

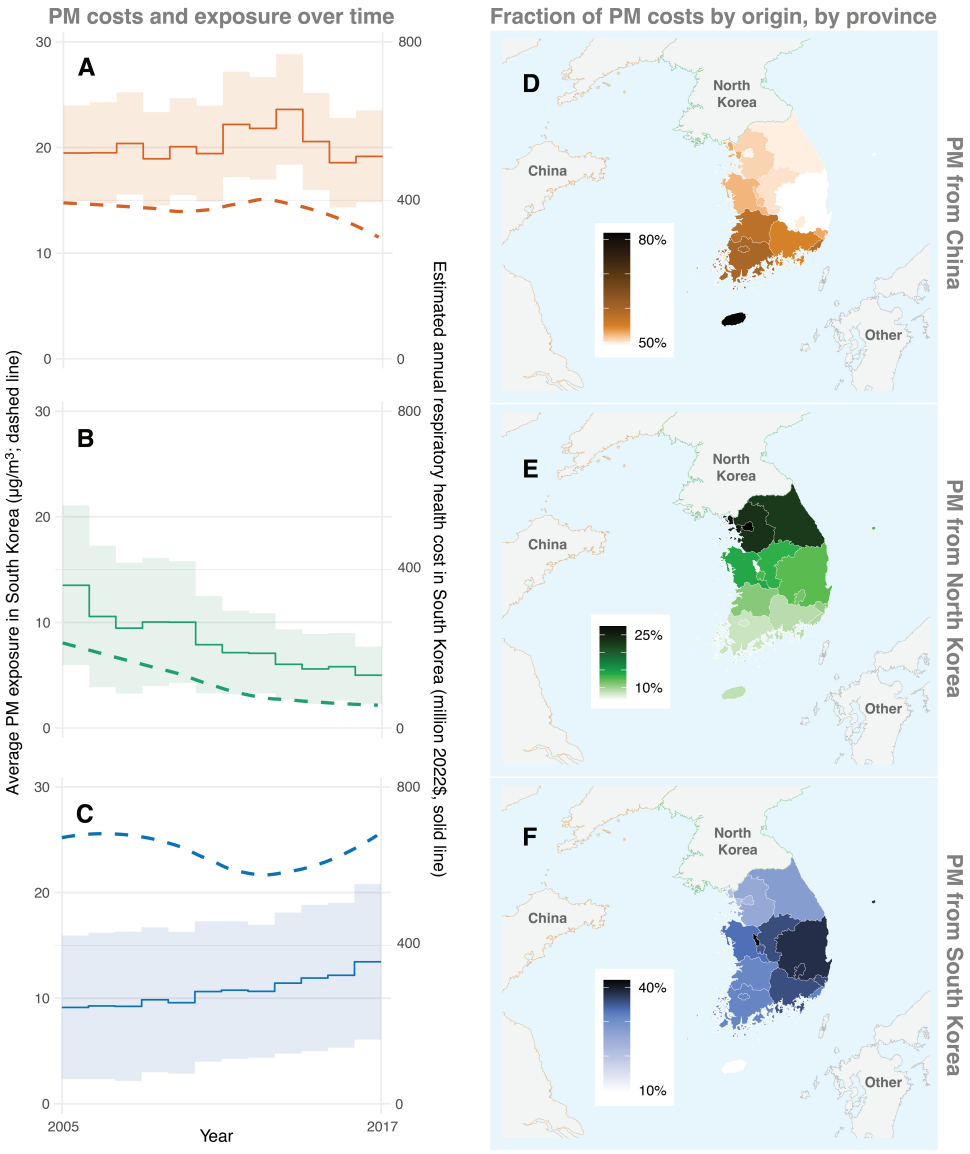

Figure 1.5: **Origin-specific Damages from PM over Time and Across Space**

Notes: (A) Trend of nationwide, population-weighted exposure in South Korea to PM from China (dashed lines, left y-axis) and annual respiratory health costs associated with PM exposures from China (solid lines, right y-axis, 95% confidence internal shown). (B)-(C) Same as (A), but for PM originating from (B) North Korea and (C) South Korea. (D) Province-level variation in the portion of respiratory health costs in South Korea attributable to anthropogenic PM from China. (E)-(F) same as (D), but for PM originating in (E) North Korea and (F) South Korea.

we have developed here can support progress in these areas by providing critical information on the relative harms attributable to particular actors.

We have also demonstrated the quantitative implications of differentiating the harm caused by PM from different origins. Our findings suggest that when identifying sources of health damage, major biases can result from assuming equal per-unit harm, as is standard in the literature. For example, in our context, this assumption causes estimates of harm from multiple countries to be incorrect by a factor of two. We believe our results suggest that this assumption should be assessed in other contexts as well. In Southeast Asia, for example, transboundary haze is considered one of the region's more serious health concerns.(Othman et al. 2014; J. S. H. Lee et al. 2016) In Sub-Saharan Africa, dust carried by winds from the Sahara is a major contributor to PM levels, though its effects may be distinct from the effects of PM from, for example, internal combustion engines.(Heft-Neal et al. 2018; Heft-Neal et al. 2020) Even within a country, the diversity of regional pollutants can lead to divergent responses to subcomponents of PM. This issue may be especially relevant for larger countries, such as the U.S., China, Brazil, and India, where internal interstate air pollution flows are a growing concern.(DeCicca and Malak 2020; Dedoussi et al. 2020; Du, Guo, et al. 2020; Chen, Li, et al. 2021) In all of these cases, the approach we have developed here can be used to empirically test whether pollutants from different origins exhibit similar or distinct per-unit damages.

Two points are worth noting when interpreting our findings. First, data presented here should not be considered a complete cost-benefit analysis. The outcome of interest—health costs associated with outpatient visits due to respiratory illnesses—is an incomplete measure of total changes in social welfare. For example, defensive investments—such as the purchase of air purifiers and face masks—are often paid privately and are not accounted for in our analysis.(Deschenes, Greenstone, and Shapiro 2017) We also do not consider mortality costs, other morbidity costs, or any potential benefits associated with transboundary PM emissions, such as economic benefits from PM-emitting industrial activity in China.(Zhang et al. 2017) We hope future work addresses these limitations.

Second, the magnitude of PM-driven health costs we measure will differ in other contexts. One reason for this is that our results are specific to South Korea: we report health effects of PM by origin, but those effects are net of any chemical or physical changes that occur to PM plumes after they are emitted. For example, because PM emitted in China must travel for many hours in the atmosphere before reaching South Korea, larger particles may have been preferentially removed or components of the emitted PM plume may have been oxidized into less harmful substances, both of

which would affect resulting health costs. In other words, while we find that PM from China is more harmful per unit to the South Korean population than PM originating domestically, this does not necessarily imply that PM originating in China is more harmful *in general*. We also expect that, overall, monetized damages from PM will be larger in other high-income countries for two reasons. First, healthcare costs in South Korea are some of the lowest among developed countries. For instance, prior analyses have estimated that in 2020, the average fee for an initial primary care visit was about $13 (₩16,140) in South Korea while it was about $109 in the U.S.(RIHP 2020) Similarly, the medical fees for hospital childbirth and appendectomy are $1,040 and $2,166 in South Korea, respectively, while the corresponding fees in the U.S. are $11,200 and $13,020.(RIHP 2021) These differences in cost contribute to total annual health expenditure per capita of only $2,600 in South Korea, compared to $10,945 in the U.S.(Chow, Bradley, and Gross 2022) Thus, the costs we report here would almost certainly be higher if our study population were under an alternative healthcare system.(Anderson, Hyun, and Lee 2022) Second, the South Korean population is very sensitive to information about PM levels, such as air quality warnings, and has already invested heavily in defensive adaptations, such as air filters.(Hahm and Yoon 2021; Anderson, Hyun, and Lee 2022) Populations that are less responsive to air quality information or that possess fewer defensive assets would likely experience larger health damages from any given quantity of PM exposure.

Lastly, our results suggest that institutions responsible for the management of transboundary pollution may need to consider origin-specific health responses to improve their assignment of damages and/or management of emissions. Since the *Trail Smelter* transboundary air pollution dispute was settled in 1941,(Henry, Kim, and Lee 2012) countries have attempted to control transboundary pollution within the frameworks of international institutions. The settlement served as the foundation for Principle 2 of the Rio Declaration, unanimously accepted by all 179 countries present at inaugural 1992 UN Earth Summit, which states "the polluter should, in principle, bear the cost of pollution."(Bratspies and Miller 2006; Rio Declaration on Environment and Development 1992) Furthermore, several commissions or organizations have been created: examples include the United Nations Economic Commission for Europe (UNECE) Convention on Long-Range Transboundary Air Pollution, the Malé Declaration on Control and Prevention of Air Pollution and Its Likely Transboundary Effects for South Asia, and the Association of Southeast Asian Nations' Agreement on Transboundary Haze Pollution.(WHO 2021) However, no international institution has yet recommended the consideration of origin-specific health responses to pollution when assessing the simultaneous impacts of transboundary and domestic air pollution. For instance, while the World Health Organization acknowledges the

possibility that PM from different origins may have different health impacts, it currently does not offer guidelines to account for origin-specific health responses.(WHO 2021) Our findings suggest that updated guidance and policies that account for these differences can improve public health.

The preceding chapter has investigated the divergent responses of public health outcomes to PM based on their originating locations. The subsequent chapter will delve into the ramifications of the previous chapter's findings within the context of applied microeconometrics.

Chapter 2

Instrumental Variables and Heterogeneity in Sources of Identifying Variations

2.1 Introduction

When using instrumental variables (IV), many studies in applied econometrics have focused on the conventional requirements for the use of IVs–the first-stage condition and the exclusion restriction–to get estimates of the causal impacts and extrapolate those coefficients to counterfactual policy settings. An issue is that the results of IV regressions could differ considerably depending on which sets of IVs are in use, even if these IVs are deemed appropriate in terms of those two conventional requirements. Identifying variations induced by a particular set of IVs can be associated with certain groups of people or channels that determine the influence of the endogenous variable on the dependent variable. These groups and channels may have different characteristics compared to those associated with other IV sets, thus leading to heterogeneous responses. (Angrist and Krueger 2001; Mogstad and Torgovitsky 2018; Mogstad, Santos, and Torgovitsky 2018; Dunning 2008) As a result, it is possible that the IV or two-stage least-square (2SLS) estimates may diverge, even though these estimates are assumed to represent one 'causal impact,' and only depict a part of the impacts associated with target variations (or policy-relevant variations (PRV)) one aims to analyze in a counterfactual analysis. However, it is still unknown to what extent the different sets of identifying variations can result in 2SLS estimates which are not qualitatively similar to those produced when other sets of IVs are used, in real-world empirical settings.

In this paper, we demonstrate the degree to which the regression results can vary depending on sets of IVs in use, drawing on real-world data sets. We pinpoint the IV sets utilized to establish the relationship between particulate matter (PM) and health outcomes as a pertinent example of this phenomenon. More specifically, we analyze the relationship between particulates less than 10 micrometers in diameter (hereafter "PM_{10}") and the respiratory health expenditure per person associated with outpatient visits. We test different sets of widely used IVs that satisfy the conventional IV conditions but may represent different identifying variations – 1) estimates of the contribution of distant anthropogenic emissions to PM observed in location of interest, 2) non-anthropogenic contributions, and 3) the changes in wind direction. We calculate IV or 2SLS regression coefficients for each set of IVs, and compare the results of extrapolating these estimates to counterfactual policy simulations. By doing so, we aim to underscore that the use of justifiable IVs may not guarantee a unique estimate of causal impacts and, therefore, the association between identifying variations and PRV should be carefully examined when discussing policy implications. Indeed, our findings show a wide range of coefficients, the largest estimate being over 17 times larger than the smallest one in magnitude, and even the sign of coefficients was estimated to be negative in some cases.

The analysis of air pollutants, including PM, is well-aligned with the goal of this study at least in two regards. First, there are some standard sets of IVs we can refer to when replicating IV construction processes. Previous studies on air pollutants have developed and standardized the use of wind-related information. Usually, wind direction dummy variables were utilized, interacted with the regional fixed effects, based on the assumption that the position of primary contributors to the level of pollution observed in a location of interest is fixed (e.g., on the western side of Michigan or the south-eastern side of San Francisco), and the changes in wind patterns randomly determine the degree of people's exposure to air pollutants. (Deryugina et al. 2019; Carneiro, Cole, and Strobl 2021; Eom et al. 2020; Zheng, Zhang, et al. 2019; Powdthavee and Oswald 2020; Anderson 2020)

Another way of using wind-related identifying variations is to capture the contribution of distant locations to the level of air pollution observed in an area of interest. This approach assumes that emissions from distant regions might be less correlated with unobservable confounders, such as the level of economic activity, compared to emissions from an area of interest. In these cases, changes in emissions from distant locations, usually proxied with pollution observations from those regions, are combined with information on wind dynamics. (Lai et al. 2021; Chen, Chen, et al. 2021; Zheng, Wang, et al. 2019; Fu, Viard, and Zhang 2022; Nam et al. 2022; Heyes and Zhu 2019; Rocha and Sant'Anna 2022; Cheung, He, and Pan 2020; Barwick et al. 2018;

Bayer, Keohane, and Timmins 2009) While most of these papers used wind direction dummies, others use a more complicated measure to construct IVs, considering the wind speed and the wind directions between the source and destination cities. (Barwick et al. 2018) Also, Bayer, Keohane, and Timmins (2009) do not directly harness wind information, but they utilize a source-receptor matrix created by the Environmental Protection Agency (EPA), which is partially based on backward trajectory models drawing on historical wind dynamics, to capture the contribution of distant emissions. A number of studies harnessed information on specific sources of pollution instead of using PM emissions or observations of remote areas. Examples include the locations of power plants, (Luechinger 2009, 2014; Chen, Li, et al. 2021; Freeman et al. 2019) agricultural and wildfires, (He, Liu, and Zhou 2020; Pullabhotla and Souza 2022; Agarwal, Sing, and Yang 2020; Agarwal, Wang, and Yang 2021; Tan Soo 2018) and sand and dust storms. Yang and Zhang (2018) and Heft-Neal et al. (2020)

Following previous studies, we construct sets of IVs that correspond to these standard groups of IVs. We test the interaction terms of wind direction category dummies and district-level fixed effects. Additionally, to gauge the estimates of the contribution of external PM sources, we draw on information on wind dynamics combined with an atmospheric model to fully utilize wind-related variations, beyond utilizing the wind direction dummies. We further break down these external contributions into anthropogenic (from a foreign country – from China – to South Korea in this study), and non-anthropogenic origins (from desert dust and wildfires) as the per-unit impacts of PM associated with these origins can be different (Lee, Wilson, and Hsiang 2023).

The possibility of heterogeneous impacts by identifying variation is the second reason that the analysis of PM can be a pertinent example for this type of study. Indeed, there are various channels through which the impact of per-unit PM10 can differ depending on the types of exogenous variations. Among others, four channels can be considered. The first channel is the physical and chemical composition. Although PM10 is generally analyzed as one pollutant, it is basically a mixture of different constituents. Therefore, the physical and chemical characteristics of PM can be different by the composition and type of PM, which, in turn, can lead to varying degrees of its adverse health impacts. (Harrison and Yin 2000; Kelly and Fussell 2012; Strak et al. 2012; Schmid and Stoeger 2016; Lee, Wilson, and Hsiang 2023)

The second channel is that the degree of behavioral responses can differ. For example, PM from specific sources can be more closely related to visible distance degradation (Y. J. Kim et al. 2006; Yuan et al. 2006; Lee, Wilson, and Hsiang 2023), and the public can notice the level of PM more easily, thus taking avoidance or

defensive behaviors (e.g., wearing masks, using air purifiers, or staying at home) accordingly.

The third channel is that population subgroups exposed to PM would respond differently. Continuing with the behavioral responses mentioned above, children are considered to be more vulnerable to the toxicity of PM compared to adults; (Pope III and Dockery 1992; Anderson, Thundiyil, and Stolbach 2012) hence, they are more likely to be guided to undertake appropriate avoidance behavior. (Kim 2021; Neidell 2009a; Anderson, Hyun, and Lee 2022) If changes in PM due to exogenous emissions from a particular source reduce visibility at a larger degree compared to other sources, thus inducing the behavioral responses of the more vulnerable group, the estimated per-unit impacts based on these variations can be different other 2SLS estimates.

The fourth channel is the functional form of the impact of PM, which is potentially nonlinear, combined with different distributional characteristics across sources. For example, the level of PM from desert dust is more highly correlated with the extreme level of total PM (e.g., PM over 1,000 $\mu g/m^3$) while other sources better represent comparatively lower levels of PM. If the local response of health outcomes associated with extreme levels of PM is different from that related to milder levels of PM because of the potential nonlinearity of the response, the 2SLS estimates of the per-unit impacts of PM would not be the same either.

Considering all those channels, we analyze the relationship between respiratory health expenditure per person by age group and various types of PM that may have different physical and chemical characteristics, thus demonstrating the extent to which these channels mentioned above can be translated into varying degrees of IV/2SLS results.

This paper contributes to at least three strands of paper. First, our analysis directly contributes to papers that analyze the impacts of air pollutants with IVs constructed based on wind dynamics, especially in the field of environmental economics. Since the pioneering work of Luechinger (2009) demonstrated how to use changes in wind patterns to construct IVs, wind-related IVs have been widely used to analyze changes in various outcomes, including health-related variables, such as mortality rates, morbidity costs, and hospitalization rates. (Deryugina et al. 2019; Anderson 2020; Luechinger 2014; Chen, Li, et al. 2021; He, Liu, and Zhou 2020; Heft-Neal et al. 2020; Yang and Zhang 2018; Rocha and Sant'Anna 2022; Ebenstein, Frank, and Reingewertz 2015; Cheung, He, and Pan 2020) Other examples of health outcomes include sleeplessness, (Heyes and Zhu 2019) memory power, (Powdthavee and Oswald 2020), hypertension risks, (Pullabhotla and Souza 2022) and pregnancy loss. Xue et al. (2021) The use of wind dynamics to obtain identifying variations was

not limited to the analysis of health outcomes. Previous studies harnessed changes in wind patterns to estimate the impacts of air pollutants on the level of happiness, (Luechinger 2009; Zheng, Wang, et al. 2019) crime rate, (Bondy, Roth, and Sager 2020) test scores, (Carneiro, Cole, and Strobl 2021; Jeong 2021) migration choices, (Zheng, Zhang, et al. 2019; Chen, Chen, et al. 2021; Lai et al. 2021; Tan Soo 2018) labor productivity, (Fu, Viard, and Zhang 2022) housing values, (Nam et al. 2022; Freeman et al. 2019) consumer satisfaction, (Agarwal, Wang, and Yang 2021) and energy consumption. (Eom et al. 2020; Yi et al. 2020; Agarwal, Sing, and Yang 2020) We aim to highlight the importance of comparing the identifying variations in use and the target variations when deriving policy implications, which has not been fully appreciated in previous studies.

Second, we contribute to a growing literature on analyzing the discrepancy between the identifying variations induced by IVs in use and PRV. Many research papers in this strand have focused on settings where the endogenous variable of interest is a binary indicator, identifying the complier group that determines the local average treatment effect (LATE) and assessing to what extent LATE can be extrapolated to the impact of another policy setting. If the target groups of a given policy are different from compliers that determine LATE, the issue of a discrepancy between LATE and a policy-relevant treatment effect (PRTE) can arise. In these cases, Mogstad and Torgovitsky (2018) and Mogstad, Santos, and Torgovitsky (2018) demonstrated that researchers could draw inferences about lower and upper bounds of PRTE based on assumptions about how exogenous variations induced by IVs at hand would interact with target groups of population. While we do not explicitly distinguish which part of identifying variations can be used as PRV, our results imply the importance of understanding the potential discrepancy between identifying variations and PRV as the 'causal estimates' in the classical sense were shown to vary substantially depending on the choice of IVs.

Broadly, our study is built upon papers that delve into the validity of IVs and the interpretations of 2SLS results. Among them, our paper is most closely related to Dunning (2008). The author raised the issue of assuming that the effect estimated based on variations induced by IVs at hand is the same as the impact associated with the variations that are not related to the IVs, since those impacts might be heterogeneous in many cases. One of the examples he provides is the case of Doherty, Gerber, and Green (2006) who analyzed the impact of income on political attitude and used lottery winnings as an instrument. Dunning (2008) argues that, to interpret the IV estimates as causal impacts, the impact of lottery winnings should be considered homogeneous compared to the impact of increasing other types of income. Theoretically, we generalize this argument to the settings of multiple sources of identifying

variations. We further introduce the concept of PRV, which is equivalent to PRTE – the core concept in the second strand of papers, thus creating a bridge between the two branches of papers.

Other papers in this strand harnessed real-world data sets to test the validity of IVs that are frequently in use. Our paper does not directly question the validity of IVs as we treat all the identifying variations as legitimate ones. Instead, we highlight the potential discrepancy between identifying variations in use, thus calling for more cautious attention when using IVs, which is aligned with the spirit of this branch of literature. Zabrocki, Alari, and Benmarhnia (2022) directly questioned the comparability between wind directions. They demonstrated that the meteorological factors, such as temperature, humidity, and precipitation, are distributed differently by wind direction, which they argue signals the different characteristics associated with each wind direction and necessitates a more rigorous matching algorithm when using wind direction IVs. Another example is Mellon (2022), who demonstrated that 192 variables used in the previous literature were associated with weather variables. This intertwined relationship between weather factors and many aspects of society may potentially invalidate exclusion restrictions when utilizing meteorological factors as IVs.

2.2 Theoretical Framework

This section describes a parsimonious theoretical framework explaining the IV issue mentioned above. To illustrate the idea, we utilize the simplest example – the linear specification – as described elsewhere. (Dunning 2008) Researchers are usually interested in identifying the coefficient of interest β in the following specification:

$$y_{it} = \beta pm_{it} + \gamma x_{it} + e_{it} \tag{2.1}$$

where y is the dependent variable of interest, such as respiratory morbidity spending. Note that we assume all variables are normalized so that their means are zero for simplicity. pm is the independent variable of interest, the level of PM10 in this study, which is potentially endogenous. x represents a confounding factor. An example of x is the level of economic activities that would impact the health conditions of the public and as well increase the level of anthropogenic emissions, i.e., $pm \perp x$. In many empirical settings, not all confounding factors are observable,

as is likely in the case of the level of economic activities. Therefore, the empirical specification is reduced to the equation as follows:

$$y_{it} = \beta' pm_{it} + e'_{it} \tag{2.2}$$

When an appropriate measure of x is absent, it is believed that using valid IVs – ones that are correlated with pm but uncorrelated with x – can help identify the β without biases. A problem occurs when the impact of PM is heterogeneous by origin so that the true model is as follows:

$$y_{it} = \beta_a pm\_a_{it} + \beta_n pm\_n_{it} + \delta x_{it} + \epsilon_{it} \tag{2.3}$$

pm_a and pm_n are PM10 from anthropogenic and non-anthropogenic origins, respectively. Their impacts are heterogeneous here, hence $\beta_a \neq \beta_n$. We further assume $pm\_a \perp pm\_b$, which is also likely in real-world settings as in the case of anthropogenic and non-anthropogenic emissions. As x represents economic activities, it is reasonably assumed to be not systematically correlated with pm_n. Therefore, $pm\_n \perp x$ and $pm\_a \not\perp x$. ϵ_{it} is the idiosyncratic error term. The issue is that the different origins of PM are difficult to capture in many empirical settings. Even when the decomposition would be possible, the need for differentiating the origins is not well recognized as discussed in Lee, Wilson, and Hsiang (2023). As a result, many researchers estimate Equation 2.2, using the total PM level ($pm\_a + pm\_n$) rather than decomposing PM by origins.[1] In this case, what the estimated coefficient implies depends on the identifying variations associated with IVs at hand. If those IVs are related to changes in the level of PM from one source, the estimated coefficient would represent the impact of PM from the same source accordingly. For example, assume that the following relationships hold:

$$pm\_a \not\perp z, \quad pm\_n_{it} = \eta z_{it} + u_{it} \tag{2.4}$$

$$pm_{it} = \eta z_{it} + u'_{it} \tag{2.5}$$

$$y_{it} = \beta_{IV} \hat{pm}_{it} + \epsilon'_{it} \tag{2.6}$$

[1]This case can also be found in other empirical settings, such as the analysis of the impact of income on political attitudes as shown in Dunning (2008).

Equation 2.4 shows the true relationship between an IV, z, and PM from two origins. z is associated with the non-anthropogenic PM, while it is orthogonal to the anthropogenic PM. Equation 2.4 leads to Equation 2.5, the first stage specification of 2SLS. Note that $pm = pm_a + pm_n$, and they are normalized, so the coefficient of z is η, the same as in Equation 2.4. Equation 2.6 is the second stage regression specification, where $\hat{pm}_{it} = \eta z_{it}$. u, u', and ϵ' are idiosyncratic errors with mean zero. Under these assumptions, it can be easily shown that β_{iV} is the same as β_n in Equation 2.3.

$$\beta_{IV} = \frac{Cov(\hat{pm}, y)}{Var(\hat{pm})} = \frac{1}{\eta}\frac{Cov(z, y)}{Var(z)} = \frac{\beta_n}{\eta}\frac{Cov(z, pm\_a)}{Var(z)} = \beta_n \tag{2.7}$$

Even though this IV estimate represents a specific type of variation within changes in the level of total PM, it can have meaningful policy implications when the identifying variations are well aligned with the target variations. For example, if a government is interested in a policy of reducing the number of forest fires, then the use of wild fire-related IVs in this type of regressions can help draw relevant policy implications. Further, if the PM impacts are homogeneous across sources of variations, i.e., $\beta = \beta_1 = \beta_2$, the interpretation of the IV coefficients can be generalized to the total PM reduction, regardless of PM sources.

Problems rise when the target variations are not closely related to the identifying variations in use, and the impacts are heterogeneous ($\beta_a \neq \beta_n$) across sources of variations. For instance, a government might be more interested in the impact of abating anthropogenic emissions rather than reducing non-anthropogenic emissions that are more difficult to control. Then, the policy implications can be misleading when using the estimates based on non-anthropogenic identifying variations to gauge the policy impact of abating anthropogenic air pollution. Therefore, when reducing the total level of PM in general is of interest, then the IVs at hand should well represent an appropriate mixture of both anthropogenic and non-anthropogenic emissions.

The above-mentioned problem can be generalized a larger number of sources of variations when the true data generating process is as follows:

$$y_{it} = \sum_{j=1}^{N} \beta_j pm\_j_{it} + \zeta x_{it} + v_{it} \tag{2.8}$$

where $pm = \sum_{j=1}^{N} pm\_j$, v is an unsystematic error term, and N is the number of identifying variations that should be considered given an empirical setting. A

larger number of N necessitates the efforts in determining which sets of identifying variations are induced by IVs at hand and to what extent these sets of variations are related with the variations of interest that would be targeted in a counterfactual policy simulation.

2.3 Data and Summary Statistics

Estimates of External Contribution to PM

To test the degree to which coefficients vary depending on IVs, we utilize estimates of the exogenous contribution of different origins to PM_{10} (particulates less than 10 micrometers in diameter, henceforth "PM") observed in South Korea["ROK"]. The unique geographical characteristic of the country, a peninsular surrounded by waters but frequently affected by various origins of distant PM emissions, allows the evaluation of sources of upwind influences according to meteorological circumstances. (Crawford et al. 2021; Jordan et al. 2020; Choi et al. 2019) For example, when the wind blows from the west or the north, the level of air quality in ROK is affected by anthropogenic emissions from China flowing over the Yellow Sea or those from North Korea ["DPRK"] crossing the border, respectively. Another example is the impact of Asian dust, which originates from deserts in Inner Mongolia and China and influences countries in their east, such as ROK, DPRK, and Japan. (Kar and Takeuchi 2004)

In our earlier work, (Lee, Wilson, and Hsiang 2023) we decompose the origin of PM by anthropogenic sources, which we further break down into country jurisdictions: ROK, China, North Korea["DPRK"], and non-anthropogenic sources including the influences of desert dust, forest fires, and sea salt. More specifically, we first used a global reanalysis data set (Inness et al. 2019) to isolate the impact of dust and sea salt on the levels of PM observed in ROK. We then create many backward trajectories starting at different times and altitudes for each PM monitor in South Korea on each day based on the Hybrid Single-Particle Lagrangian Integrated Trajectory model (HYSPLIT), one of the standard atmospheric transport models (Draxler and Hess 1998; Stunder 2004) We combine these trajectories with the distribution map of emissions due to anthropogenic sources (European Commission, Joint Research Centre (JRC)/Netherlands Environmental Assessment Agency (PBL) 2019) and fires (Werf et al. 2017; Randerson et al. 2012; Giglio, Randerson, and Werf 2013), applying chemical decay and deposition rates, which provides us with estimates of the contribution of distant human emissions and forest fires to the level of PM observed

on a monitor on a certain day.[2]

Figure 2.1 demonstrates the decomposition process and the results. Figure 2.1A shows a set of backward trajectories created by HYSPLIT, which traces back 96 hours of historical wind dynamics from a single district in Busan, the second most populous city in ROK, for one month, April 2016. The trajectories of two particular dates – April 5 and 11 – are colored yellow and pink, respectively. For these two respective dates, Figures 2.1B and 2.1C depict the result of combining the trajectories with emission estimates. The opacity of each cell on each trajectory describes the degree to which the emissions from each location contribute to the levels of PM in Busan. The colors of cells are differentiated according to their jurisdiction. The violin plots located in the left-bottom corner of Figures 2.1B and 2.1C demonstrate the distribution of the contribution levels by origin. Figure 2.1D shows the daily variations in total PM during 2016, and Figure 2.1F depicts the distribution of contribution levels by origin, weighted with the number of population, with various origins colored differently. Emissions from ROK and China constitute a majority of PM in ROK throughout the year. However, PM from dust becomes the largest contributor when Yellow Dust flows over the Yellow Sea, recording extremely high levels of PM above 100 $\mu g/m^3$. PM associated with forest fires contributes to the total PM10 with a smaller amount, but its contributions are noticeable during July and August. These distributional and temporal differences imply that the identifying variations induced by each IV may also not be the same, potentially resulting in qualitatively dissimilar results.

Wind Direction and Meteorological Factors

Another set of IVs that we test in this paper is the wind direction indicators interacted with regional dummy variables. We collected information on the hourly wind direction from monitors managed by the Korea Meteorological Administration (KMA). For each monitor, the wind direction is recorded in one of 16 directions or as 'no wind direction,' which means no specific wind direction can be detected due to weak wind speed. We use the dominant wind direction category on a certain day given a district as a daily representative wind direction of the area. We then interpolated the missing observations using the nearest-neighbor algorithm.

We found that the level of PM10 is associated with the direction of the wind, while the magnitude of the relative difference between directions varies by geographic location. As shown in Figure 2.2, in Seoul, the capital of ROK, the level of PM10

[2]The method section of our previous work describes further details on the decomposition procedures. (Lee, Wilson, and Hsiang 2023)

is greater when the wind blows from the west and southwest compared to the other directions, especially the east wind. In the case of Gwangju, a metropolitan city located in the southwest of ROK, the easterly wind is again associated with the lower degree of PM exposure, with the relative difference being larger as the PM exposure linked to the westerly wind is nearly as twice as that linked to the easterly wind. In Ulsan, one of the most industrialized areas in the country, the PM levels associated with the wind from the east and southeast are greater, as residential areas and air pollution monitors are located further inland to the northwest, while industrial complexes are developed in the coastal areas. In all of the example cities, when the wind direction is not recorded due to lower wind speed, the level of exposure is considerably large compared to the exposure levels related to 16 wind directions, potentially due to the fact that air pollution cannot be dispersed easier when the wind speed is slower.

We observe that changes in wind direction are also associated with the components of PM. In Figure 2.3, we incorporated the information on wind direction and the aforementioned estimates of PM origin decomposition. For ease of displaying the results, we incorporated slightly ordinal directions into ordinal directions (e.g., NNW and WNW to NW). In all the sample cities, when the wind direction is not detected, the contribution of ROK itself is the largest. The westerly winds are more associated with PM due to desert dust and the Chinese anthropogenic emissions flowing over the Yellow Sea. Our data shows that geographical adjacency plays a role as cities near foreign countries are under a higher influence of those countries than cities far from borders. The contribution of DPRK is larger in general in Seoul than the others, with the northwestern winds being related to the largest DPRK contribution, and Gwangju is impacted harder by PM from dust with the westerlies and the Chinese emissions than Ulsan is.

Other meteorological variables, such as precipitation and temperature, were collected from the database managed by the same agency and used as control variables. We collected hourly observations of those weather variables and interpolated missing observations using inverse-distance weighting drawing on the readings of the nearest five monitors. These variables were then aggregated by day of sample and district.

Medical Expenditure

We combine the estimates of origin decomposition and information on wind direction with changes in health outcomes. Our health variable of interest is the morbidity expenditure associated with outpatient visits due to respiratory diseases. South Korea has a universal healthcare system through which more than 97% of the entire

population is insured. We were granted access to the medical transactions data of about 10% sample of insured people, which are only accessible through the data center managed by the National Health Insurance Service (NHIS). We aggregated individual-level transactions by date and district of residence and calculated outpatient medical expenditure per person. Our outcome of interest covers all types of outpatient visits – e.g., visits to emergency, doctor's offices, and general hospitals. We focus on respiratory diseases – J-category illnesses according to the International Classification of Diseases, 10^{th} revision, as the impact of PM on health outcomes would be most pronounced in respiratory symptoms. To determine the heterogeneous impacts of PM by age group, we also calculated medical expenditure per person by three age groups – minors (0−19), adults (20-64), and older adults (65 or more). The period of analysis spans from 2005 to 2016.

Summary Statistics

Summary statistics of variables are described in Table 2.1 and Table B1. The first sub-panel of Table 2.1 summarizes our health outcome of interest. The average respiratory outpatient expenditure per person is the largest among minors, followed by older adults. The second sub-panel shows the statistics related to PM and its constituents. As depicted in Figure 2.1F, PM emissions estimated to have originated in ROK and China are the first and second largest contributors to PM observed in ROK. In our decomposition data, we observe that PM due to desert dust is the third contributor to the total level of PM, however, it becomes the main driver of extremely high levels of PM. The estimated maximum level of PM from desert dust is over 950 $\mu g/m^3$, the case of which coincides with the case of the maximum PM10 level over 1,000 $\mu g/m^3$. The pollution contribution of DPRK anthropogenic emissions was estimated to be less than 8 percent, which is followed by PMs originating from forest fires, salt, and other countries' industrial emissions (e.g., Russia, Taiwan, Japan, etc.). Lastly, Table B1 shows the ratio of wind direction category given a province. The ratio of each wind direction group significantly varies by geographical location. For example, the portion of the 'no-wind-direction' category ranges from 6.2 (Jeju, an island having stronger wind speeds than the other provinces) to 68.2 (Chungcheongbuk-do, an inland province with weaker wind speeds).

In our analysis, we focus on selected PM constituents, considering the methods of constructing IVs in previous literature. We analyze three categories of IVs – 1) estimates of the anthropogenic contribution of distant regions, 2) those of non-anthropogenic contribution, and 3) the wind direction dummies interacted with region indicators. For the first set, we use the estimates of the Chinese PM, as its contribution is the largest except for ROK itself. For the second category, we use

our estimates of PM from desert dust and forest fires. For the last group of IVs, we interact the wind directions with district dummy variables.

2.4 Empirical Analysis

Comparison of Fitted Values

We first compare the fitted values and the residuals obtained from using each set of IVs based on the following specification:

$$PM_{it} = \boldsymbol{IV}_{it} \cdot \boldsymbol{\beta}_1 + \boldsymbol{X}_{1it} \cdot \boldsymbol{\gamma}_1 + \boldsymbol{\theta}_{1it} + \boldsymbol{\phi}_{1t} + \boldsymbol{\delta}_{1i} + \varepsilon_{it} \tag{2.9}$$

where PM_{it} is the total level of PM, IV_{it} is the set of IVs in use, X_{it} is the weather control variables. We include an extensive set of fixed effects following Deryugina et al. (2019): θ_{it} is the interaction of province dummies and month fixed effects, ϕ_{1t} represents time fixed effects – year by month fixed effects, the day of the week, and holidays, and δ_{1i} controls the spatial – district – fixed effects. ε_{it} is an error term assumed to be distributed normal.

Based on Equation 2.9, we first obtain the fitted values of PM, $\hat{PM}$. Figure 2.4 compares these fitted values across the total level of PM10 based on a district in Busan, a metropolitan city located in the southeast of ROK. Compared to the fitted values associated with distant human emissions (PM from China), forest fires, and wind direction dummies, identifying variations induced by desert dust are shown to capture the higher level of PM10 better. On the other hand, PM from China shows a better performance in capturing very low levels of PM. Forest fires and wind dummies are showing similar performances, as the patterns of fitted values depicted in the lower panel of the figure. Figure 2.5 compares them focusing on year 2016 to present which parts of temporal variations are captured by each set of IVs. Compared to other sets of IVs, the desert dust was able to capture the huge increase in total PM10 in the late spring season.

Table 2.2 compares the results of the first-stage regressions. The adjusted R^2 associated with desert dust is greater than that of other sets of IVs since it works better to capture the extreme levels of PM. The regression coefficients are expected to be around one, but they were estimated to be statistically significantly lower than one in the case of distant human emissions and forest fires or larger than one in the case of desert dust. This is partially due to the fact that the various fixed effects are

also correlated with the identifying variations and the total level of PM10, resulting in those coefficients being different from one.

2SLS Regression Results

We run the reduced form and the second stage of regressions as follows:

$$Spending_{it} = \boldsymbol{IV}_{it} \cdot \boldsymbol{\beta}_2 + \boldsymbol{X}_{2it} \cdot \boldsymbol{\gamma}_2 + \boldsymbol{\theta}_{2it} + \boldsymbol{\phi}_{2t} + \boldsymbol{\delta}_{2i} + \epsilon_{it} \tag{2.10}$$

$$Spending_{it} = \boldsymbol{P\hat{M}}_{it} \cdot \boldsymbol{\beta}_3 + \boldsymbol{X}_{3it} \cdot \boldsymbol{\gamma}_3 + \boldsymbol{\theta}_{3it} + \boldsymbol{\phi}_{3t} + \boldsymbol{\delta}_{3i} + \epsilon'_{it} \tag{2.11}$$

where $Spending_{it}$ is the healthcare expenditure due to respiratory illnesses per person associated with outpatient visits, and $\hat{PM}$ is the fitted values of PM from Equation 2.9. While the meanings of other variables are the same, the subscripts 2 and 3 indicate that these equations are different from Equation 2.9.

The first panel of Table 2.3 presents the reduced form results. We found that the reduced-form estimates show a varying degree of magnitudes, even the signs of coefficients being sometimes different. The IV estimates based on forest fires show coefficients consistently statistically significant except for the older-adult group. Their magnitudes were the largest compared to the cases of other sets of IVs, and the coefficient for the minors group is about 40 times larger than the coefficient based on distant human emissions. On the other hand, the signs of the coefficients associated with desert dust were estimated to be negative, and all the results were not statistically significant at the 10% level. The use of distant human emissions, PM originating from China, resulted in regression coefficients that are only statistically significant for the elderly group at 10% level. These reduced-form results align with the heterogeneous responses by PM origin highlighted in our previous work. (Lee, Wilson, and Hsiang 2023)

The bottom panel of Table 2.3 shows the coefficients amplified according to the first-stage results in the three columns in the middle. This panel further demonstrates the results based on the interaction terms of wind direction dummies and district-level fixed effects in the last column. The 2SLS coefficients were estimated to be all negative and statistically insignificant. Stark differences are observed compared to the case of forest fires, even though the adjusted R-squared value and the fitted value graph were shown to be similar. The differences are more pronounced when comparing the columns of forest fires and distant human emissions in the total population group, as the magnitude of coefficients is over 200 times larger in the fourth column.

The variability in IV estimates leads to huge differences in a counterfactual policy simulation. Table 2.4 shows to what extent our health outcome of interest – the expenditure due to respiratory outpatient visits – would change for the total population in ROK when the level of PM10 is mitigated by 10 $\mu g/m^3$ on average, throughout one year. The mitigation simulation results vary substantially, as possibly inferred from the previous tables. When a government project the impact of the 10-unit mitigation of the total PM10 based on the results associated with forest fire IV, the nearly two-million USD decrease in healthcare expenditure would not be realized unless the 10-unit decrease only aims at the PM emitted from forest fires.

2.5 Conclusion

In this paper, we demonstrated the degree to which the regression results can vary depending on sets of IVs in use, drawing on real-world data sets. We test different sets of widely used IVs that satisfy the conventional IV conditions but may represent different identifying variations. We calculate IV or 2SLS regression coefficients for each set of IVs, and compare the results of extrapolating these estimates to counterfactual policy simulations. Indeed, our findings show a wide range of coefficients, the largest estimate being 200 times larger than the smallest one in magnitude, and even the sign of coefficients was estimated to be negative in some cases. These findings are our greatest contribution to previous literature as there has not yet been studies showing the variability of 2SLS results depending on the choice of particular IVs, based on the real-world data sets and the detailed estimates of the various sources of variations.

The variability itself may not be an obstacle to the applied econometricians who intend to utilize IVs. If the homogeneous responses across various sources of variations can be justified, policy implications can be drawn regarding the potential changes in the total level of an endogenous variable of interest. Also, even if heterogeneous responses are reasonably assumed, one can determine whether the target variations of a counterfactual simulation are well connected to the identifying variations at hand, thus justifying the extrapolation of IV/2SLS estimates to the simulation.

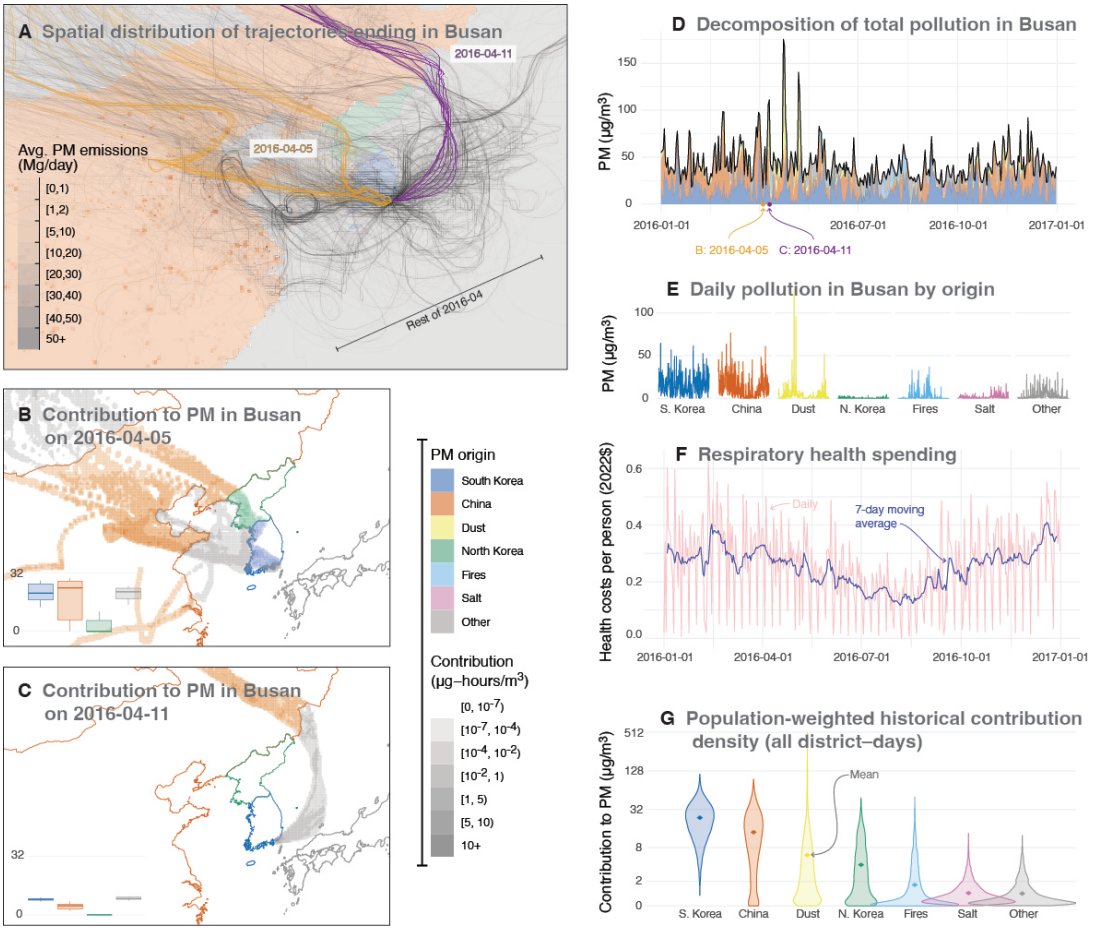

Figure 2.1: Source Decomposition Process and Results (Reprinted from Lee, Wilson, and Hsiang 2023)

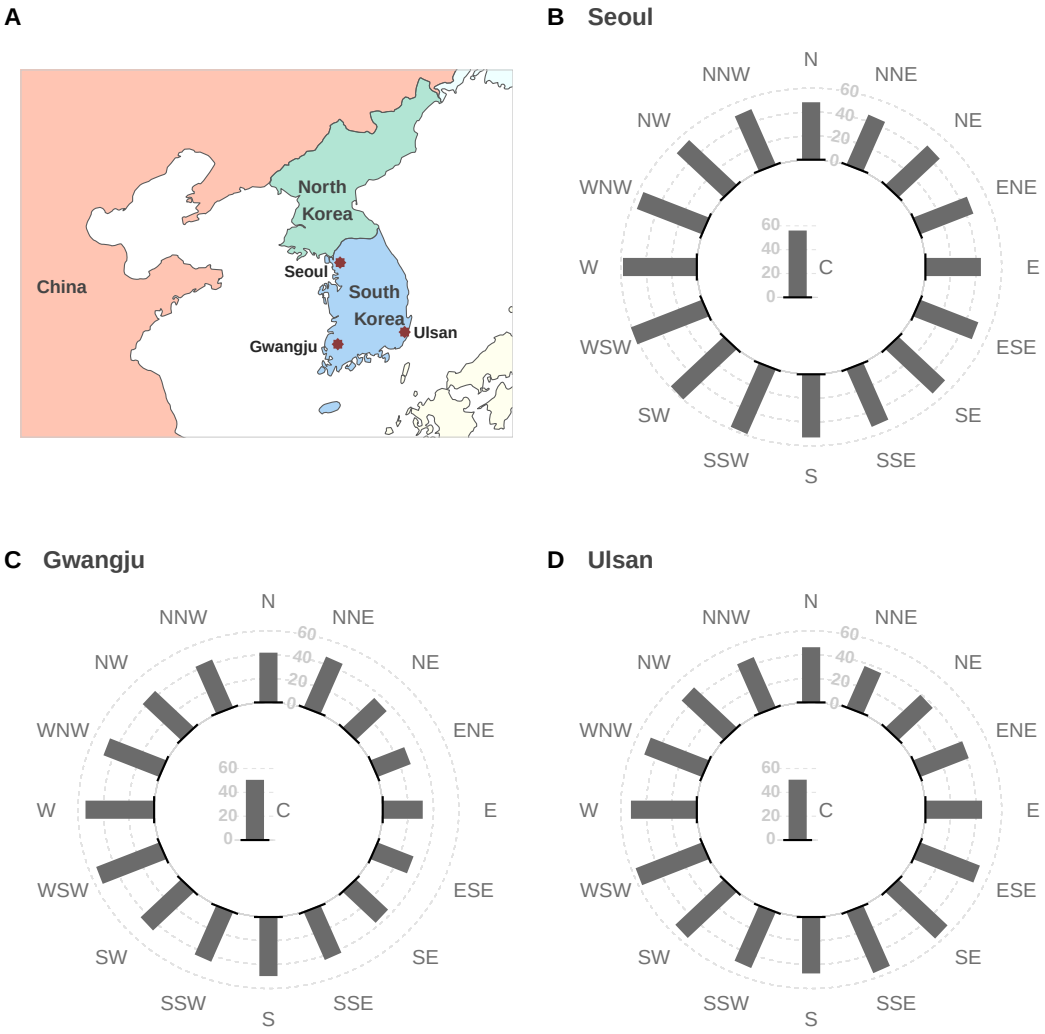

Figure 2.2: Population-weighted Exposure to PM10 by Wind Direction in Selected Cities

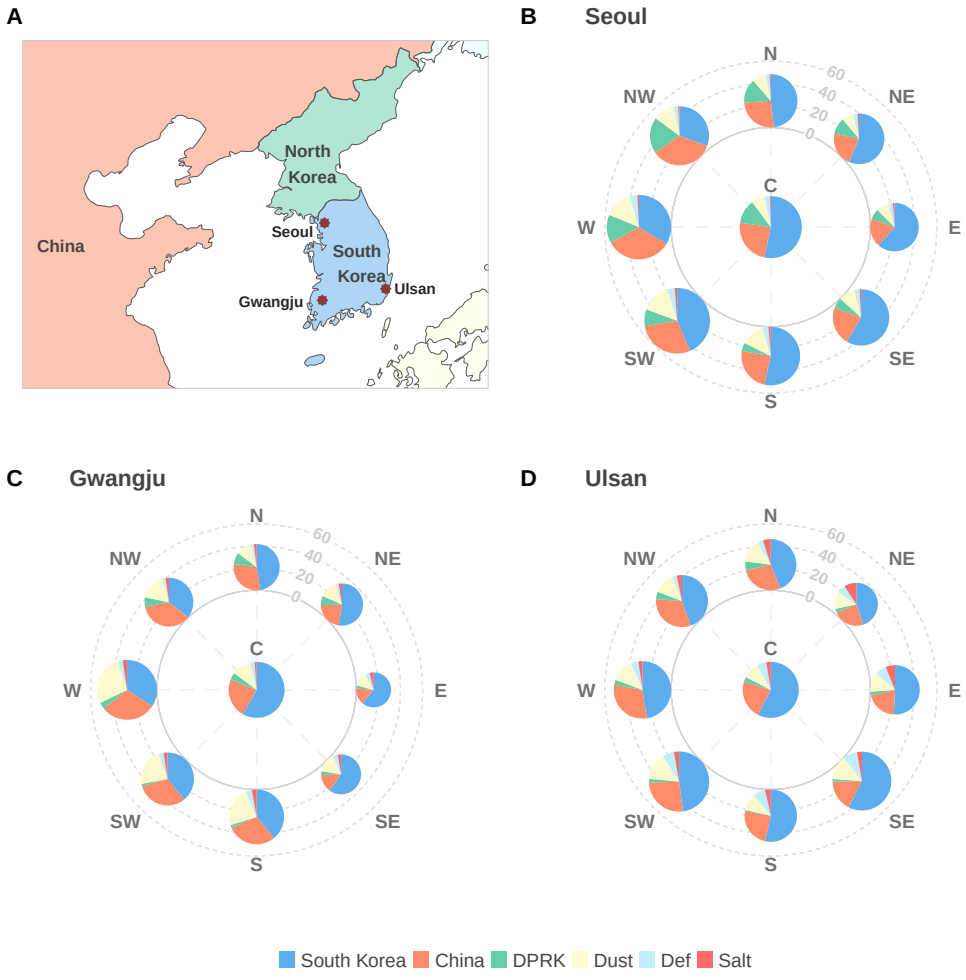

Figure 2.3: PM10 Origin Decomposition by Wind Direction in Selected Cities

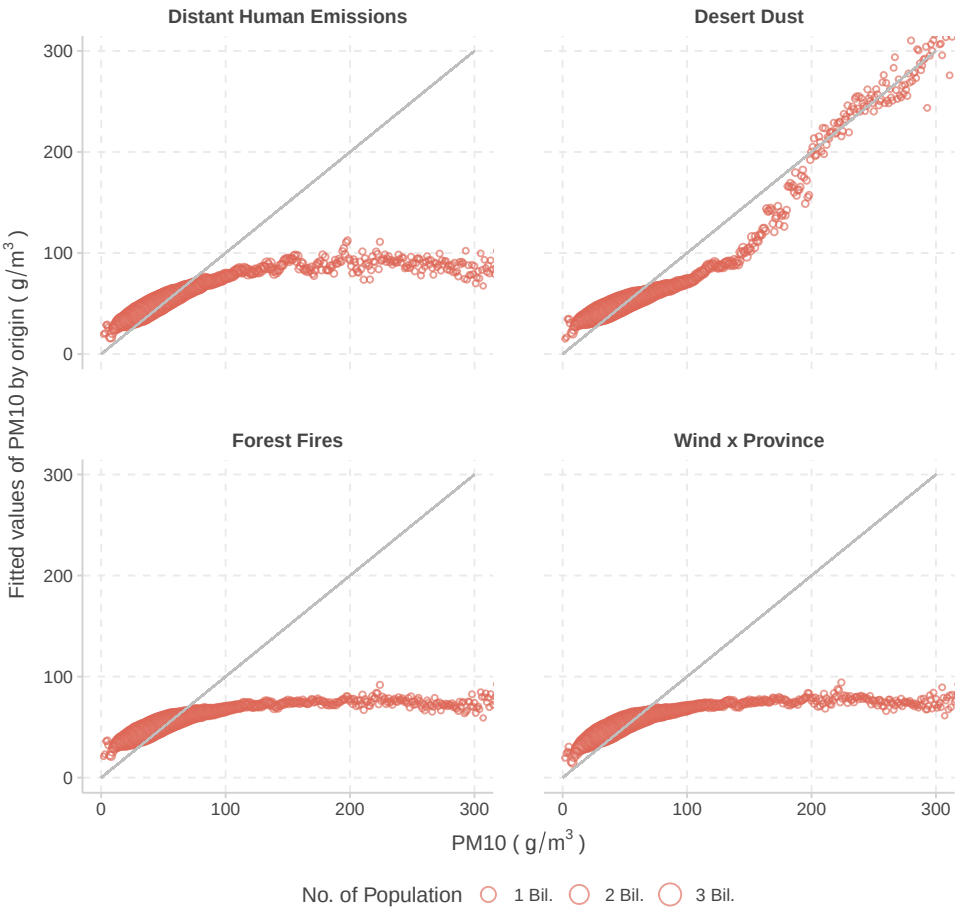

Figure 2.4: Comparison of Fitted and Actual Values

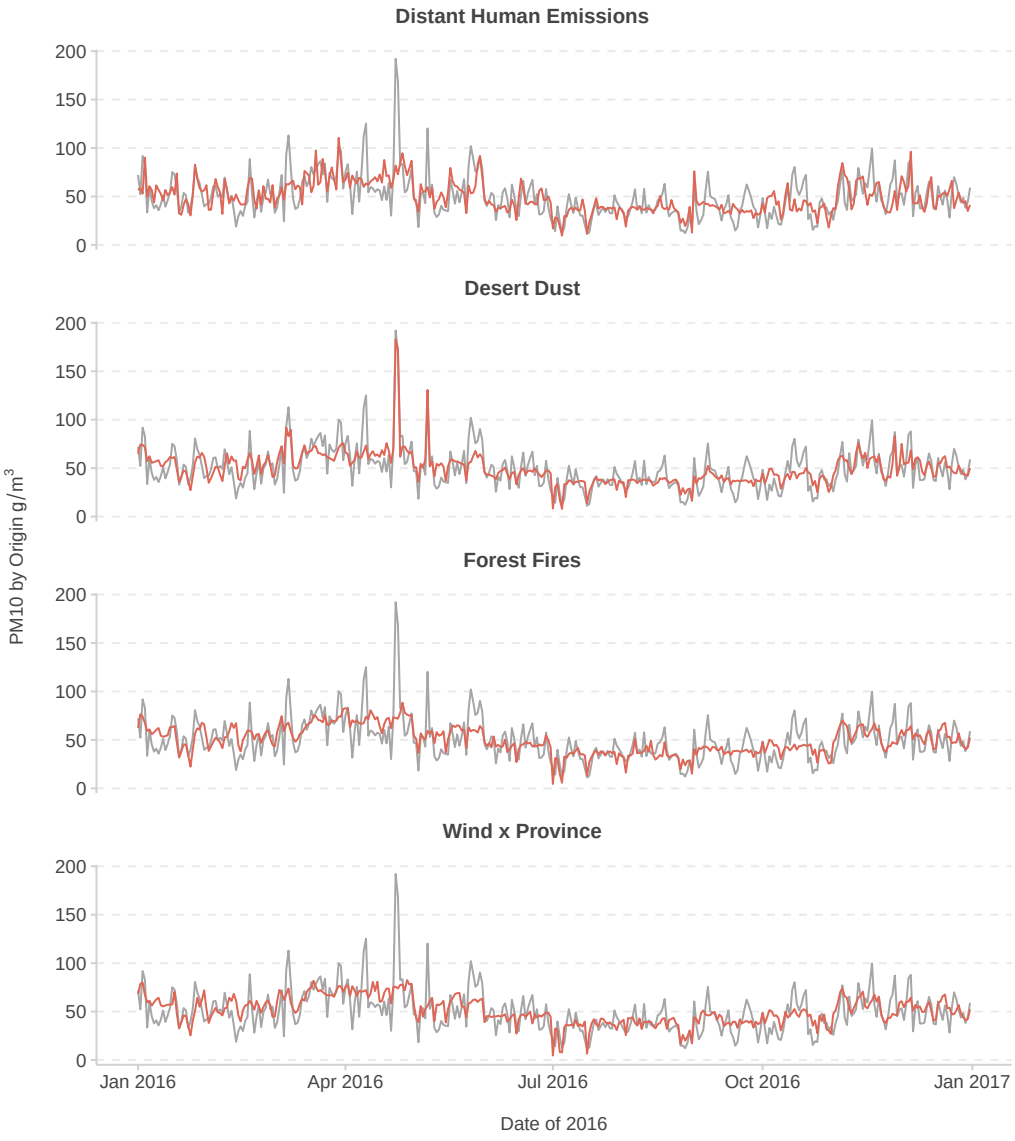

Figure 2.5: Comparison of Fitted and Actual Values in a District in Busan by Date in 2016

Table 2.1: Summary Statistics

	Mean	St. Dev.	Min	Max
Health Outcome				
Respiratory Expenditure (USD per capita)	0.569	0.203	0.012	2.498
Age Groups				
Minors (0−19)	0.760	0.291	0.015	3.935
Adults (20−64)	0.365	0.140	0.005	1.266
Older Adults (≥65)	0.612	0.269	0	3.502
PM Variables				
PM10 ($\mu g/m^3$)	51.251	30.513	2.030	1,022.278
Anthropogenic PM Sources	42.206	21.252	0.507	195.110
ROK	23.208	17.297	0	164.348
China	13.893	14.507	0	170.951
DPRK	4.023	7.164	0	103.587
Other Countries	1.082	3.183	0	74.843
Non-Anthropogenic PM Sources	9.034	20.446	0	952.813
Desert Dust	6.285	19.865	0	951.445
Forest Fires	1.663	4.404	0	103.686
Salt	1.086	1.849	0	78.950
Control Variables				
Temperature (°C)	13.029	9.970	−19.100	33.200
Precipitation (mm)	3.507	13.331	0	449.500

Notes: The number of observations is 600,119. All the variables are aggregated daily by district. The number of districts is 137, and the period of analysis is 2005−2016. Some of the districts have observations fewer than 12 years since air quality monitors were installed more recently in those districts. We excluded districts with fewer than three-year observations. For the Korean Won (KRW) and US Dollar (USD) conversion, the exchange rate of 1175 KRW:1 USD was used.

Table 2.2: First-stage Result Comparison

	Instrumental Variables			
	Distant Human Emissions	Desert Dust	Forest Fires	Wind Direction **x** Region
First-Stage Dependent: PM10 ($\mu g/m^3$)				
All Groups[(a)]	0.893 (0.032)	1.049 (0.020)	0.584 (0.060)	_[(b)]
Adjusted R^2	0.385	0.677	0.271	0.284
No. of Obs.	600,119			

Notes: (a) The results for each of the sub-population groups – minors, adults, and older adults – are in the appendix. (b) 17 wind-related indicators (16 directions and a no-wind dummy) interacted with district dummies were included. District, year-by-month, and province-by-month fixed effects are controlled. Linear and quadratic precipitation and temperature terms are included but not reported. Observations are weighted with district-level population. Standard errors are noted with parentheses. Errors are clustered by day of sample and district.

Table 2.3: Results of Respiratory Health Outcome Analysis

		Instrumental Variables			
	OLS[a] Benchmark	Distant Human Emissions	Desert Dust	Forest Fires	Wind Direction **x** Region
Reduced Form					
All Groups	0.006	0.0004	−0.006	0.063	_[b]
	(0.004)	(0.009)	(0.005)	(0.020)	
Minors (0−19)	0.005	−0.002	−0.007	0.091	_[b]
	(0.006)	(0.013)	(0.007)	(0.032)	
Adults (20−64)	0.004	0.002	−0.004	0.034	_[b]
	(0.003)	(0.006)	(0.004)	(0.012)	
Older Adults (≥65)	0.009	0.020	−0.003	0.019	_[b]
	(0.005)	(0.011)	(0.008)	(0.021)	
2SLS					
All Groups	0.006	0.0005	−0.006	0.104	−0.017
	(0.004)	(0.001)	(0.005)	(0.035)	(0.016)
Minors (0−19)	0.005	−0.002	−0.006	0.150	−0.014
	(0.006)	(0.015)	(0.007)	(0.057)	(0.023)
Adults (20−64)	0.004	0.003	−0.004	0.057	−0.014
	(0.003)	(0.007)	(0.004)	(0.019)	(0.009)
Older Adults (≥65)	0.009	0.023	−0.003	0.031	−0.020
	(0.005)	(0.013)	(0.008)	(0.034)	(0.016)
No. of Obs.	598,392				

Notes: The unit of the dependent variable is US Cent (1 USD = 1,175 KRW, therefore 1 US Cent = 11.75 KRW).(a) For the OLS benchmark, the results using the reduced form and those using 2SLS are the same. (b) 9 wind-related indicators (8 directions and a no-wind dummy) interacted with province dummies were included. District, year-by-month, and province-by-month fixed effects are controlled. Linear precipitation and temperature terms are included but not reported. Observations are weighted with district-level population. Standard errors are noted with parentheses. Errors are clustered by day of sample and district.

Table 2.4: Comparison of the Estimated Impacts of 10-unit PM Mitigation Efforts

		Instrumental Variables			
Million USD	OLS Benchmark	Distant Human Emissions	Desert Dust	Forest Fires	Wind Direction **x** Region
All Groups	−10.6	−0.9	+10.5[(a)]	**−194.0**[(b)]	+10
Minors (0−19)	−1.8	+0.8	+2.3	**−53.8**	−0.9
Adults (20−64)	−4.8	−3.5	+5.2	**−70.5**	+8.8
Older Adults (≥65)	**−2.4**	**−5.9**	0.7	−8	+2.3

Notes: (a) A plus sign implies that the 10-unit abatement of the annual average PM level would lead to deterioration of health outcomes: the increase of respiratory illness-related spending. (b) The results that are statistically significant at least at 10% are in bold.

Returning to the core objective of alleviating public health burdens, the next chapter delves into the role of information disclosure, specifically focusing on air quality warnings.

Chapter 3

Bounds, Benefits, and Bad Air: Welfare Impacts of Pollution Alerts

3.1 Introduction

Air quality alert systems, which notify individuals of unhealthy pollution levels, are widespread throughout the world and cover over 1.7 billion people. For example, the United States (US) Environmental Protection Agency (EPA) manages the Air Quality Alert Program in the New England Area, and California air quality districts each run their own alert systems. In the United Kingdom, the Department for Environment, Food, and Rural Affairs issues pollution alerts. In Beijing, environmental authorities enacted a four-tier warning policy in 2013, expanded nationwide in 2014, and the South Korean government in 2015 launched a new air quality alert system (AQAS) as well (see Appendix Table C1 for additional examples). These programs encourage the public to wear particulate-filtering masks, stay indoors, and reduce strenuous activities to mitigate health damages from air pollution.

Despite their increasing popularity, there has been little empirical analysis of the welfare impacts of these programs. In this work, we exploit the structure of the South Korean AQAS to estimate a regression discontinuity (RD) design using pollution measurements as the running variable. Combining economic theory with our estimates, we establish a lower bound on the health-related net benefits of the AQAS and an upper bound on the operating costs. This yields lower bounds on net benefits and benefit-cost ratios. Importantly, our estimates are net of the welfare loss

due to avoidance behavior.

Our analysis contributes directly to two strands of literature. The first strand focuses on the health impacts of air-quality alerts. In seminal work, Neidell (2009a) exploited high-frequency time-series variation to demonstrate that minors with asthma benefited from ozone alerts via a decrease in Los Angeles inpatient hospital admissions due to breathing difficulties. Janke (2014) generalized these results to England and further established an effect on emergency department (ED) admissions for minors. H. Chen et al. (2018) found marginally significant reductions in asthma-related ED visits in Toronto due to alerts.[1] Mullins and Bharadwaj (2015) and Aguilar-Gomez (2020) demonstrated that when combined with driving restrictions, environmental warnings reduced elderly mortality in Chile and ED visits in Mexico City, respectively.

The second emerging strand examines the effects of air pollution information on welfare measures. Ito and Zhang (2020) found that the willingness to pay for air purifiers in China increased following the 2013 disclosure of air-quality information by the US Embassy in Beijing. Barwick et al. (Conditionally accepted) demonstrated that avoidance behaviors, such as air purifier sales and the timing of credit-card purchases, changed in response to the Chinese government providing real-time air quality monitoring data to the public. Gao, Song, and Timmins (2021) exploited the disclosure of PM2.5 data in China to estimate the impact of relaxing information constraints on hedonic valuation.

More generally, our paper contributes to a broad literature exploring the value of information provision to the public. Previous studies found that public information provision can affect behavior in many contexts, including restaurant hygiene (Jin and Leslie 2003), sales taxes (Chetty, Looney, and Kroft 2009), calorie labeling (Bollinger, Leslie, and Sorensen 2011), restaurant quality (Anderson and Magruder 2012), and toxic releases (Mastromonaco 2015). Further, targeting of information may affect choices in a variety of contexts as well, from school choice to health insurance to electricity consumption (Hastings and Weinstein 2008; Kling et al. 2012; Ito 2014; Jessoe and Rapson 2014). It also relates to work on establishing bounds for welfare analysis in situations with limited information (Manski et al. 1997; Finkelstein and Hendren 2020; Kang and Vasserman 2021).

Finally, our paper is relevant to a series of studies investigating potential efforts to manipulate pollution information for political or economic gain. Several stud-

[1] A related body of research explores who responds to air quality alerts but does not estimate effects on health outcomes (Noonan 2014; Ward and Beatty 2016; Saberian, Heyes, and Rivers 2017).

ies found evidence that particulate matter (PM) measurements cluster right below politically-significant thresholds, compliance with which is important for government officials' promotions (Andrews 2008; Y. Chen et al. 2012; Ghanem and Zhang 2014; Zou 2021). Recent work demonstrated that reported PM concentrations increased following the automation of pollution monitoring (Greenstone, He, Jia, et al. 2021). Though our analysis does not focus on the manipulation of air pollution observations, our results demonstrate the potential welfare consequences of such information distortion.

We make several contributions to the literature. First, our work represents, to the best of our knowledge, the first welfare analysis of these widespread alert systems (as opposed to general air-quality monitoring). This contribution is possible because we analyze health expenditures, rather than raw visit counts or deaths, and we apply a theoretical framework that, combined with our novel health expenditure data, allows us to estimate sharp lower bounds on benefits that are net of the costs of avoidance behavior.[2] Second, while previous work on the benefits of alert systems exploited time-series or panel variation, we implement a RD design to study health-related outcomes.[3] Finally, while most analyses of AQASs have occurred in developed countries, the pollution levels in our study region are more representative of developing and middle-income countries.[4]

3.2 Background and Data

South Korea is an advanced economy that nevertheless suffers from high levels of particulate pollution. According to the Organization for Economic Cooperation and

[2]In much of the existing literature on air quality alerts, the avoidance behavior is the object of interest, but its welfare impact cannot be quantified. Barwick et al. (Conditionally accepted) addresses avoidance behavior costs by estimating two specific types of avoidance behavior: air purifier purchases and outdoor shopping trips. These behaviors are less relevant to air quality alerts since air purifiers are durable goods, and many of the benefits of alerts accrue to minors.

[3]The one exception we are aware of is H. Chen et al. (2018), which implements a RD to study health outcomes. Their study appears underpowered, however, yielding a single significant t-statistic of exactly 2.0 across 12 outcomes tested, with no visual evidence of a break for any health outcome. Ito and Zhang (2020) exploits a spatial pollution discontinuity at the Huai River, but the study's effect of information disclosure is identified using a post-2013 indicator. Neidell (2009a), Neidell (2010), and Liu, He, and Lau (2018) estimate RD designs in the context of avoidance behavior.

[4]The only AQAS studies in developing and middle-income countries that we are aware of are Mullins and Bharadwaj (2015), Aguilar-Gomez (2020), and Rivera (2021), all of which establish impacts of driving restrictions but cannot reject the null hypothesis that alerts in isolation have no effects.

Development (OECD), South Korea's level of PM2.5 (particulates less than 2.5 micrometers in diameter) is the highest among all OECD countries. The average PM2.5 concentration level recorded in 2015 was over 30 $\mu g/m^3$, while the mean of other member countries was under 15 $\mu g/m^3$ (Organization for Economic Cooperation and Development 2018). In response, the South Korean government launched a new air quality alert system in 2015. The primary objective of the alert system is to reduce negative health effects by providing citizens with the necessary information to take precautionary measures.

Municipal governments of major cities issue the alerts. When the level of PM2.5 or PM10 exceeds a certain threshold in an alert region within a city, the local government announces a PM warning for the region (Figure 3.1). Citizens are encouraged to curtail outdoor activities, wear face masks, drinking water, and use public transportation (Table 3.1). Authorities disseminate public health warnings through mass media (e.g., radio, television, and online news articles), public road signs, and wireless services (text messages and mobile applications).

Given the widespread dissemination, most people are likely informed when air quality warnings are issued. To determine whether citizens are more cognizant of air quality when alerts are issued, we analyzed internet search keywords in NAVER, a search engine accounting for 75% of all web searches in South Korea. The keywords include three phrases: (i) air pollution alert; (ii) particulate matter; and (iii) air quality. Figure 3.2 indicates that searches for these keywords increased dramatically during the days on which alerts were issued.

PM alerts are triggered based on hourly monitor readings of PM2.5 and PM10. When the new alert system began, both the 24-hour average and the 2-hour minimum values served as measurement criteria for issuing the alerts. After about a year, the Ministry of Environment (MOE) settled on the 2-hour minimum value as the sole standard. Advisories were then issued when the hourly average PM2.5 (PM10) in an alert region was over 90 $\mu g/m^3$ (150 $\mu g/m^3$) for two consecutive hours (Table 3.1). These advisories remained in effect until the 1-hour level of PM2.5 (PM10) dropped below 50 $\mu g/m^3$ (100 $\mu g/m^3$).[5] We retrieved the alert information from the website of the Korea Environment Corporation (KECO). There were a total of 412 region-days

[5]When the level of PM is more extreme, governments issue a second-level warning. The PM thresholds are 180 $\mu g/m^3$ and 300 $\mu g/m^3$ for PM2.5 and PM10, respectively. Our identification strategy utilizes observations around the threshold of the first-level warnings, as second-level warnings are rare. Therefore, we use terms such as advisory, alert, and warning interchangeably to indicate the first-level warning. Also note that in July 2018, the PM2.5 thresholds for issuance and cancellation were lowered to 75 $\mu g/m^3$ and 35 $\mu g/m^3$, respectively. This date lies outside of our analytic data set.

or 2,562 district-days with alerts during 2016–2018, the coverage period of our health spending data.[6] While alerts are relatively infrequent in this context (e.g., occurring on approximately 5% of potential district-days), the PM levels that trigger alerts are not uncommon in other Asian countries. For example, PM2.5 levels in Delhi exceeded the alert threshold on approximately 80% of days during our sample (Sharma and Mauzerall 2022), and PM2.5 levels in Beijing exceeded the threshold on the majority of days during our sample.

Our health spending data cover daily per-capita spending by district in 2016 and 2017.[7] The dataset comes from the National Health Insurance Service (NHIS) of South Korea, which covers the country's entire population (all individuals must join). Our data represent a 10% random sample of insurance subscribers in seven major cities: Seoul, Busan, Daegu, Daejeon, Incheon, Gwangju, and Ulsan. Their combined population is 23 million, or 44% of the population of South Korea. Hence, our dataset includes about 2.3 million individuals. We requested separate spending measures by disease type (cardiovascular disease and respiratory disease) and age group (minors: 0−19; adults: 20−64; and older adults: 65 and older).[8] We focused on respiratory and cardiovascular diseases because air pollution should directly affect the respiratory system, and previous work has established high-frequency temporal associations between PM and cardiovascular morbidity and mortality (Pope and Dockery 1999). The health spending data are summarized in Table 3.2.

Our data cover most healthcare expenditures, including outpatient care (e.g., clinics and doctors' offices), hospitals (inpatient and emergency department visits), public health centers, and most prescription medications. Three features are noteworthy. First, while the data include inpatient hospital visits (i.e., overnight stays), there is often a temporal gap of a week or more between the onset of symptoms and an inpatient admission, as an inpatient hospitalization requires several rounds of referrals for all but the most acute cases. As the temporal unit of our data is daily, we exclude spending on inpatient stays from our analysis to reduce the noise in our dependent variable.

Second, we further exclude outpatient visits to tertiary hospitals in our primary analysis. In the South Korean healthcare system, outpatient visits to primary (clin-

[6]Our dataset includes 73 districts across 14 alert regions.

[7]Due to privacy concerns, the dataset can be used only in selected data centers in South Korea. Furthermore, NHIS does not allow the sharing or publication of any type of processed data, except for summary statistics, figures, and regression results.

[8]Cardiovascular diseases are those in the "I" category according to the International Classification of Diseases, 10th revision (ICD-10). Respiratory diseases are those in the "J" category according to ICD-10.

ics) and secondary facilities (hospitals and general hospitals) typically do not require referrals, but visits to tertiary general hospitals do (see Appendix Table C3 for definitions of these institutions). The referral process leads to a delay between the onset of symptoms and actual outpatient visits, and our main dependent variables accordingly exclude tertiary visit healthcare costs. Nevertheless, we test the robustness of our results to this exclusion by running regressions that include tertiary outpatient visits. The results are qualitatively similar to the main results, with coefficients and standard errors of generally comparable magnitudes.

Third, our health expenditure data consist of the sum of private copayments and public coverage. Therefore, our regression coefficients can be interpreted as changes in total health expenditures in the covered categories. It is worth noting that the out-of-pocket payment ratio ranges from 10% to 50%, implying substantial coverage by the social health care system (see Appendix Table C4 for details on insurance coverage by treatment location). Overall, the South Korean healthcare system subsidized 70% of the total healthcare spending on outpatient visits. We thus interpret 70% of the spending to represent external costs from the patient's perspective.

The final primary data set in our analysis is a credit card spending data set provided by one of the largest credit card companies in South Korea, whose market share is approximately 25%. We use these data to look for evidence of avoidance behavior. The data include daily per capita credit card consumption expenditures of members at the district of residence level.[9] The consumption data sets cover the same spatial boundaries and seven metropolitan cities as the healthcare expenditure data, but the coverage dates (2017−2018) differ. We test the RD validity assumptions — e.g. treatment discontinuity, control continuity, and manipulation of the running variable — separately for this different coverage period.

Our credit card data set covers a range of spending categories. Examples include larger retailers (e.g. department stores, large-sized supermarkets, and electrical appliance stores) and smaller retailers (e.g. grocery stores, bakeries, butcher shops, dollar stores, convenience stores, clothing stores, cosmetics shops, and eyewear shops). Entertainment, sports, and leisure activities, such as transactions in movie theaters, art exhibitions, museums, karaoke, bowling alleys, fitness centers, swimming pools, golf courses, and indoor golf driving ranges, are also included in our credit card expenditure data set. In addition, our data set includes expenditures in restaurants and bars.

[9]Due to privacy concerns, our consumption data sets are not accessible on an individual member basis. Instead, they are aggregated to the district-by-day level, across multiple spending categories, and then divided by the number of active members in each district, thus providing information on the card consumption expenditures per person.

In the data extraction procedure, we requested the exclusion of selected categories — specifically, cars, furniture, and spending on educational institutions. Spending in these categories is high variance and seems unlikely to be related to daily variation in pollution information, potentially increasing noise in the dependent variable. Spending on medical expenditures was also excluded to avoid duplication between the card spending data and the medical expenditure data; the national health insurance data set provides a more complete accounting of health expenditures.

In addition to the credit card expenditure data aggregated across different consumption categories, we obtained information on expenditures per member for four selected consumption categories: restaurants and bars, fashion outlets, and travel accommodations. The first category, restaurants and bars, represents one of the most frequently occurring daily consumption activities and accounts for a significant portion of daily card transactions (almost 30%). In contrast, spending on fashion outlets represents less frequent consumption activities. However, fashion stores in South Korea are typically situated in outdoor marketplaces, and we thus expect them to be more susceptible to the impact of air quality information disclosure. Conversely, we anticipate the impact on the travel and accommodations spending category to be minimal since most of these expenditures are booked in advance and difficult to change. The third panel in Table 3.2 presents summary statistics of card expenditures per member for the different categories.

While credit and debit cards are not the only forms of payment, in South Korea they account for a majority of expenditure-weighted transactions. According to the Bank of Korea, in 2019 credit cards accounted for 53.8% of expenditures, followed by cash (17.4%), debit cards (15.3%), bank transfers (8.0%), and mobile payments (3.8%). Credit and debit cards thus comprise approximately 70% of payments during our sample period.

3.3 Theoretical Framework

We develop a parsimonious model of an individual's avoidance behavior to motivate and interpret our empirical analysis. Consider a representative individual i choosing an activity level a. The individual gains utility from activities that involve pollution exposure and loses utility from getting sick. Her utility function is:

$$U_i(a_i, pm) = b_i(a_i) - s_i^{pvt} p_s(a_i, pm) \tag{3.1}$$

where $b_i(a)$ represents the benefits of activity level a, s_i^{pvt} represents the private costs (pecuniary and non-pecuniary) of getting sick, and $p_s(a, pm)$ represents the

probability of getting sick given activity level a and PM level pm. One could imagine more general utility functions — e.g. pm could affect b as well — but to motivate our bounding exercise this model suffices.

To interpret our RD estimand, note that it compares days on which the PM level is just above the alert threshold ($pm \downarrow c$) to those on which it is just below the alert threshold ($pm \uparrow c$). Thus, pm itself remains approximately constant near the threshold c (confirmed in Appendix Table C5), but perceived PM, denoted as pm_i, changes.[10] Specify individual beliefs as

$$pm_i = \begin{cases} pm^{avg} & \text{if} \quad pm = pm \uparrow c \\ pm^{hi} & \text{if} \quad pm = pm \downarrow c \end{cases}$$

where pm^{avg} represents average PM conditional on being below the threshold c and pm^{hi} represents average PM conditional on being above the threshold c. For our bounding exercise we assume that $pm^{hi} \approx c$, or at least that $|pm^{hi} - c| << |pm^{avg} - c|$. This representation is a reasonable approximation of our actual PM data.[11] More generally, the approximation only needs to be sufficiently accurate that the alerts do not cause individuals to behave *less* optimally than they would absent the alert's information.[12]

Individuals maximize utility by choosing activity levels $a_i = \text{argmax}_a \, U_i(a, pm_i)$. Then

$$U_i = \begin{cases} U_i(a_i(pm^{avg}), c) & \text{if} \quad pm = pm \uparrow c \\ U_i(a_i(pm^{hi}), c) & \text{if} \quad pm = pm \downarrow c \end{cases}$$

An individual's private change in utility from PM crossing the alert threshold is

[10] In our actual data, the hourly PM level is distinct from the running variable, as the latter depends on the maximum 2-hour minimum PM level. For notational simplicity, we treat PM as the running variable in the theoretical model, but in Appendix C.1 we show that our conclusions generalize to a model in which the running variable is a function of PM.

[11] For example, in our PM2.5 data, $pm^{avg} = 22.7$, $pm^{hi} = 66.7$, and $c = 57.5$. Thus pm^{hi} is much closer to c than pm^{avg} is. In this context c represents the average PM2.5 level when the running variable is close to the threshold, which differs from the running variable itself (see previous note).

[12] Of course, if individuals already have accurate information on PM levels (e.g. via real-time monitoring), then alerts will have no impact on behavior, and our research design should estimate null effects. In that case we would correctly conclude that the alerts generate no benefits.

$$\Delta\ U_i = U_i(a_i(pm^{hi}), c) - U_i(a_i(pm^{avg}), c) = \\ [b_i(a_i(pm^{hi})) - b_i(a_i(pm^{avg}))] - s_i^{pvt}[p_s(a_i(pm^{hi}), c) - p_s(a_i(pm^{avg}), c)]. \tag{3.2}$$

Naturally $\Delta\ U_i \geq 0$ since $pm^{hi} \approx c$ and $a_i = \text{argmax}_a\ U_i(a, pm_i)$ — i.e. more accurate PM information can only (weakly) increase the individual's utility — but accurately quantifying $\Delta\ U_i$ is challenging even with good data on s_i^{pvt}. This challenge arises because it is difficult to estimate $b_i(a_i)$, the benefits of different activities (and thus the costs of avoidance behaviors). In particular, a_i may be high dimensional, and researchers rarely have data on all, or even most, elements of a_i.

To motivate our welfare-bounding exercise, consider the public net benefits of the individual's choices:

$$W_i = U_i(a_i, pm) + E_i. \tag{3.3}$$

W_i, the social welfare accruing from i's choices, equals private welfare U_i plus the externalities associated with i's choices, E_i. Then

$$\Delta\ W_i = \Delta\ U_i + \Delta\ E_i. \tag{3.4}$$

Since $\Delta\ U_i \geq 0$, $\Delta\ E_i$ represents a lower bound on the social net benefits of crossing the alert threshold. By aggregating $\Delta\ E_i$ across individuals and alert days, we can estimate a lower bound on the gross social benefits of the alert system. Combined with data on the costs of the system, we can estimate lower bounds on benefit-cost ratios. Importantly, as established in Equation (3.2), these bounds are already net of any individual costs of avoidance behavior, e.g. choosing to avoid outdoor events or keeping a vulnerable child home from school.

One caveat for this result is that if authorities or event organizers engage in mass avoidance behavior by canceling outdoor events in response to alerts, then $\Delta\ U_i$ need not be weakly positive, as some individuals would then be engaging in involuntary avoidance behavior. In our specific context, this issue does not arise, as we estimate effects of "Level 1" alerts that correspond to modestly elevated pollution levels and do not trigger large-scale cancellations.[13] In other contexts, however, researchers

[13]We conducted extensive searches for any instances of pollution-related events or school cancellations. The small number of examples of event cancellations that we found, such as several baseball games in 2018 and 2021, were in response to PM levels many times higher than the first-level alert

applying this framework would need to confirm that involuntary avoidance behavior is not enforced, or that enforcement of such behavior does not result in negative private net benefits (i.e., on average $\Delta\ U_i$ is non-negative).

For the bound to be nontrivial, the researcher must have data on meaningful externalities associated with individuals' choices. In our context, health expenditures — the majority (about 70%) of which are reimbursed by public funds — represent such an externality.[14]

3.4 Regression discontinuity design

We employ a RD design to estimate the causal impact of PM alerts on health spending. The RD focuses on the point where the running variable (RV) exceeds a threshold at which the probability of treatment changes discontinuously. The identifying assumption is that the only difference between observations right above and below the threshold is the assignment of the treatment; other factors affecting the outcome are continuous around the threshold. It then follows that we can attribute the discontinuous change of the outcome variable to the treatment assignment.

In this paper, the issuance of advisories corresponds to the treatment, with health spending as the outcome. The running variable is the daily maximum of 2-hour minimum PM values. For example, in the case of PM2.5, an advisory occurs when the PM2.5 level is over 90 $\mu g/m^3$ for two consecutive hours. Hence, when the 2-hour minimum exceeds 90 $\mu g/m^3$, the alert triggers. We calculate the daily maximum of these hourly 2-hour minimum values and code the running variable at the daily level (for a given region).

As discussed in Section 3.2, there are two pollutants that trigger the issuance of alerts, PM2.5 and PM10. Following Cattaneo et al. (2020), we calculate the daily maximum of 2-hour minimum values for PM2.5 and PM10, normalize them by their respective thresholds (90 $\mu g/m^3$ and 150 $\mu g/m^3$), and take the larger one as the assignment variable for the RD. By doing so, we construct one normalized assignment

threshold that we study (Yoo 2021). Even at the second-level alert threshold, schools may only receive, at most, non-compulsory recommendations for closure (Ahn and Dabee 2018).

[14]Our bounds are conservative in that they ignore the marginal cost of public funds (Dahlby 2008). Incorporating a positive marginal cost of public funds would increase the estimated net benefits.

variable whose treatment threshold is zero (Table 3.1).[15] This running variable is similar to the minimum distance to the nearest threshold elucidated in Cattaneo et al. (2020).

The running variable does not perfectly determine alert issuance for (at least) two reasons. First, municipal governments also consider weather conditions when determining whether to announce an alert. Thus alerts are not issued on some days on which the normalized running variable exceeds zero. Second, the thresholds for issuance and cancellation are different. For example, suppose that an alert was issued at 2 PM Monday, when the 2-hour minimum PM2.5 exceeded 90 $\mu g/m^3$. If the hourly PM2.5 level remains at 60 $\mu g/m^3$ until the end of Tuesday, the alert remains in effect through Tuesday, as the PM2.5 cancellation threshold is 50 $\mu g/m^3$. Nevertheless, the normalized running variable for Tuesday is -30. For these reasons, we estimate a fuzzy RD (FRD) design.[16]

After setting a bandwidth h around the threshold, we retain observations with running-variable values falling within h units of the threshold. We run the following first-stage and reduced-form regressions:

$$Alert_{it} = \gamma_1 \mathbb{1}(\widetilde{PM}_{it} \geq 0) + \gamma_2 \widetilde{PM}_{it} + \gamma_3 \widetilde{PM}_{it} \mathbb{1}(\widetilde{PM}_{it} \geq 0) + \boldsymbol{X_{1it}\theta}_1 + \boldsymbol{X_{2t}\phi}_1 + \boldsymbol{\delta_{1i}} + u_{it} \tag{3.5}$$

$$Y_{it} = \beta_1 \mathbb{1}(\widetilde{PM}_{it} \geq 0) + \beta_2 \widetilde{PM}_{it} + \beta_3 \widetilde{PM}_{it} \mathbb{1}(\widetilde{PM}_{it} \geq 0) + \boldsymbol{X_{1it}\theta}_2 + \boldsymbol{X_{2t}\phi}_2 + \boldsymbol{\delta_{2i}} + \varepsilon_{it} \tag{3.6}$$

Y_{it} represents health expenditures per person or credit card expenditures per person in district i on day t, $\widetilde{PM}_{it}$ is the normalized running variable (described above), and $Alert_{it}$ is an indicator variable for an air-quality alert. $\boldsymbol{X_{1it}}$ includes temperature and precipitation controls, $\boldsymbol{X_{2t}}$ includes year-month, day-of-week, and holiday fixed effects, and $\boldsymbol{\delta_i}$ are district fixed effects.[17] While these controls are not strictly necessary for identification, they substantially improve the precision of our

[15] For additional details on calculating the running variable, see Appendix C.2.

[16] A concern may arise regarding the discrepancy between the thresholds of issuance and cancellation. To address this concern, we also present FRD results without these cases, and these results are comparable to our baseline FRD estimates (see Appendix Table C10).

[17] In the case of credit card expenditure, we added a before-holiday fixed effect that indicates whether day t is a day before a holiday since consumption increases substantially not only on holidays but also before the holidays.

regressions (Cellini, Ferreira, and Rothstein 2010).[18] We population weight our regressions to make the estimates more representative and further improve precision,[19] and we cluster the standard errors by running variable value or date to account for spatial correlation in alerts and health spending across districts.[20] When discussing t-statistics, to be conservative we default to whichever of the two standard errors is larger.

To estimate the FRD and recover the local average treatment effect (LATE), we divide $\hat{\beta}_1$ by $\hat{\gamma}_1$, yielding:

$$\hat{\tau}_{FRD} = \frac{\hat{\beta}_1}{\hat{\gamma}_1} \tag{3.7}$$

In practice we estimate $\hat{\tau}_{FRD}$ using two-stage least squares (2SLS). Equations (3.6) and (3.7) estimate the contemporaneous effect of an alert on health expenditures. The panel nature of our data, however, introduces additional considerations that are absent from most cross-sectional RDs. First, the asymmetry in the thresholds for issuance and cancellation ensures that many air quality alerts last for two to three consecutive days.[21] One could thus conceptualize the treatment as a single 48- to 72-hour alert. Second, the possibility of dynamic effects represents a potential violation of the stable unit treatment value assumption (SUTVA) — the treatment on day t could have spillover effects on the outcome on day $t+1$.

We address this complication in two ways. First, as a robustness check, we trim the estimation sample to exclude days following a day with an air quality alert. This estimation sample yields similar results. Second, while the contemporaneous regressions (Equations (3.6) and (3.7)) appear to generate estimates that are internally valid (based on the results referenced above), they may yield an incomplete picture of the total effect of an air quality alert. In particular, they do not capture any dynamic effects of an alert that persist beyond one day. In principle, these effects could shift the net impact in either direction. For example, if avoidance behavior

[18] The adjusted R^2 in our main outcome regressions is in the range of 0.8 to 0.9 (Tables 3.4 and 3.5), implying that including the controls reduces the standard errors by a factor of 2 to 3.

[19] For the card expenditure analysis we weight by the number of members.

[20] Unlike typical panel data sets, serial correlation over time has little impact in our context, because the independent variable of interest, $\gamma_1 \mathbb{1}(\widetilde{PM}_{it} \geq 0)$, exhibits very modest time-series correlation. Clustering by district (to account for time-series correlation) generates much smaller standard errors, and two-way clustering by district and date generates standard errors that are similar in size to clustering by date.

[21] Out of the total 134 region-by-alert episodes, 45 episodes were single-day alerts, and the remaining 89 warnings were issued for two days or more in a row.

yields health benefits beyond 24 hours, the dynamic effects could increase the net impact. Alternatively, if individuals intertemporally substitute activities, resulting in higher-than-average activity on the day after an alert, then accounting for dynamic effects could decrease the net impact.

To capture dynamic effects, we estimate an alternative fuzzy RD that specifies the dependent variable as a rolling 3-day sum of health expenditures. Specifically, we estimate the reduced-form regression as:

$$Y_{it}^{+} = \beta_1 \mathbb{1}(\widetilde{PM}_{it} \geq 0) + \beta_2 \widetilde{PM}_{it} + \beta_3 \widetilde{PM}_{it} \mathbb{1}(\widetilde{PM}_{it} \geq 0) + \boldsymbol{X_{1it}\theta}_2 + \boldsymbol{X_{2t}\phi}_2 + \boldsymbol{\delta_{2i}} + \varepsilon_{it} \tag{3.8}$$

Y_{it}^{+} represents health expenditures or credit card expenditures in district i on days t, $t+1$, and $t+2$ (i.e. $Y_{it}^{+} = \sum_{s=0}^{2} Y_{it+s}$). Other variables remain as defined before, and we continue to population weight the regression. Since the treatment is effectively a multi-day alert (given the asymmetry of the activation and cancellation thresholds), we also estimate a specification in which we omit treated days whose previous dates were also treated with an air quality alert. For example, if an alert was issued on January 1 and 2, January 2 is omitted to avoid "double counting" the alert's impact when conducting policy simulations in Section 3.6.[22]

Before presenting the estimates, we note two details about the FRD regressions. First, FRD estimates may be sensitive to the polynomial degree of the running variable. For robustness, we also check results using a specification with a quadratic in the running variable.[23] Second, the FRD results may be sensitive to the choice of bandwidth, h. To find a default bandwidth for our analysis, we follow Calonico, Cattaneo, and Titiunik (2014, 2015) (CCT). The CCT criteria yield optimal bias-corrected bandwidths ranging from 17 to 22 for our dataset (Appendix Table C6), so we chose $h = 20$ as the default bandwidth. To demonstrate robustness, however, we report results from bandwidth choices of 16, 20, and 24.

[22] As an alternative strategy, we considered supplementing Equation (3.6) with lagged values of the treatment, similar to the "one-step" estimator in Cellini, Ferreira, and Rothstein (2010). This specification, however, would require us to trim the sample on multiple dimensions. For example, with two lagged values of treatment, we would need to trim the estimation sample based on the contemporaneous running variable and one- and two-day lags of the running variable. In practice, this would reduce our estimation sample to an impractical degree. Given that almost all treatment episodes consist of two consecutive days of alerts, we chose to instead sum the outcome over several days and regard each episode of two-day treatments as a single treatment. This strategy also avoids the need to consider different sequences of treatments (Lechner 2009; Anderson 2017).

[23] Following the arguments in Gelman and Imbens (2019), we do not try higher-order polynomials in the running variable.

3.5 Results

Contemporaneous effects

Figure 3.3 plots treatment probability by the running variable using a binned scatter plot.[24] The figure demonstrates a large discontinuity in the probability of treatment around the RD threshold. Table 3.3 presents corresponding first-stage estimates of Equation (3.5) for three bandwidth choices (16, 20, and 24). Crossing the RD threshold corresponds to an approximate 60 percentage point increase in the probability of an alert. This discontinuity is robust to the choice of bandwidth and highly significant in all cases, with F-statistics between 25 and 50. There is no significant "first-stage" effect on average PM levels (Appendix Table C5), however, which is consistent with the lack of any binding alert-associated restrictions on activity or emissions. We thus interpret our RD health effects as resulting purely from avoidance behavior rather than from reductions in ambient pollution levels.

Figure 3.4 plots health expenditures, converted to spending per capita in US cents, by the running variable using a binned scatter plot. The left panels present respiratory-illness expenditures, while the right panels present cardiovascular-illness expenditures. From top to bottom, the panels present expenditures for minors (under age 20), adults (age 20-64), and older adults (over age 64).

The top-left panel reveals a sharp decline in respiratory expenditures for minors at the RD threshold, and a notable, though less pronounced, decline in these expenditures for adults. In contrast, there is less evidence of a decline for older adults. The top-right panel reveals no change in cardiovascular expenditures for minors, likely because cardiovascular diagnoses are rare for this age group. The middle-right and bottom-right panels, however, reveal drops in cardiovascular-illness expenditures for adults and older adults at the RD threshold.

Tables 3.4 and 3.5 present corresponding reduced-form and 2SLS estimates of Equations (3.6) and (3.7) for the preferred bandwidth of $h = 20$. Table 3.4 reports results for respiratory disease, while Table 3.5 reports results for cardiovascular disease. In each table, the top panel presents reduced-form estimates (i.e. estimates corresponding to Figure 3.4), and the bottom panel presents 2SLS estimates. Each

[24]For the 2017−2018 data, Figure C3 presents an analogous plot, which shows a clearer discontinuity around the threshold.

column corresponds to a different age group: minors, adults, older adults, and all ages.

The tables confirm the patterns observed in Figure 3.4. In Table 3.4, an alert induces a highly significant decrease in respiratory-illness expenditures for minors ($t = -3.2$). The point estimate implies a reduction of 15 cents per capita, or approximately 30% percent of mean expenditures below the RD threshold.[25] For older age groups the change in respiratory-illness expenditures is insignificant at the RD threshold. Nevertheless, the overall reduction in respiratory-illness expenditures at the threshold is statistically significant ($t = -2.4$).

In Table 3.5, an alert induces significant decreases in cardiovascular-illness expenditures for adults (age 20-64) and older adults ($t = -2.9$ and $t = -2.5$ respectively). The point estimates imply reductions of 2.8 and 9.6 cents per capita respectively, or about 23% and 14% of mean expenditures below the RD threshold. For minors, there is no significant change in cardiovascular-illness expenditures at the RD threshold. The overall reduction in cardiovascular-illness expenditures at the threshold is statistically significant ($t = -3.0$), however.

Figure 3.5 presents an outcome discontinuity plot for credit card spending data that is analogous to Figure 3.4. The top-left panel plots expenditures aggregated across all spending categories. The top-right, bottom-left, and bottom-right panels represent restaurant and bar, fashion store, and travel accommodation expenditures respectively. There is some evidence of a drop in total credit card expenditures at the discontinuity threshold. The change in restaurant and bar expenditures is not as pronounced at the threshold, but there is a sharp decline in fashion outlet expenditures at the threshold. This drop is consistent with the outdoor and discretionary nature fashion outlet expenditures. In contrast, the travel accommodations category does not display any discontinuous decrease at the threshold. This null effect is consistent with the significant cost of canceling these expenditures on short notice and also suggests that alert days are not unusual in an *ex ante* sense.

Table 3.8 reports the results of FRD regressions with credit card expenditures as the outcome. These results confirm the patterns visible in Figure 3.5. We observe significant negative impacts of air pollution alerts on restaurant and fashion outlet expenditures. The overall impact of an alert on expenditures is -25.7 US cents per person (-3.8%); however, the point estimate does not reach statistical significance.[26]

[25] When calculating percentage effects, we take the mean of the dependent variable when the running variable lies between -20 and 0.

[26] While it does not reach significance, the point estimate is of the same magnitude as the result

The effect on restaurant expenditures, reported in Column (2), is −12.4 US cents per person (−6.6%, $t = -2.6$). An alert decreases fashion store expenditures by −3.0 US cents per person (−11.3%, $t = -3.1$). Travel accommodation expenditures increase by a statistically insignificant 0.9 US cents per person (3.6%, $t = 0.8$).

Dynamic effects

Air pollution alerts may have lagged effects — either because an alert lasts more than one day or because avoidance behavior yields dividends over multiple days — further decreasing healthcare costs beyond the dates of alert issuance. It is also possible that the healthcare costs rebound, attenuating the magnitude of the decreases demonstrated in Tables 3.4 and 3.5. To incorporate lagged effects into our analysis of social net benefits, we estimate FRD regressions with a rolling sum of 3-day healthcare expenditures as the dependent variable (Equation (3.8)).

Table 3.6 reports results from estimating Equation (3.8). The coefficient magnitudes are larger than the corresponding coefficients presented in Tables 3.4 and 3.5, by factors ranging from 2.5 to 2.8 when focusing on all age groups and the first row of each sub-panel. The larger magnitudes can be partially explained by the nature of the South Korean AQAS, where many alerts last for at least one day beyond the initial date of issuance. Indeed, 80 of 134 unique alerts were issued for more than one day, and the average number of days per alert is approximately 1.87. Nevertheless, this figure cannot fully explain the differences in the magnitudes mentioned above, which hints at potential lagged decreases in healthcare costs even after an alert expires.

To avoid double counting benefits when we conduct policy simulations, the estimation sample for the second row in each panel of Table 3.6 omits alert days on which the previous day was covered by an alert.[27] In general, the coefficients decrease in size; nevertheless, they are still approximately comparable in overall magnitude. Compared to the results in the first rows, the overall effects decrease by 8% to 19%. Compared to estimates of contemporaneous effects, the coefficients are 2.2 or 2.5 times larger — figures above 1.87, or the average number of days per alert.

in Barwick et al. (Conditionally accepted), which finds that, following monitoring programs, a doubling of air pollution reduces credit card transactions by three percentage points.

[27]Consider an alert that lasts for two consecutive days. If both days from the alert are within the analysis bandwidth (defined by PM levels), the 3-day impacts of both alert days would be counted separately even though there is a two-day overlap between the two 3-day sums of healthcare spending. By dropping alert days that immediately follow an alert day, we filter out any secondary sets of overlapping 3-day sums for that particular alert.

Lagged effects are also possible with credit card expenditures, since consumers may intertemporally substitute their consumption activities. Table 3.9 presents results from estimating Equation (3.8) using credit card spending. The first row reports coefficients larger than those in Table 3.8, but no coefficient reaches statistical significance. In contrast to the health expenditure analysis, estimating coefficients while eliminating alert days that immediately follow another alert day yields different point estimates — the coefficient magnitudes decrease to near zero for restaurant and fashion outlet expenditures. Overall these results suggest that consumers may engage in some intertemporal substitution, which would reduce the net impact of air pollution alerts on consumption activities.[28]

Robustness

We first test the robustness of our results by incorporating health expenditures from outpatient visits to tertiary hospitals. The medical referral process, which is required when visiting a tertiary hospital, generates a gap between the onset of symptoms and actual outpatient visits. We excluded those visits in our main analysis to clearly identify the immediate impacts of the AQAS, and we do not expect their inclusion to qualitatively change our main results since these expenditures comprise less than 15% of the total outpatient expenditures. Tables C7 and C8 confirm that our estimates are robust to the inclusion of tertiary outpatient visits. The coefficients and standard errors are of similar magnitudes to the analogous estimates in Tables 3.4 and 3.5.

Table 3.7 estimates a variety of alternative specifications to demonstrate the robustness of our results to specification choices. The most important modeling choice in most RD studies is the bandwidth for the local linear regressions. The first three rows in each table present reduced-form estimates utilizing bandwidths of 16, 20 (our baseline specification), and 24.[29] In the top panel of Table 3.7, the magnitude and significance of respiratory-illness effects for minors and all age groups remain stable across all bandwidths. In the bottom panel, cardiovascular-illness effects for both adult groups and all ages are statistically significant for the smaller bandwidth, in line with the main results, but they become insignificant for the larger bandwidth.

[28] In the context of our model, intertemporal substitution in consumption activities reduces the sensitivity of $b(a)$ to a, if a represents activity for a single day. Alternatively, if consumption activities feature perfect intertemporal substitution over a several day period, then a could represent activity summed over several days.

[29] 2SLS estimates are identical to the reduced-form estimates after rescaling coefficients and standard errors by 1.6, as the first-stage estimates are insensitive to bandwidth choice.

We note, however, that the motivation for choosing a larger bandwidth is to trade off increased bias for a smaller standard error; in this context the standard error actually rises with the bandwidth, likely due to the increased mean-squared error associated with higher pollution levels (see Figure 3.4), suggesting little gain from using a larger bandwidth. Appendix Table C9 reports analogous results for the dynamic effects specification; for both disease categories, the pooled age-group results remain statistically significant at all three bandwidths (16, 20, and 24).

Another concern in our context is the timing of advisories. In some instances, alerts may be triggered early in the morning but cancelled by 9 am; in others they may not be triggered until the evening. In either case, we would not expect the alerts to have meaningful effects on behavior. The last row in both panels of Table 3.7 filters out days with alerts cancelled before 9 am or triggered after 7 pm. As expected, the coefficients become slightly larger in magnitude and remain statistically significant.

In Appendix C.3, we report a wide range of alternative specifications and robustness checks for the main results. Briefly, we find no visual evidence of manipulation of the running variable near the RD threshold (Appendix Figures C1 and C2) or a discontinuity in the control variables (Appendix Figure C6).[30] Removing alert days on which the air quality warning was issued too late or too early yields similar results, as does accounting for the asymmetry in thresholds for alert issuance and cancellation (Appendix Table C10). We demonstrate that controlling for a quadratic of the running variable, a quadratic of the temperature variable, or the air quality variables (PM10, PM2.5, PM10 and PM2.5, and the Air Quality Index (AQI)) does not change our main conclusions (Appendix Tables C11 and C12). Our findings are also robust to using alternative sets of time fixed effects (Appendix Table C11) or clustering at different levels (Appendix Table C13). To test for spatial spillovers of alerts, we estimate the FRD regressions with the largest running variable observed in an adjacent alert region; Appendix Table C14 finds no effect of an adjacent region's alert on the focal region's health expenditures. Finally, we perform falsification tests by changing the RD threshold by 20, 30, or 50 units from the true threshold; Appendix Table C14 demonstrates no statistically significant results at these placebo thresholds.

We conduct similar robustness checks for the credit card expenditure results. The first three rows of Table 3.10 present coefficients and standard errors with dif-

[30] We also conducted the statistical manipulation test based on a local polynomial density estimation technique proposed by (Cattaneo, Jansson, and Ma 2018) and does not reject the hypothesis that the density of the score does not change discontinuously at the cutoff point. For 2016−2017, the p-values are 0.509, 0.554, and 0.690 for the bandwidths 16, 20, and 24, respectively. For 2017−2018, the corresponding p-values are 0.248, 0.257, and 0.206, respectively.

ferent bandwidths. The restaurant and fashion outlet results remain significant for all bandwidths, though they decrease in magnitude for wider bandwidths. The fourth row shows the results estimated with data that filter out days with advisories issued too late or canceled too early. The estimates are similar to Table 3.8. The fifth row uses only data from before the change in the threshold for PM2.5 advisories at the end of June 2018. Again the estimates are similar to Table 3.8.

3.6 Discussion

We highlight several of our empirical findings. First, our results provide new insights on responses across broader disease categories. Previous studies on air pollution alerts have primarily analyzed respiratory symptoms — Neidell (2009a) found effects on asthma-related hospitalizations, and Janke (2014) found effects on respiratory emergency admissions.[31] Our findings suggest that effects are not limited to respiratory diagnoses, as cardiovascular disease spending of adults also decreased significantly. At the same time, our credit-card spending results corroborate previous findings that alerts can induce avoidance behavior for certain activities (Neidell 2009a; Janke 2014).

Second, our results yield novel findings of alerts' effects for adults. Neidell 2009a and Janke 2014 found statistically significant impacts of air quality warnings for the youngest ages.[32] In contrast, our results reveal that the benefits of air quality warnings may not be restricted to minors. While minors' health spending was reduced by 12.6 million USD, prime-age and older adults also demonstrated significant health expenditure decreases due to alerts, amounting to 20.4 million and 8 million USD, respectively. Our results imply that alerts can motivate all age groups to take appropriate avoidance measures, reducing the negative impacts of air pollution.

Our results represent effects of avoidance behavior, but there are two mechanisms that could underlie these effects. First, avoidance behavior could improve health, reducing expenditures. Second, avoidance behavior could directly reduce healthcare visits if individuals avoid leaving their residences. In theory both mechanisms generate positive benefits via reductions in expenditures, but rescheduling of visits or

[31] H. Chen et al. (2018) also find weak evidence of an effect on asthma-related visits.

[32] Mullins and Bharadwaj (2015) and Aguilar-Gomez (2020) both find effects of pollution warnings on elderly health outcomes. In their contexts, however, the warnings also reduce pollution levels, suggesting a direct effect of pollution on health. Our study estimates the pure effect of alerts on health expenditures, as measured PM does not change at the RD threshold. Furthermore, our welfare analysis framework would not apply to policies which reduce emissions, as these policies entail additional implicit net costs.

longer-term health complications could attenuate the benefits if the second mechanism drives the results.

In practice, the evidence suggests that the first mechanism seems likely to be the primary one. First, we do find evidence of general avoidance behavior in the credit-card spending data — individuals appear to avoid outdoor shopping experiences and, to a lesser extent, dining away from home. This implies that they are not solely avoiding healthcare visits. Second, the multi-day dynamic effects on health expenditures are considerably larger than the contemporaneous effects. For example, if we study only alert episodes with a single alert day, we find 3-day dynamic effects that are 2.8 times larger than contemporaneous effects for youth respiratory expenditures and 6.0 times larger for elderly cardiovascular expenditures. If postponed healthcare visits were the primary mechanism, we would expect the 3-day dynamic effects to be weakly smaller than the contemporaneous effects, as both visit rescheduling and complications from avoided visits would attenuate the first-day effects.

To calculate total benefits from decreased healthcare expenditures, we first tabulate the number of people exposed to the alerts in the seven major South Korean cities. As the FRD estimates measure the reduction in health spending per capita, we multiply the FRD estimates by the population affected by the alerts. Based on the coefficients of spending in the both disease categories across all ages, which sum to 9.1 cents per capita, the total reduction in health expenditures during $2016-2017$ in seven major cities was approximately 41 million USD. This estimate considers only the alerts' contemporaneous effects. Incorporating dynamic effects into the calculation increases the reduction by about one third, for a total reduction in health expenditures of approximately 52 million USD.[33]

Combined with our theoretical framework, the empirical findings presented above can provide a lower bound on the gross benefits from the AQAS. Specifically, our framework implies that the reduction in *public* healthcare expenditures represents a lower bound on the gross benefits of the AQAS. Our health expenditure data contain the sum of private copayments and public coverage, with an approximate ratio of 7:3. Thus, approximately 70% of the FRD coefficients represents a reduction in public expenditures. Applying this share to the total expenditure reductions computed above yields lower bounds on gross benefits that amount to 18.4 million USD (respiratory) and 10.2 million USD (cardiovascular) respectively. Figure 3.6 presents lower

[33]For this calculation we must assume that the benefits of alerts do not decrease as the pollution level rises above the RD threshold, as our RD estimates are local to the RD threshold. This assumption seems plausible, however, as health damages must weakly increase with pollution, so the benefits of avoidance behavior likely increase as well.

bounds on gross benefits by age group, with non-elderly adults realizing the largest gross benefits. Benefits using estimates from the dynamic specification (Table 3.6) are somewhat larger than those using estimates from the contemporaneous specification (Tables 3.4 and 3.5) (24.5 million USD for respiratory and 12.2 million USD for cardiovascular), as the former captures a larger change in health expenditures than the latter.

To quantify AQAS net benefits and benefit-cost ratios, we collected reports on environmental expenditures from the websites of the seven major cities' municipal governments. The cost of managing the alert system in 2017 was estimated at 2 million USD. To be conservative we include a wide range of expenditures in this estimate, from the price of sending alerts via text messages to the maintenance cost of the air pollution monitors.[34] As we could not obtain complete expenditure information for 2016, we assume that costs would be similar to 2017, yielding a total cost of 4 million USD in 2016−2017.[35] The cost is considerably lower than the total health benefit calculated above, 28.6 million USD, yielding an approximate benefit:cost ratio of 7.1:1 and a net benefit of 24.6 million USD for 2016−2017. Incorporating the dynamic effects further increases the net benefits and the benefit:cost ratio to 32.7 million USD and 9.2:1, respectively. [36]

We also explore the potential welfare gains from expanding the alert system's covered range. For this analysis we consider two scenarios. In the first scenario, we assume that advisories are issued on *all* days on which the running variable exceeds zero (i.e. the fuzzy RD becomes a sharp RD). In the second scenario, we assume that the government tightens the advisory criterion for PM2.5 from 90 $\mu g/m^3$ to 75 $\mu g/m^3$ during our analysis period (2016−2017). This corresponds to an actual policy the government enacted starting July 2018. In both scenarios we assume that the magnitudes of the alerts' effects remain similar to our FRD estimates.[37,38]

[34]Appendix Tables C15 and C16 list the expenditure items and the sum of these expenditures by metropolitan city, respectively. See Appendix C.2 for additional details.

[35]Government expenditures may vary year-to-year. We collected similar information for 2018 and found that total 2018 expenditures were approximately 2.8 million USD.

[36]Utilizing the 2018 expenditures as the reference cost leads to the total costs of 5.6 million USD. The corresponding net benefit is about 23 million USD, with a benefit:cost ratio of approximately 5.1:1. When considering dynamic effects, the total net benefit is 31.1 million USD, and the associated benefit:cost ratio is 6.6:1.

[37]Concerns may arise regarding "alert fatigue" in these simulations, as the number of days with alert issuance necessarily increases. It is worth noting, however, that the number of treated days remains modest even in those scenarios. The rates of alert district-days are 2.67%, 2.81%, and 4.57% in the baseline scenario, Scenario A, and Scenario B, respectively. We thus assume that alert fatigue does not become a serious concern in these simulations.

[38]A related concern is that non-advisory days on which the running variable exceeds zero ("non-

We find that expanding the alert system's coverage could yield significant benefits. Figure 3.7 presents net benefits for the baseline scenario and the two alternative scenarios. Issuing alerts whenever the RD threshold is exceeded would have reduced health expenditures by an additional 5.7 million USD (Scenario A) during our sample period, bringing the total reduction to 42.4 million USD (right panel). Lowering the threshold for alert issuance from 90 $\mu g/m^3$ to 75 $\mu g/m^3$ (for PM2.5) would have reduced total health expenditures by 76.5 million USD (Scenario B) during our sample period (right panel), or a 109% increase from the baseline policy. Notably, this corresponds to the current alert criteria, implemented in July 2018. In all scenarios the benefits greatly exceed the costs, indicated by the solid or dashed horizontal lines for comparison.

3.7 Conclusion

Combining our RD estimates with a theoretical framework, we find lower bounds on the benefits of the South Korean air pollution alert system that greatly exceed the costs of operating the system. Given the insignificant changes in average PM levels at the RD threshold, we interpret our results as a "pure" effect of avoidance behavior, rather than a combined effect of avoidance behavior and reduced ambient pollution levels. Our results thus stand in contrast to those from some recent work, which found effects only in contexts in which alerts were combined with policies to reduce ambient pollution levels (Mullins and Bharadwaj 2015; Aguilar-Gomez 2020). Our theoretical framework is likely to prove applicable in other settings in which individuals endogenously respond to information provision but there are substantial externalities. For example, one might bound the welfare benefits of restaurant hygiene grade cards using the reduction in insurance-covered hospitalization costs (Jin and Leslie 2003) or the benefits of electricity usage information using the reduction in environmental damages (Jessoe and Rapson 2014).

Our study also highlights that manipulation of air pollution information for economic and political gains may be costly. If pollution alerts are not issued due to

compliant" days) systematically differ from advisory days on which the running variable exceeds zero ("compliant" days). Indeed, as shown in Table 3.1, weather conditions influence alert issuance. We thus compared precipitation and temperature across non-compliant and compliant days falling within the running variable interval of [0, 40]. Average precipitation and temperature on non-compliant days were 0.65 mm and 3.121 C, respectively, with standard deviations of 5.12 mm and 2.24 C. Average precipitation and temperature on compliant days were 1.215 mm and 7.618 C, respectively, with standard deviations of 6.12 mm and 3.79 C. We assume that these modest meteorological differences would not yield large differences in the alerts' impacts.

manipulation, the public may not engage in welfare-enhancing avoidance behaviors. Despite the alerts' benefits, governments may have incentives to distort air pollution information if they worry about temporary economic declines from decreased outdoor activities (Min 2019). Furthermore, local government officials may have incentives to manipulate air pollution levels for more favorable evaluations (Andrews 2008; Y. Chen et al. 2012; Ghanem and Zhang 2014; Zou 2021). Our findings imply that these distortions can reduce public health and generate additional healthcare expenditures.

A primary limitation of our study is that the results apply specifically to South Korean metropolitan areas. While these areas are economically important in themselves, with a combined population of over 23 million, our estimates may not generalize to other countries. Nevertheless, there are good reasons to believe that our main qualitative finding — an AQAS can generate meaningful welfare gains — applies to other contexts. First, previous studies have found significant reductions in some types of healthcare utilization due to air-quality alerts. For example, Neidell (2009a) found that alert-induced avoidance behavior decreased Los Angeles asthma hospitalizations between 12 and 60 percent, and Janke (2014) found that even alerts for "moderate" pollution levels reduced asthma admissions by 8 percent in England. Furthermore, South Korean healthcare prices are remarkably low by developed-country standards. For example, relative to South Korea, 2016 per capita health expenditures (PPP-adjusted) were 60 percent higher in the United Kingdom, 77 percent higher in France, 113 percent higher in Sweden, and 270 percent higher in the United States (Lorenzoni and Koechlin 2017). Thus, even if avoidance behavior or high pollution levels are less prevalent in other countries than in South Korea, overall impacts on health expenditures may still be of similar magnitude.

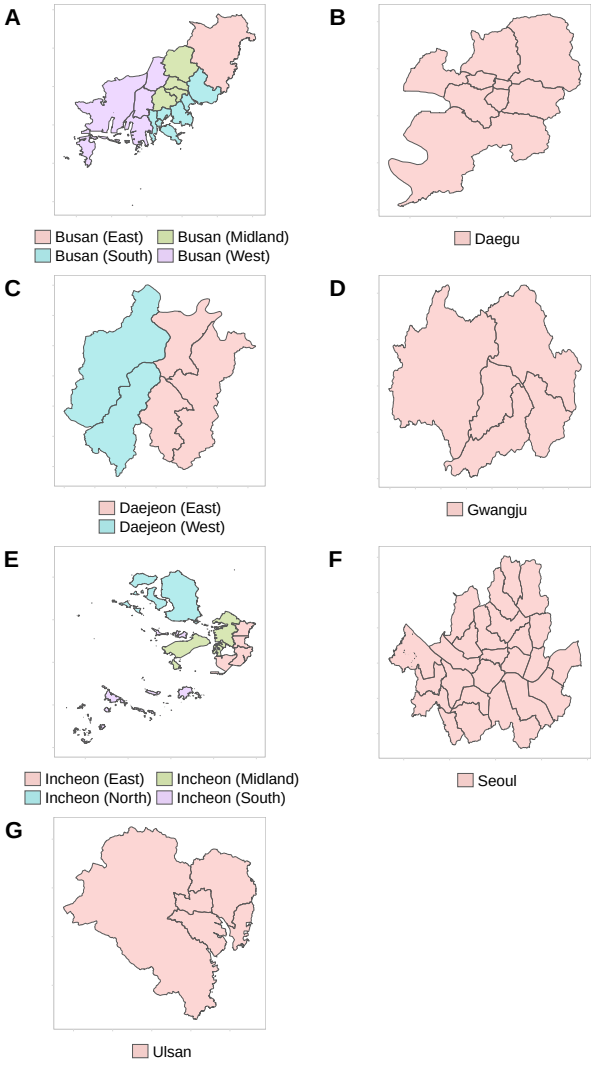

Figure 3.1: Alert Clusters for Seven Major Cities in South Korea

Notes: Panels A through G depict the alert clusters in Busan, Daejeon, Daegu, Gwangju, Incheon, Seoul, and Ulsan respectively. Different colors (in a given city) represent different alert clusters. Border lines separate districts in each major city area.

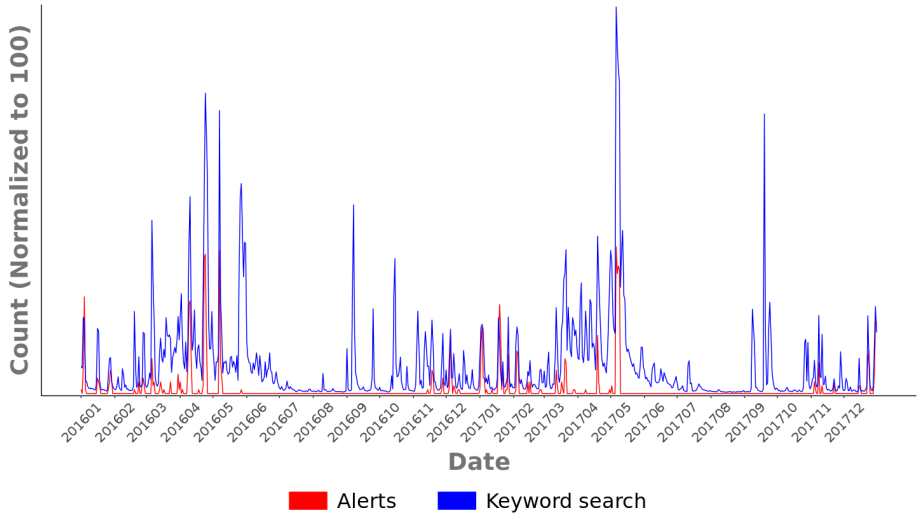

Figure 3.2: Alert counts and keyword search results related to air quality information

Notes: The red series represents the daily count of air quality alerts, and the blue series represents searches for "air pollution alert", "particulate matter", or "air quality" on NAVER. The maximum value of daily keyword search counts is set to 100.

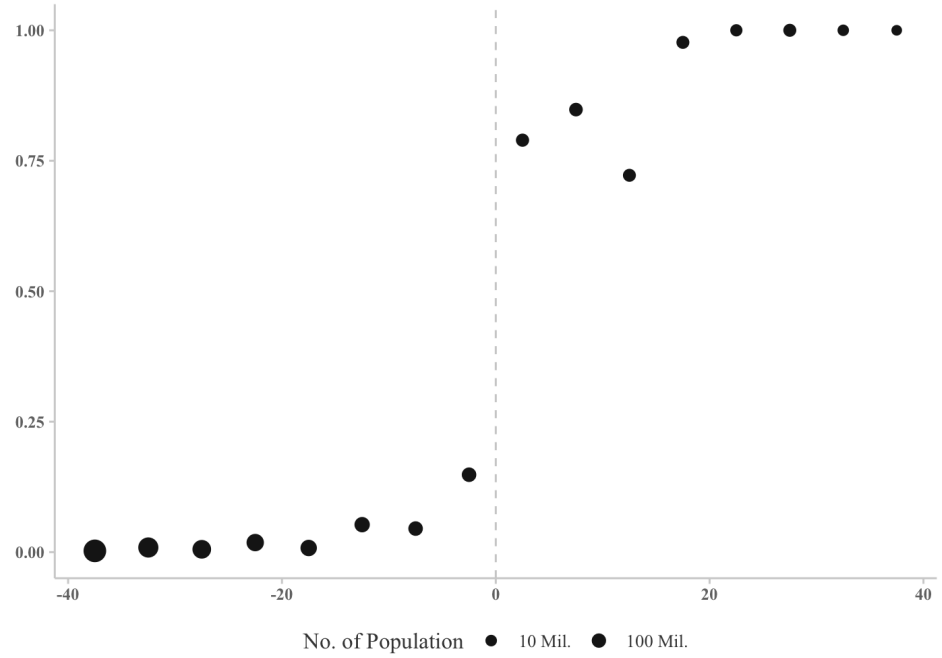

Notes: Each point represents the population-weighted average of observations in a given bin, the width of which is five. The y-axis indicates the average probability of a particulate matter advisory. The x-axis indicates the value of the running variable (a threshold-normalized function of PM).

Figure 3.3: Treatment Discontinuity

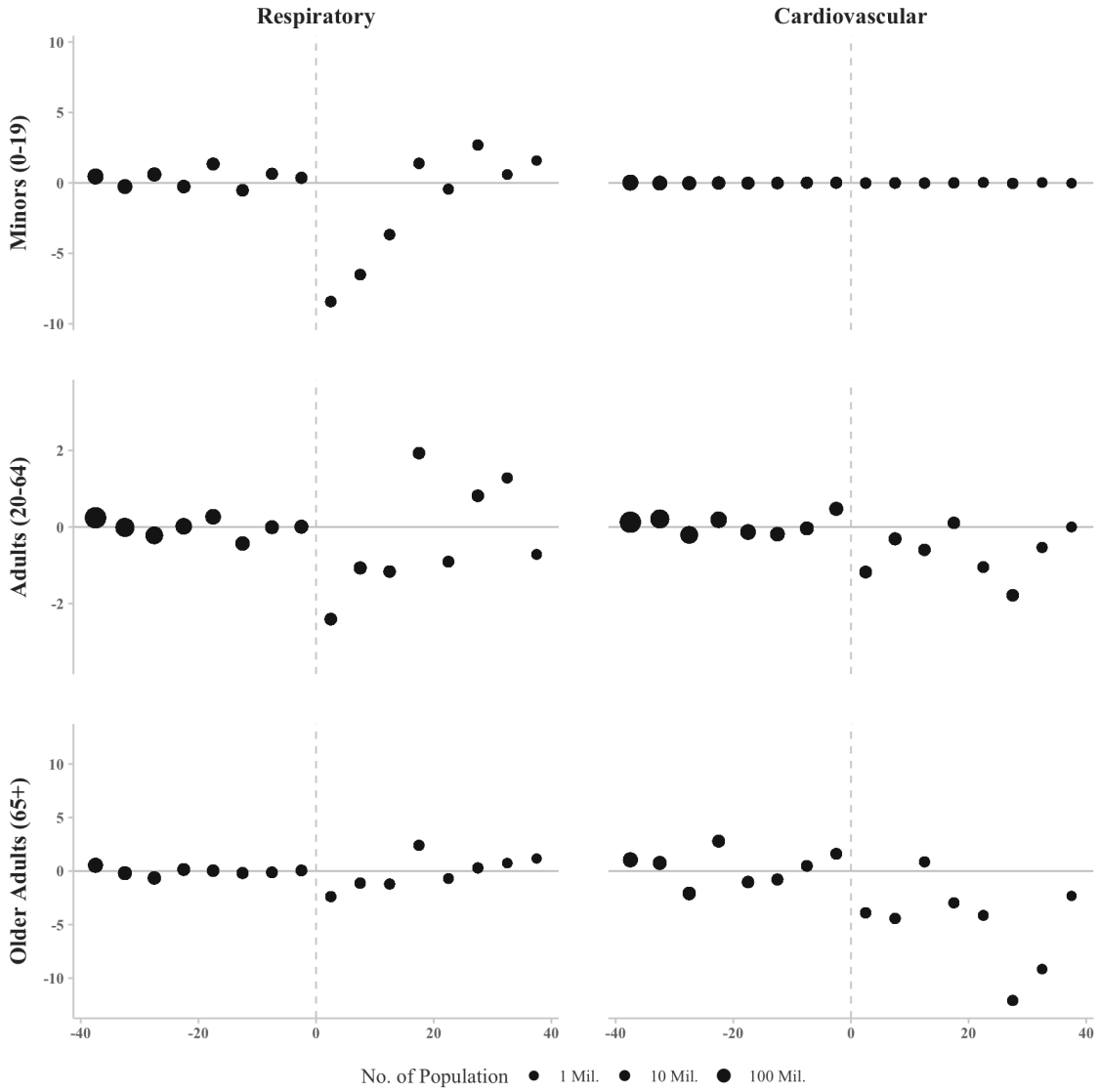

Notes: Each point represents the population-weighted average of observations in a given bin, the width of which is five. The y-axis indicates the per capita level of residualized health expenditures, in US cents (11.5 KRW = 0.01 USD). The residualization was performed with respect to day-of-week, year-by-month, holiday, and district fixed effects. The x-axis indicates the value of the running variable (a threshold-normalized function of PM). The period of the analysis is 2016−2017.

Figure 3.4: Outcome Discontinuity - Health Spending

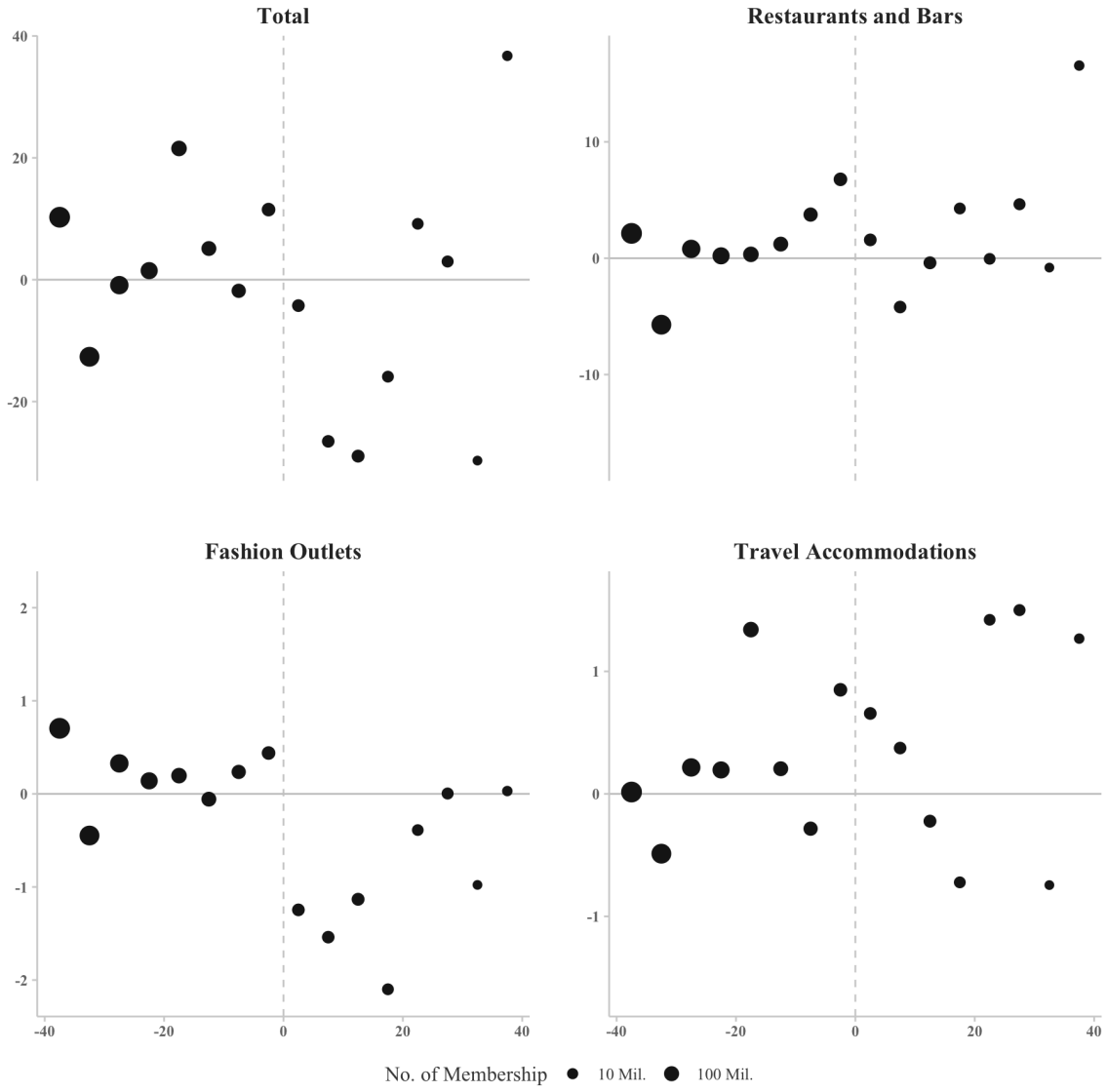

Figure 3.5: Outcome Discontinuity - Credit Card Spending

Notes: Each point represents the number-of-membership-weighted average of observations in a given bin, the width of which is five. The y-axis indicates the per capita level of residualized credit card expenditure, in US cents (11.5 KRW = 0.01 USD). The residualization was performed with respect to day-of-week, year-by-month, holiday, one-day-before-holiday, and district fixed effects. The x-axis indicates the value of the running variable (a threshold-normalized function of PM). The period of the analysis is 2017−2018.

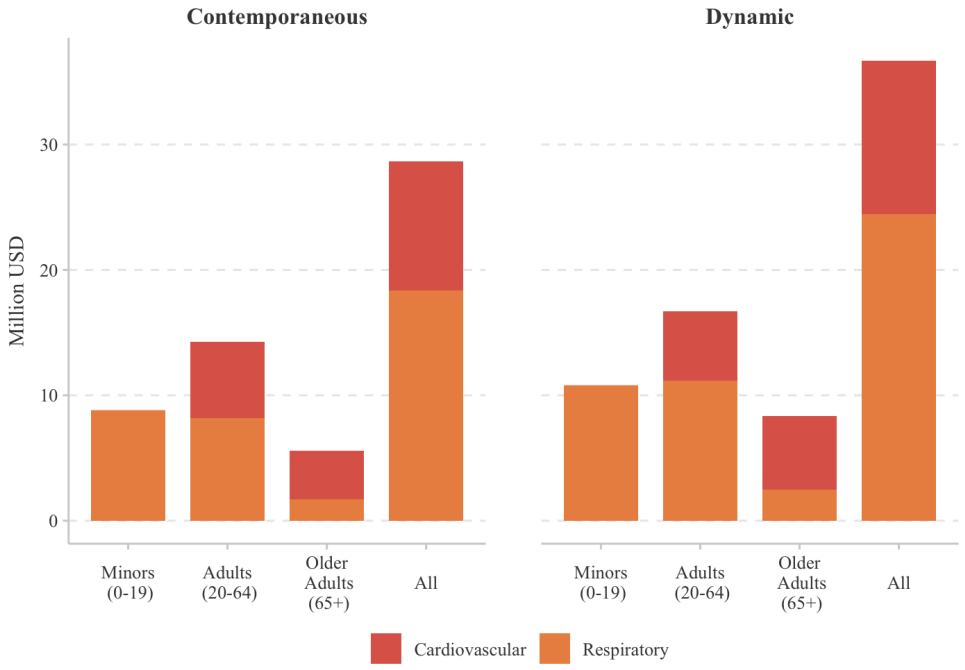

Figure 3.6: Potential Health Benefits by Age Group

Notes: The left (right) panel plots lower bounds on gross benefits by age groups using estimates from Tables 3.4 and 3.5 (Table 3.6). To bound gross benefits we scale the table coefficients by the average share of health expenditures that are publicly covered (70%).

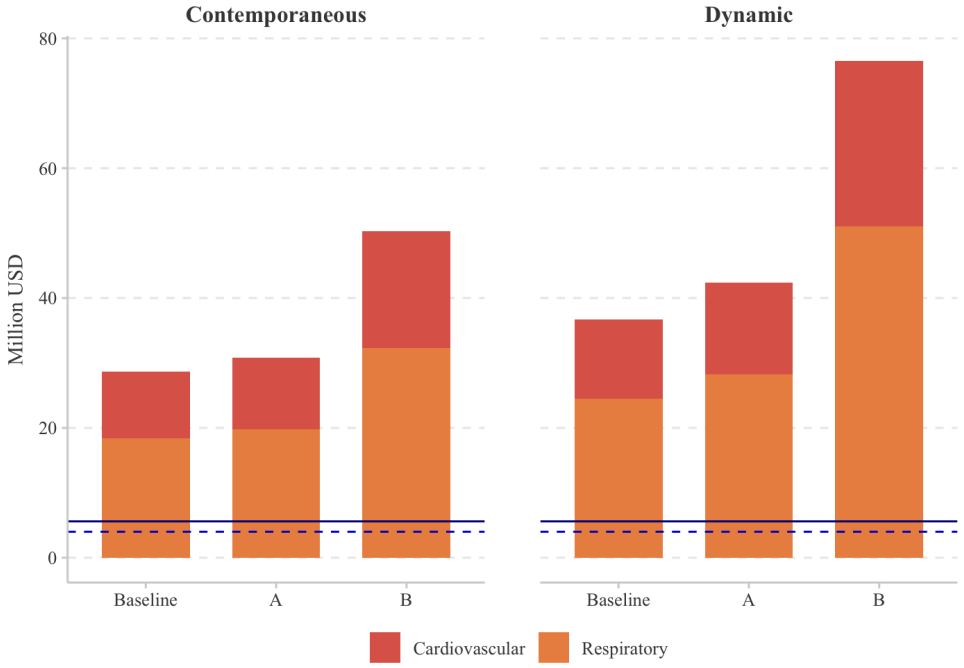

Figure 3.7: Cost-Benefit Comparison and Potential Health Benefits

Notes: The left (right) panel plots lower bounds on gross benefits by scenario using estimates from Tables 3.4 and 3.5 (Table 3.6). To bound gross benefits we scale the table coefficients by the average share of health expenditures that are publicly covered (70%). "Baseline" represents the policy during the sample period, "Scenario A" represents a policy that triggers an alert whenever the running variable crosses the relevant threshold, and "Scenario B" represents a policy that lowers the PM2.5 threshold to the value adopted in July 2018. The solid (dashed) line represents the total system maintenance cost for the analytic period (2016−2017) using 2018 (2017) as the reference year for costs.

Table 3.1: Thresholds and Guidelines of South Korean PM Advisories

	PM Advisory Thresholds	
	PM10	PM2.5
Issuance	Over 150 $\mu g/m^3$ for 2 hours	Over 90 (75)† $\mu g/m^3$ for 2 hours
Cancellation	Under 100 $\mu g/m^3$ for 1 hour	Under 50 (35)† $\mu g/m^3$ for 1 hour
Target Groups	**Guidelines**	
General Population	· Stay indoors and reduce outdoor activities · Wear hygiene masks when you go outside · Reduce emissions (e.g. use public transportation) · Avoid roadways and construction sites	
Children & Teenagers	· Reduce or forbid outdoor classes. · Replace outdoor activities with indoor activities. · Enhance the hygiene management of dining facilities	
The Elderly	· Enhance the hygiene management of dining facilities	

†The numbers in the parentheses indicate the thresholds that were changed after June 28, 2018.
Source: AirKorea, Korea Environment Cooperation
https://www.airkorea.or.kr/, accessed on Sep 30, 2021

Table 3.2: Summary Statistics

	Full Sample				Bandwidth = 40			
Respiratory Expenditures	Mean	SD	Min	Max	Mean	SD	Min	Max
Minors (0−19)	46.0	23.2	0	201.8	50.1	24.9	0	171.6
Adults (20−64)	21.3	14.0	0	239.8	23.3	14.8	0	147.2
Older Adults(≥65)	13.8	7.8	0	59.6	15.2	8.3	0	50.6
Cardiovascular Expenditures								
Minors (0−19)	0.1	1.7	0	316.5	0.1	3.1	0	316.5
Adults (20−64)	12.2	7.5	0	107.6	12.0	7.4	0	107.6
Older Adults(≥65)	65.1	42.7	0	268.9	64.3	42.1	0	248.5
Credit Card Expenditures								
Total	675.2	169.6	0	3,197	676.9	177.6	0	1,713
Restaurants & Bar	189.3	49.4	0	387.5	189.2	52.8	0	381.2
Fashion Outlets	25.8	9.4	0	314.6	26.3	9.5	0	225.2
Travel	25.9	14.0	0	226.1	25.7	14.4	0	144.5
Treatment & Covariates								
Alert	0.03	0.2	0	1	0.1	0.3	0	1
PM10 ($\mu g/m^3$)	44.5	22.0	2.8	253.9	68.4	18.8	19.3	170.3
PM25 ($\mu g/m^3$)	25.1	12.9	1.6	109.5	41.8	13.4	6.6	109.5
Precipitation (mm)	3.1	12.2	0	313.8	1.1	4.5	0	67
Temperature (°C)	13.8	9.9	-16.4	32.5	10.7	8.3	-9.3	32

Notes: The number of district-day observations is 53,363 (73 districts, 761 days, 2016−2017) and 10,547 for the full sample and the sample based on a bandwidth of 40, respectively. The corresponding numbers for the credit card consumption data are 53,290 (73 districts, 760 days, 2017−2018) and 11,324, respectively. Morbidity and credit card spending variables are presented in US cents per capita (11.5 KRW = 0.01 USD). The summary statistics of the treatment variable and other covariates for 2017−2018 are presented in Appendix (Table C2)

Table 3.3: First-stage Regression Results

	Bandwidth		
	16	20	24
$\mathbb{1}(RV >= 0)$	0.636	0.622	0.618
	(0.091)	(0.091)	(0.092)
	[0.122]	[0.114]	[0.110]
Adjusted R^2	0.708	0.720	0.728
F-statistics	46.029	65.351	89.686
N	1,857	2,530	3,380

Notes: This table reports three first-stage estimates of the change in advisory likelihood when the running variable crosses the RD threshold. These estimates are based on coefficients from three separate local-linear regressions, one for each reported bandwidth. The dependent variable in all regressions is an advisory indicator, and the independent variable of interest is an indicator for the running variable being above the RD threshold. All regressions control for the running variable, an interaction between the running variable and the indicator for the running variable being above the RD threshold, temperature, precipitation, and year-by-month and day-of-week fixed effects. The level of observation is the district by day, and observations are population weighted. Parentheses (square brackets) contain standard errors clustered by the running variable (day of sample).

Table 3.4: RD Results for Respiratory Diseases

	Age Group			
	Minors (0-19)	Adults (20-64)	Older Adults (65+)	All
Reduced form				
$\mathbb{1}(RV >= 0)$	−9.412	−2.346	−2.661	−3.624
	(2.326)	(1.391)	(1.674)	(1.437)
	[2.930]	[1.379]	[1.860]	[1.528]
RV	−0.074	−0.041	0.002	−0.038
	(0.143)	(0.043)	(0.062)	(0.056)
	[0.140]	[0.045]	[0.069]	[0.057]
RV $\cdot \mathbb{1}(RV >= 0)$	0.645	0.214	0.167	0.270
	(0.167)	(0.113)	(0.129)	(0.110)
	[0.225]	[0.078]	[0.108]	[0.088]
2SLS				
$\mathbb{1}(RV >= 0)$	−15.03	−3.777	−4.303	−5.829
	(4.709)	(2.195)	(2.753)	(2.397)
	[5.674]	[2.127]	[2.804]	[2.495]
RV	0.039	−0.013	0.035	−0.006
	(0.204)	(0.062)	(0.084)	(0.084)
	[0.170]	[0.055]	[0.083]	[0.071]
RV $\cdot \mathbb{1}(RV >= 0)$	0.596	0.204	0.156	0.254
	(0.243)	(0.112)	(0.127)	(0.120)
	[0.305]	[0.078]	[0.106]	[0.105]
Adjusted R^2	0.836	0.866	0.797	0.893
N	2,530			

Notes: This table reports results from four reduced-form local-linear regressions (top panel) and four 2SLS local-linear regressions (bottom panel). The dependent variable in all regressions is respiratory disease expenditures for the relevant age group, measured in cents per capita (11.5 KRW = 0.01 USD), and the independent variable of interest in the reduced-form (2SLS) regressions is an indicator for the running variable being above the RD threshold (advisory indicator). All regressions control for the running variable, an interaction between the running variable and the indicator for the running variable being above the RD threshold, temperature, precipitation, and year-by-month and day-of-week fixed effects. The level of observation is the district by day, and observations are population weighted. Parentheses (square brackets) contain standard errors clustered by the running variable (day of sample). The bandwidth is set to 20 in all regressions.

Table 3.5: RD Results for Cardiovascular Diseases

	Age Group			
	Minors (0-19)	Adults (20-64)	Older Adults (65+)	All
Reduced form				
$\mathbb{1}(RV >= 0)$	−0.025	−1.757	−5.962	−2.026
	(0.021)	(0.513)	(2.070)	(0.573)
	[0.022]	[0.481]	[2.250]	[0.622]
RV	0.003	0.056	0.234	0.066
	(0.001)	(0.023)	(0.102)	(0.024)
	[0.001]	[0.020]	[0.113]	[0.026]
RV $\cdot \mathbb{1}(RV >= 0)$	−0.003	0.012	−0.083	0.006
	(0.002)	(0.035)	(0.158)	(0.038)
	[0.002]	[0.037]	[0.213]	[0.049]
2SLS				
$\mathbb{1}(RV >= 0)$	−0.040	−2.828	−9.641	−3.259
	(0.032)	(0.976)	(3.849)	(1.086)
	[0.035]	[0.767]	[3.677]	[1.008]
RV	0.003	0.077	0.308	0.090
	(0.001)	(0.029)	(0.104)	(0.030)
	[0.001]	[0.023]	[0.124]	[0.029]
RV $\cdot \mathbb{1}(RV >= 0)$	−0.003	0.005	−0.109	−0.003
	(0.002)	(0.042)	(0.152)	(0.039)
	[0.002]	[0.045]	[0.228]	[0.055]
Adjusted R^2	0.029	0.794	0.847	0.869
N	2,530			

Notes: This table reports results from four reduced-form local-linear regressions (top panel) and four 2SLS local-linear regressions (bottom panel). The dependent variable in all regressions is cardiovascular disease expenditures for the relevant age group, measured in cents per capita (11.5 KRW = 0.01 USD), and the independent variable of interest in the reduced-form (2SLS) regressions is an indicator for the running variable being above the RD threshold (advisory indicator). All regressions control for the running variable, an interaction between the running variable and the indicator for the running variable being above the RD threshold, temperature, precipitation, and year-by-month and day-of-week fixed effects. The level of observation is the district by day, and observations are population weighted. Parentheses (square brackets) contain standard errors clustered by the running variable (day of sample). The bandwidth is set to 20 in all regressions.

Table 3.6: Dynamic Impacts

	Age Group			
	Minors (0-19)	Adults (20-64)	Older Adults (65+)	All
Respiratory Illness				
Dependent Variable				
3-day Spending	−38.220 (11.551) [13.769]	−10.703 (3.952) [4.661]	−12.977 (4.951) [6.624]	−16.125 (4.777) [5.935]
3-day Spending without Later Alert Days	−38.616 (12.422) [16.370]	−7.122 (3.258) [3.262]	−8.202 (4.427) [4.651]	−13.005 (4.473) [5.381]
Cardiovascular Illness				
Dependent Variable				
3-day Spending	−0.064 (0.086) [0.075]	−5.279 (1.907) [1.993]	−30.388 (12.229) [12.987]	−8.042 (2.657) [3.057]
3-day Spending without Later Alert Days	0.023 (0.100) [0.094]	−4.486 (1.706) [2.040]	−36.044 (11.875) [13.975]	−7.414 (2.515) [3.303]

Notes: This table reports results from 16 2SLS local-linear regressions. The dependent variable in all regressions is three-day respiratory or cardiovascular disease expenditures (from day t to day $t + 2$) for the relevant age group, measured in cents per capita (11.5 KRW = 0.01 USD), and the independent variable of interest is an advisory indicator. All regressions control for the running variable, an interaction between the running variable and the indicator for the running variable being above the RD threshold, temperature, precipitation, and year-by-month and day-of-week fixed effects. The level of observation is the district by day, and observations are population weighted. Parentheses (square brackets) contain standard errors clustered by the running variable (day of sample). The bandwidth is set to 20 in all regressions. N = 2,530 in the first row of each panel. The last row of each panel drops from the sample advisory district-days on which the previous district-day experienced an advisory, which results in N = 2,228.

Table 3.7: Robustness Checks - Health Spending

	Age Group			
	Minors (0-19)	Adults (20-64)	Older Adults (65+)	All
Respiratory Illness				
Sample Modification				
Bandwidth: 16	−12.504	−4.357	−4.468	−5.851
	(4.256)	(2.293)	(2.626)	(2.492)
	[4.779]	[2.071]	[2.752]	[2.391]
Bandwidth: 20	−15.033	−3.777	−4.303	−5.829
	(4.709)	(2.195)	(2.753)	(2.397)
	[5.674]	[2.127]	[2.804]	[2.495]
Bandwidth: 24	−14.049	−2.876	−2.393	−4.867
	(4.521)	(2.008)	(2.918)	(2.254)
	[5.666]	[2.009]	[2.857]	[2.387]
Without Late/Early Advisories	−16.274	−4.093	−4.687	−6.320
	(5.243)	(2.316)	(2.944)	(2.550)
	[6.248]	[2.268]	[2.996]	[2.675]
Cardiovascular Illness				
Sample Modification				
Bandwidth: 16	−0.042	−2.781	−7.426	−2.994
	(0.039)	(0.889)	(2.897)	(0.900)
	[0.035]	[0.675]	[3.327]	[0.864]
Bandwidth: 20	−0.153	−3.022	−9.691	−3.431
	(0.095)	(1.024)	(3.930)	(1.168)
	[0.113]	[0.789]	[3.786]	[1.073]
Bandwidth: 24	−0.019	−1.654	−4.469	−1.870
	(0.030)	(1.016)	(4.320)	(1.219)
	[0.035]	[0.838]	[3.850]	[1.087]
Without Late/Early Advisories	−0.043	−3.064	−10.502	−3.533
	(0.034)	(1.050)	(4.217)	(1.160)
	[0.038]	[0.834]	[4.012]	[1.091]

Notes: This table reports results from 32 2SLS local-linear regressions. The dependent variable in all regressions is respiratory or cardiovascular disease expenditures for the relevant age group, measured in cents per capita (11.5 KRW = 0.01 USD), and the independent variable of interest is an advisory indicator. All regressions control for the running variable, an interaction between the running variable and the indicator for the running variable being above the RD threshold, temperature, precipitation, and year-by-month and day-of-week fixed effects. The level of observation is the district by day, and observations are population weighted. Parentheses (square brackets) contain standard errors clustered by the running variable (day of sample). The bandwidth is set to 20 unless otherwise noted. For bandwidths of 16, 20, and 24, N = 1,857, 2,530, and 3,380 respectively. The last row in each panel drops from the sample advisory district-days on which the advisory was cancelled before 9 am or triggered after 7 pm, which results in N = 2,443.

Table 3.8: RD Results for Credit Card Spending

	Spending Category			
	All	Restaurant	Fashion	Travel
Reduced form				
$\mathbb{1}(RV >= 0)$	−18.977	−9.177	−2.191	0.676
	(13.820)	(3.096)	(0.608)	(0.799)
	[12.537]	[2.895]	[0.645]	[0.851]
RV	0.247	0.470	0.095	−0.034
	(1.018)	(0.144)	(0.028)	(0.044)
	[0.861]	[0.166]	[0.035]	[0.050]
RV $\cdot \mathbb{1}(RV >= 0)$	−1.778	−0.536	−0.103	−0.079
	(1.273)	(0.353)	(0.061)	(0.079)
	[1.423]	[0.354]	[0.067]	[0.085]
2SLS				
$\mathbb{1}(RV >= 0)$	−25.713	−12.434	−2.969	0.916
	(20.331)	(4.837)	(0.963)	(1.044)
	[17.333]	[4.430]	[0.874]	[1.123]
RV	1.224	0.535	0.111	−0.038
	(0.538)	(0.212)	(0.041)	(0.045)
	[0.455]	[0.186]	[0.034]	[0.054]
RV $\cdot \mathbb{1}(RV >= 0)$	−2.306	−0.629	−0.125	−0.073
	(0.841)	(0.373)	(0.068)	(0.076)
	[0.778]	[0.338]	[0.065]	[0.085]
Adjusted R^2	0.915	0.923	0.784	0.820
N			2,905	

Notes: This table reports results from five reduced-form local-linear regressions (top panel) and fiver 2SLS local-linear regressions (bottom panel). The dependent variable in all regressions is credit card expenditures for the relevant item group, measured in cents per capita (11.5 KRW = 0.01 USD), and the independent variable of interest in the reduced-form (2SLS) regressions is an indicator for the running variable being above the RD threshold (advisory indicator). All regressions control for the running variable, an interaction between the running variable and the indicator for the running variable being above the RD threshold, temperature, precipitation, and year-by-month, day-of-week, and 1-day-before holiday fixed effects. The level of observation is the district by day, and observations are credit-card-user weighted. Parentheses (square brackets) contain standard errors clustered by the running variable (day of sample). The bandwidth is set to 20 in all regressions.

Table 3.9: Dynamic Impacts (Credit Card Spending)

	Spending Category			
	All	Restaurant	Fashion	Travel
Credit Card Spending				
Dependent Variable				
3-day Spending	−96.534	−25.672	−3.817	−0.604
	(56.747)	(17.382)	(2.477)	(2.678)
	[66.468]	[17.621]	[2.655]	[2.802]
3-day Spending without Later Alert Days	−34.709	−1.424	−1.408	1.849
	(39.292)	(8.717)	(1.427)	(1.985)
	[40.405]	[9.315]	[1.567]	[2.259]

Notes: This table reports results from 10 2SLS local-linear regressions. The dependent variable in all regressions is three-day credit card expenditures (from day t to day $t + 2$) for the relevant age group, measured in cents per capita (11.5 KRW = 0.01 USD), and the independent variable of interest is an advisory indicator. All regressions control for the running variable, an interaction between the running variable and the indicator for the running variable being above the RD threshold, temperature, precipitation, and year-by-month, day-of-week, and 1-day-before holiday fixed effects. The level of observation is district by day, and observations are weighted by the population. Parentheses (square brackets) contain standard errors clustered by the running variable (day of the sample). The bandwidth is set to 20 in all regressions. N = 2,905 in the first row of each panel. The last row of each panel drops from the sample advisory district-days on which the previous district-day experienced an advisory, which results in N = 2,701.

Table 3.10: Robustness Checks (Credit Card Spending)

	Spending Category			
	All	Restaurant	Fashion	Travel
Credit Card Spending				
Sample Modification				
Bandwidth: 16	−20.235	−16.284	−3.226	0.122
	(21.801)	(6.078)	(1.145)	(1.347)
	[22.422]	[5.839]	[1.070]	[1.477]
Bandwidth: 20	−25.713	−12.434	−2.969	0.916
	(20.331)	(4.837)	(0.963)	(1.044)
	[17.333]	[4.430]	[0.874]	[1.123]
Bandwidth: 24	−32.576	−9.888	−2.032	0.367
	(23.868)	(4.717)	(0.929)	(1.180)
	[16.887]	[4.320]	[0.906]	[1.116]
Without Late/Early Advisories	−22.308	−11.066	−2.979	1.219
	(19.843)	(4.995)	(0.956)	(1.204)
	[18.761]	[4.454]	[0.913]	[1.269]
Before Threshold Changes	−27.420	−14.566	−3.723	1.378
	(20.427)	(5.094)	(0.943)	(1.174)
	[20.607]	[5.421]	[0.973]	[1.332]

Notes: This table reports results from 25 2SLS local-linear regressions. The dependent variable in all regressions is credit card expenditures for the relevant item group, measured in cents per capita (11.5 KRW = 0.01 USD), and the independent variable of interest is an advisory indicator. All regressions control for the running variable, an interaction between the running variable and the indicator for the running variable being above the RD threshold, temperature, precipitation, and year-by-month, day-of-week, and 1-day-before holiday fixed effects. The level of observation is the district by day, and observations are credit-card-user weighted. Parentheses (square brackets) contain standard errors clustered by the running variable (day of sample). The bandwidth is set to 20 unless otherwise noted. For bandwidths of 16, 20, and 24, N = 2,277, 2,905, and 3,997 respectively. The last row in each panel drops from the sample advisory district-days on which the advisory was cancelled before 9 am or triggered after 7 pm, which results in N = 2,701.

Bibliography

Achilleos, S., M.-A. Kioumourtzoglou, C.-D. Wu, J. D. Schwartz, P. Koutrakis, and S. I. Papatheodorou. 2017. "Acute effects of fine particulate matter constituents on mortality: A systematic review and meta-regression analysis." *Environment International* 109:89–100.

Agarwal, S., T. F. Sing, and Y. Yang. 2020. "The impact of transboundary haze pollution on household utilities consumption." *Energy Economics* 85:104591.

Agarwal, S., L. Wang, and Y. Yang. 2021. "Impact of transboundary air pollution on service quality and consumer satisfaction." *Journal of Economic Behavior & Organization* 192:357–380.

Aguilar-Gomez, S. 2020. *Adaptation and mitigation of pollution: evidence from air quality warnings.* Technical report. Working paper.

Aguilar-Gomez, S., H. Dwyer, J. Graff Zivin, and M. Neidell. 2022. "This Is Air: The "Nonhealth" Effects of Air Pollution." *Annual Review of Resource Economics* 14 (1): 403–425. doi:10.1146/annurev-resource-111820-021816. eprint: https://doi.org/10.1146/annurev-resource-111820-021816. https://doi.org/10.1146/annurev-resource-111820-021816.

Aguilera, R., T. Corringham, A. Gershunov, and T. Benmarhnia. 2021. "Wildfire smoke impacts respiratory health more than fine particles from other sources: observational evidence from Southern California." *Nature communications* 12 (1): 1493.

Ahn, S., and L. Dabee. 2018. ""학교 보내는데 죄인된 기분"...미세먼지 '나쁨' 등 굣길 풍경 ["Feels not right to let my children go to school"...on the way to school when the fine dust level is 'bad']." *Chosun Ilbo* (March 27). Accessed March 27, 2018. https://www.chosun.com/site/data/html_dir/2018/03/27/2018032701653.html.

Air Quality Modeling Group, U.S. Environmental Protection Agency. 2004. *User's guide for the AMS/EPA regulatory model (AERMOD).*

Alam, K., S. Qureshi, and T. Blaschke. 2011. "Monitoring spatio-temporal aerosol patterns over Pakistan based on MODIS, TOMS and MISR satellite data and a HYSPLIT model." *Atmospheric Environment* 45 (27): 4641–4651.

Anderson, J. O., J. G. Thundiyil, and A. Stolbach. 2012. "Clearing the air: a review of the effects of particulate matter air pollution on human health." *Journal of medical toxicology* 8 (2): 166–175.

Anderson, M. L. 2017. "The benefits of college athletic success: An application of the propensity score design." *Review of Economics and Statistics* 99 (1): 119–134.

———. 2020. "As the wind blows: The effects of long-term exposure to air pollution on mortality." *Journal of the European Economic Association* 18 (4): 1886–1927.

Anderson, M. L., M. Hyun, and J. Lee. 2022. *Bounds, Benefits, and Bad Air: Welfare Impacts of Pollution Alerts.* Technical report. National Bureau of Economic Research.

Anderson, M., and J. Magruder. 2012. "Learning from the crowd: Regression discontinuity estimates of the effects of an online review database." *The Economic Journal* 122 (563): 957–989.

Andrews, S. Q. 2008. "Inconsistencies in air quality metrics:'Blue Sky'days and PM_{10} concentrations in Beijing." *Environmental Research Letters* 3 (3): 034009.

Angrist, J. D., and A. B. Krueger. 2001. "Instrumental variables and the search for identification: From supply and demand to natural experiments." *Journal of Economic perspectives* 15 (4): 69–85.

Angrist, J. D., and J. Pischke. 2008. *Mostly Harmless Econometrics: An Empiricist's Companion.* Princeton University Press.

ApSimon, H. M., and R. F. Warren. 1996. "Transboundary air pollution in Europe." *Energy Policy* 24 (7): 631–640.

Barwick, P. J., S. Li, L. Lin, and E. Zou. Conditionally accepted. "From fog to smog: The value of pollution information." *American Economic Review.*

Barwick, P. J., S. Li, D. Rao, and N. B. Zahur. 2018. *The healthcare cost of air pollution: Evidence from the world's largest payment network.* Technical report. National Bureau of Economic Research.

Bayer, P., N. Keohane, and C. Timmins. 2009. "Migration and hedonic valuation: The case of air quality." *Journal of Environmental Economics and Management* 58 (1): 1–14.

Bellis, D., A. Cox, I. Staton, C. McLeod, and K. Satake. 2001. "Mapping airborne lead contamination near a metals smelter in Derbyshire, UK: spatial variation of Pb concentration and 'enrichment factor' for tree bark." *Journal of Environmental Monitoring* 3 (5): 512–514.

Binkowski, F. S., and S. J. Roselle. 2003. "Models-3 Community Multiscale Air Quality (CMAQ) model aerosol component 1. Model description." *Journal of Geophysical Research: Atmospheres* 108 (D6).

Bollinger, B., P. Leslie, and A. Sorensen. 2011. "Calorie posting in chain restaurants." *American Economic Journal: Economic Policy* 3 (1): 91–128.

Bondy, M., S. Roth, and L. Sager. 2020. "Crime is in the air: The contemporaneous relationship between air pollution and crime." *Journal of the Association of Environmental and Resource Economists* 7 (3): 555–585.

Braithwaite, I., S. Zhang, J. B. Kirkbride, D. P. Osborn, and J. F. Hayes. 2019. "Air pollution (particulate matter) exposure and associations with depression, anxiety, bipolar, psychosis and suicide risk: a systematic review and meta-analysis." *Environmental Health Perspectives* 127 (12): 126002.

Bratspies, R. M., and R. A. Miller. 2006. *Transboundary harm in international law: lessons from the*
Trail Smelter arbitration. Cambridge University Press.

Burke, M., A. Driscoll, S. Heft-Neal, J. Xue, J. Burney, and M. Wara. 2021. "The changing risk and burden of wildfire in the United States." *Proceedings of the National Academy of Sciences* 118 (2): e2011048118.

Burkhardt, J., J. Bayham, A. Wilson, E. Carter, J. D. Berman, K. O'Dell, B. Ford, E. V. Fischer, and J. R. Pierce. 2019. "The effect of pollution on crime: Evidence from data on particulate matter and ozone." *Journal of Environmental Economics and Management* 98:102267.

Calonico, S., M. D. Cattaneo, and R. Titiunik. 2014. "Robust nonparametric confidence intervals for regression-discontinuity designs." *Econometrica* 82 (6): 2295–2326.

———. 2015. "rdrobust: An R Package for Robust Nonparametric Inference in Regression-Discontinuity Designs." *The R Journal* 7 (1): 38.

Carleton, T., A. Jina, M. Delgado, M. Greenstone, T. Houser, S. Hsiang, A. Hultgren, R. E. Kopp, K. E. McCusker, I. Nath, et al. 2022. "Valuing the global mortality consequences of climate change accounting for adaptation costs and benefits." *The Quarterly Journal of Economics* 137 (4): 2037–2105.

Carneiro, J., M. A. Cole, and E. Strobl. 2021. "The effects of air pollution on students' cognitive performance: Evidence from brazilian university entrance tests." *Journal of the Association of Environmental and Resource Economists* 8 (6): 1051–1077.

Cattaneo, M. D., M. Jansson, and X. Ma. 2018. "Manipulation testing based on density discontinuity." *The Stata Journal* 18 (1): 234–261.

Cattaneo, M. D., L. Keele, R. Titiunik, and G. Vazquez-Bare. 2020. "Extrapolating treatment effects in multi-cutoff regression discontinuity designs." *Journal of the American Statistical Association:* 1–12.

Cellini, S. R., F. Ferreira, and J. Rothstein. 2010. "The value of school facility investments: Evidence from a dynamic regression discontinuity design." *The Quarterly Journal of Economics* 125 (1): 215–261.

Chay, K. Y., and M. Greenstone. 2003. "The impact of air pollution on infant mortality: evidence from geographic variation in pollution shocks induced by a recession." *The Quarterly Journal of Economics* 118 (3): 1121–1167.

Chen, D., S. Cheng, L. Liu, T. Chen, and X. Guo. 2007. "An integrated MM5–CMAQ modeling approach for assessing trans-boundary PM_{10} contribution to the host city of 2008 Olympic summer games—Beijing, China." *Atmospheric Environment* 41 (6): 1237–1250.

Chen, H., Q. Li, J. S. Kaufman, J. Wang, R. Copes, Y. Su, and T. Benmarhnia. 2018. "Effect of air quality alerts on human health: a regression discontinuity analysis in Toronto, Canada." *The Lancet Planetary Health* 2 (1): e19–e26.

Chen, J., G. Hoek, K. De Hoogh, S. Rodopoulou, Z. J. Andersen, T. Bellander, J. Brandt, D. Fecht, F. Forastiere, J. Gulliver, et al. 2022. "Long-Term Exposure to Source-Specific Fine Particles and Mortality— A Pooled Analysis of 14 European Cohorts within the ELAPSE Project." *Environmental Science and Technology* 56 (13): 9277–9290.

Chen, L., J. Lin, R. Martin, M. Du, H. Weng, H. Kong, R. Ni, J. Meng, Y. Zhang, L. Zhang, et al. 2022. "Inequality in historical transboundary anthropogenic $PM_{2.5}$ health impacts." *Science Bulletin* 67 (4): 437–444.

Chen, S., Y. Chen, Z. Lei, and J.-S. Tan-Soo. 2021. "Chasing clean air: Pollution-induced travels in China." *Journal of the Association of Environmental and Resource Economists* 8 (1): 59–89.

Chen, S., Y. Li, G. Shi, and Z. Zhu. 2021. "Gone with the wind? Emissions of neighboring coal-fired power plants and local public health in China." *China Economic Review* 69:101660.

Chen, Y., G. Z. Jin, N. Kumar, and G. Shi. 2012. "Gaming in air pollution data? Lessons from China." *The BE Journal of Economic Analysis & Policy* 13 (3).

Cheng, S., F. Wang, J. Li, D. Chen, M. Li, Y. Zhou, Z. Ren, et al. 2013. "Application of trajectory clustering and source apportionment methods for investigating trans-boundary atmospheric PM_{10} pollution." *Aerosol and Air Quality Research* 13 (1): 333–342.

Chetty, R. 2009. "Sufficient Statistics for Welfare Analysis: A Bridge Between Structural and Reduced-Form Methods." *Annual Review of Economics* 1 (1): 451–488. doi:10.1146/annurev.economics.050708.142910.

Chetty, R., A. Looney, and K. Kroft. 2009. "Salience and taxation: Theory and evidence." *American Economic Review* 99 (4): 1145–77.

Cheung, C. W., G. He, and Y. Pan. 2020. "Mitigating the air pollution effect? The remarkable decline in the pollution-mortality relationship in Hong Kong." *Journal of environmental economics and management* 101:102316.

Choi, J., R. J. Park, H.-M. Lee, S. Lee, D. S. Jo, J. I. Jeong, D. K. Henze, J.-H. Woo, S.-J. Ban, M.-D. Lee, et al. 2019. "Impacts of local vs. trans-boundary emissions from different sectors on $PM_{2.5}$ exposure in South Korea during the KORUS-AQ campaign." *Atmospheric Environment* 203:196–205.

Chow, R. D., E. H. Bradley, and C. P. Gross. 2022. "Comparison of Cancer-Related Spending and Mortality Rates in the U.S. vs 21 High-Income Countries." In *JAMA Health Forum,* vol. 3,5, e221229–e221229. American Medical Association.

Conley, T. G. 1999. "GMM estimation with cross sectional dependence." *Journal of Econometrics* 92 (1): 1–45.

Crawford, J. H., J.-Y. Ahn, J. Al-Saadi, L. Chang, L. K. Emmons, J. Kim, G. Lee, J.-H. Park, R. J. Park, J. H. Woo, et al. 2021. "The Korea–United States Air Quality (KORUS-AQ) field study." *Elementa: Science of the Anthropocene* 9 (1): 00163.

Crippa, M., E. Solazzo, G. Huang, D. Guizzardi, E. Koffi, M. Muntean, C. Schieberle, R. Friedrich, and G. Janssens-Maenhout. 2020. "High resolution temporal profiles in the Emissions Database for Global Atmospheric Research." *Scientific Data* 7, no. 1 (April): 121. ISSN: 2052-4463. doi:10.1038/s41597-020-0462-2. https://doi.org/10.1038/s41597-020-0462-2.

Dahlby, B. 2008. *The marginal cost of public funds: Theory and applications.* MIT press.

DeCicca, P., and N. Malak. 2020. "When good fences aren't enough: The impact of neighboring air pollution on infant health." *Journal of Environmental Economics and Management* 102:102324.

Dedoussi, I. C., S. D. Eastham, E. Monier, and S. R. Barrett. 2020. "Premature mortality related to United States cross-state air pollution." *Nature* 578 (7794): 261–265.

Del Rio-Salas, R., J. Ruiz, M. De la O-Villanueva, M. Valencia-Moreno, V. Moreno-Rodrıguez, A. Gómez-Alvarez, T. Grijalva, H. Mendivil, F. Paz-Moreno, and D. Meza-Figueroa. 2012. "Tracing geogenic and anthropogenic sources in urban dusts: Insights from lead isotopes." *Atmospheric Environment* 60:202–210.

Deryugina, T., G. Heutel, N. H. Miller, D. Molitor, and J. Reif. 2019. "The mortality and medical costs of air pollution: Evidence from changes in wind direction." *American Economic Review* 109 (12): 4178–4219.

Deschenes, O., M. Greenstone, and J. S. Shapiro. 2017. "Defensive investments and the demand for air quality: Evidence from the NO_x budget program." *American Economic Review* 107 (10): 2958–2989.

Diao, B., L. Ding, J. Cheng, and X. Fang. 2021. "Impact of transboundary $PM_{2.5}$ pollution on health risks and economic compensation in China." *Journal of Cleaner Production* 326:129312.

Doherty, D., A. S. Gerber, and D. P. Green. 2006. "Personal income and attitudes toward redistribution: A study of lottery winners." *Political Psychology* 27 (3): 441–458.

Draxler, R. R., and G. Hess. 1998. "An overview of the HYSPLIT_4 modelling system for trajectories." *Australian Meteorological Magazine* 47 (4): 295–308.

Du, X., H. Guo, H. Zhang, W. Peng, and J. Urpelainen. 2020. "Cross-state air pollution transport calls for more centralization in India's environmental federalism." *Atmospheric Pollution Research* 11 (10): 1797–1804.

Du, X., X. Jin, N. Zucker, R. Kennedy, and J. Urpelainen. 2020a. "Transboundary air pollution from coal-fired power generation." *Journal of Environmental Management* 270:110862.

———. 2020b. "Transboundary air pollution from coal-fired power generation." *Journal of Environmental Management* 270:110862.

Dunning, T. 2008. "Model specification in instrumental-variables regression." *Political Analysis* 16 (3): 290–302.

Ebenstein, A., E. Frank, and Y. Reingewertz. 2015. "Particulate Matter Concentrations, Sandstorms and Respiratory Hospital Admissions in Israel." *The Israel Medical Association Journal: IMAJ* 17 (10): 628–632.

Eom, J., M. Hyun, J. Lee, and H. Lee. 2020. "Increase in household energy consumption due to ambient air pollution." *Nature Energy* 5 (12): 976–984.

Escudero, M., A. Stein, R. Draxler, X. Querol, A. Alastuey, S. Castillo, and A. Avila. 2006. "Determination of the contribution of northern Africa dust source areas to PM_{10} concentrations over the Central Iberian Peninsula using the Hybrid Single-Particle Lagrangian Integrated Trajectory model (HYSPLIT) model." *Journal of Geophysical Research: Atmospheres* 111 (D6).

European Commission, Joint Research Centre (JRC)/Netherlands Environmental Assessment Agency (PBL). 2019. *Emission Database for Global Atmospheric Research (EDGAR), release version 5.0.* Technical report. `http://edgar.jrc.ec.europa.eu`. European Commission, Joint Research Centre (JRC)/Netherlands Environmental Assessment Agency (PBL).

Finkelstein, A., and N. Hendren. 2020. "Welfare Analysis Meets Causal Inference." *Journal of Economic Perspectives* 34, no. 4 (November): 146–67.

Freeman, R., W. Liang, R. Song, and C. Timmins. 2019. "Willingness to pay for clean air in China." *Journal of Environmental Economics and Management* 94:188–216.

Fu, S., V. B. Viard, and P. Zhang. 2022. "Trans-boundary air pollution spillovers: Physical transport and economic costs by distance." *Journal of Development Economics* 155:102808.

Gao, X., R. Song, and C. Timmins. 2021. *The Role of Information in the Rosen-Roback Framework.* Technical report. National Bureau of Economic Research.

Gasparrini, A., Y. Guo, M. Hashizume, E. Lavigne, A. Zanobetti, J. Schwartz, A. Tobias, S. Tong, J. Rocklöv, B. Forsberg, et al. 2015. "Mortality risk attributable to high and low ambient temperature: a multicountry observational study." *The Lancet* 386 (9991): 369–375.

Gelman, A., and G. Imbens. 2019. "Why high-order polynomials should not be used in regression discontinuity designs." *Journal of Business and Economic Statistics* 37 (3): 447–456.

Ghanem, D., and J. Zhang. 2014. "'Effortless Perfection:'Do Chinese cities manipulate air pollution data?" *Journal of Environmental Economics and Management* 68 (2): 203–225.

Giglio, L., J. T. Randerson, and G. R. van der Werf. 2013. "Analysis of daily, monthly, and annual burned area using the fourth-generation global fire emissions database (GFED4)." *Journal of Geophysical Research: Biogeosciences* 118 (1): 317–328. doi:`https://doi.org/10.1002/jgrg.20042`.

Gilmour, M. I., J. McGee, R. M. Duvall, L. Dailey, M. Daniels, E. Boykin, S.-H. Cho, D. Doerfler, T. Gordon, and R. B. Devlin. 2007. "Comparative toxicity of size-fractionated airborne particulate matter obtained from different cities in the United States." *Inhalation Toxicology* 19 (sup1): 7–16.

Gobbi, G., F. Barnaba, and L. Ammannato. 2007. "Estimating the impact of Saharan dust on the year 2001 PM_{10} record of Rome, Italy." *Atmospheric Environment* 41 (2): 261–275.

Greene, W. H. 2003. *Econometric Analysis*. Upper Saddle River, NJ. Prentice Hall.

Greenstone, M., G. He, R. Jia, and T. Liu. 2021. "Can Technology Solve the Principal-Agent Problem? Evidence from China's War on Air Pollution." *American Economic Review: Insights*.

Greenstone, M., G. He, S. Li, and E. Y. Zou. 2021. "China's war on pollution: Evidence from the first 5 years." *Review of Environmental Economics and Policy* 15 (2): 281–299.

Gu, Y., and S. H. L. Yim. 2016. "The air quality and health impacts of domestic trans-boundary pollution in various regions of China." *Environment International* 97:117–124.

Hahm, Y., and H. Yoon. 2021. "The impact of air pollution alert services on respiratory diseases: generalized additive modeling study in South Korea." *Environmental Research Letters* 16 (6): 064048.

Han, S.-B., S.-K. Song, Z.-H. Shon, Y.-H. Kang, J.-H. Bang, and I. Oh. 2021. "Comprehensive study of a long-lasting severe haze in Seoul megacity and its impacts on fine particulate matter and health." *Chemosphere* 268:129369.

Han, X., J. Cai, M. Zhang, and X. Wang. 2021. "Numerical simulation of interannual variation in transboundary contributions from Chinese emissions to $PM_{2.5}$ mass burden in South Korea." *Atmospheric Environment* 256:118440.

Harrison, R. 2012. *Lead pollution: causes and control.* Springer Science & Business Media.

Harrison, R. M., and J. Yin. 2000. "Particulate matter in the atmosphere: which particle properties are important for its effects on health?" *Science of the Total Environment* 249 (1-3): 85–101.

Hastings, J. S., and J. M. Weinstein. 2008. "Information, school choice, and academic achievement: Evidence from two experiments." *The Quarterly Journal of Economics* 123 (4): 1373–1414.

He, G., T. Liu, and M. Zhou. 2020. "Straw burning, PM2. 5, and death: Evidence from China." *Journal of Development Economics* 145:102468.

He, X., Z. Luo, and J. Zhang. 2022. "The impact of air pollution on movie theater admissions." *Journal of Environmental Economics and Management* 112:102626.

Heft-Neal, S., J. Burney, E. Bendavid, and M. Burke. 2018. "Robust relationship between air quality and infant mortality in Africa." *Nature* 559 (7713): 254–258.

Heft-Neal, S., J. Burney, E. Bendavid, K. K. Voss, and M. Burke. 2020. "Dust pollution from the Sahara and African infant mortality." *Nature Sustainability* 3 (10): 863–871.

Heim, E., J. Dibb, E. Scheuer, P. C. Jost, B. A. Nault, J. L. Jimenez, D. Peterson, C. Knote, M. Fenn, J. Hair, et al. 2020. "Asian dust observed during KORUS-AQ facilitates the uptake and incorporation of soluble pollutants during transport to South Korea." *Atmospheric Environment* 224:117305.

Henry, L. S., J. Kim, and D. Lee. 2012. "From smelter fumes to Silk Road winds: Exploring legal responses to transboundary air pollution over South Korea." *Washington University Global Studies Law Review* 11:565.

Heo, S. W., K. Ito, and R. Kotamarthi. 2023. *International Spillover Effects of Air Pollution: Evidence from Mortality and Health Data.* Technical report. National Bureau of Economic Research.

Heyes, A., and M. Zhu. 2019. "Air pollution as a cause of sleeplessness: Social media evidence from a panel of Chinese cities." *Journal of Environmental Economics and Management* 98:102247.

Hsiang, S. 2016. "Climate econometrics." *Annual Review of Resource Economics* 8:43–75.

Hsiang, S. M. 2010. "Temperatures and cyclones strongly associated with economic production in the Caribbean and Central America." *Proceedings of the National Academy of Sciences* 107 (35): 15367–15372.

Inness, A., M. Ades, A. Agustí-Panareda, J. Barré, A. Benedictow, A. Blechschmidt, J. Dominguez, et al. 2019. *CAMS global reanalysis (EAC4).* `https://ads.atmosphere.copernicus.eu/cdsapp#!/dataset/cams-global-reanalysis-eac4?tab=overview`. Copernicus Atmosphere Monitoring Service (CAMS) Atmosphere Data Store (ADS).

Ito, K. 2014. "Do consumers respond to marginal or average price? Evidence from nonlinear electricity pricing." *American Economic Review* 104 (2): 537–63.

Ito, K., and S. Zhang. 2020. "Willingness to pay for clean air: Evidence from air purifier markets in China." *Journal of Political Economy* 128 (5): 1627–1672.

Janke, K. 2014. "Air pollution, avoidance behaviour and children's respiratory health: Evidence from England." *Journal of Health Economics* 38:23–42.

Jazil, M. O., and J. A. Brown. 2012. "The Cross-State Air Pollution Rule: Will EPA Learn from Experience?" *Trends* 44:24.

Jeong, S. 2021. *Essays in Public Economics and Applied Econometrics.* Stanford University.

Jessoe, K., and D. Rapson. 2014. "Knowledge is (less) power: Experimental evidence from residential energy use." *American Economic Review* 104 (4): 1417–38.

Jia, R., and H. Ku. 2019. "Is China's pollution the culprit for the choking of South Korea? Evidence from the Asian dust." *The Economic Journal* 129 (624): 3154–3188.

Jin, G. Z., and P. Leslie. 2003. "The effect of information on product quality: Evidence from restaurant hygiene grade cards." *The Quarterly Journal of Economics* 118 (2): 409–451.

Jordan, C. E., J. H. Crawford, A. J. Beyersdorf, T. F. Eck, H. S. Halliday, B. A. Nault, L.-S. Chang, J. Park, R. Park, G. Lee, et al. 2020. "Investigation of factors controlling $PM_{2.5}$ variability across the South Korean peninsula during KORUS-AQ." *Elementa: Science of the Anthropocene* 8.

Jouanneau, S., L. Recoules, M. Durand, A. Boukabache, V. Picot, Y. Primault, A. Lakel, M. Sengelin, B. Barillon, and G. Thouand. 2014. "Methods for assessing biochemical oxygen demand (BOD): A review." *Water Research* 49:62–82.

Jung, J., A. Choi, and S. Yoon. 2022. "Transboundary air pollution and health: evidence from East Asia." *Environment and Development Economics* 27 (2): 120–144.

Kang, Z. Y., and S. Vasserman. 2021. *Robust Bounds for Welfare Analysis.* Technical report. Stanford University Working Paper.

Kar, A., and K. Takeuchi. 2004. "Yellow dust: an overview of research and felt needs." *Journal of Arid Environments* 59 (1): 167–187.

Kelly, F. J., and J. C. Fussell. 2012. "Size, source and chemical composition as determinants of toxicity attributable to ambient particulate matter." *Atmospheric Environment* 60:504–526.

Kim, I. S., and Y. P. Kim. 2019. "Characteristics of Energy Usage and Emissions of Air Pollutants in North Korea." *Journal of Korean Society for Atmospheric Environment (in Korean)* 35 (1): 125–137.

Kim, I. S., J. Y. L. Lee, and Y. P. Kim. 2011. "Energy Usage and Emissions of Air Pollutants in North Korea." *Journal of Korean Society for Atmospheric Environment (in Korean)* 27 (3): 303–312.

Kim, K. W., et al. 2015. "Optical properties of size-resolved aerosol chemistry and visibility variation observed in the urban site of Seoul, Korea." *Aerosol and Air Quality Research* 15 (1): 271–283.

Kim, M. J. 2021. "Air pollution, health, and avoidance behavior: evidence from South Korea." *Environmental and Resource Economics* 79 (1): 63–91.

Kim, N. K., Y. P. Kim, Y. Morino, J.-i. Kurokawa, and T. Ohara. 2014. "Verification of NOx emission inventories over North Korea." *Environmental Pollution* 195:236–244.

Kim, W.-H., J.-M. Song, H.-J. Ko, J. S. Kim, J. H. Lee, and C.-H. Kang. 2012. "Comparison of Chemical Compositions of Size-segregated Atmospheric Aerosols between Asian Dust and Non-Asian Dust Periods at Background Area of Korea." *Bulletin of the Korean Chemical Society* 33 (11): 3651–3656.

Kim, Y. J., K. W. Kim, S. D. Kim, B. K. Lee, and J. S. Han. 2006. "Fine particulate matter characteristics and its impact on visibility impairment at two urban sites in Korea: Seoul and Incheon." *Atmospheric Environment* 40:593–605.

Kling, J. R., S. Mullainathan, E. Shafir, L. C. Vermeulen, and M. V. Wrobel. 2012. "Comparison friction: Experimental evidence from Medicare drug plans." *The Quarterly Journal of Economics* 127 (1): 199–235.

Koen, V., and J. Beom. 2020. *North Korea: The last transition economy?* Technical report 1607. OECD Economics Department. doi:https://doi.org/https://doi.org/10.1787/82dee315-en. https://www.oecd-ilibrary.org/content/paper/82dee315-en.

Korea Meteorological Administration (KMA). *황사업무 - 관측업무 [Yellow Dust - Observation].* https://www.kma.go.kr/kma/biz/asiandust01.jsp. Accessed: July 7, 2023.

———. *황사업무 - 예보업무 [Yellow Dust - Forecast].* https://www.kma.go.kr/kma/biz/asiandust03.jsp. Accessed: July 7, 2023.

Kowalska, J. B., R. Mazurek, M. Gasiorek, and T. Zaleski. 2018. "Pollution indices as useful tools for the comprehensive evaluation of the degree of soil contamination–A review." *Environmental Geochemistry and Health* 40 (6): 2395–2420.

Lai, W., H. Song, C. Wang, and H. Wang. 2021. "Air pollution and brain drain: Evidence from college graduates in China." *China Economic Review* 68:101624.

Lechner, M. 2009. "Sequential causal models for the evaluation of labor market programs." *Journal of Business & Economic Statistics* 27 (1): 71–83.

Lee, J., A. Wilson, and S. Hsiang. 2023. *Simultaneous estimation of damage from transboundary and domestic air pollution.* Technical report. Unpublished manuscript.

Lee, J. S. H., Z. Jaafar, A. K. J. Tan, L. R. Carrasco, J. J. Ewing, D. P. Bickford, E. L. Webb, and L. P. Koh. 2016. "Toward clearer skies: Challenges in regulating transboundary haze in Southeast Asia." *Environmental Science and Policy* 55:87–95.

Lee, S., M. Kim, S.-Y. Kim, D.-W. Lee, H. Lee, J. Kim, S. Le, and Y. Liu. 2021. "Assessment of long-range transboundary aerosols in Seoul, South Korea from Geostationary Ocean Color Imager (GOCI) and ground-based observations." *Environmental Pollution* 269:115924.

Lee, Y. W., Y. P. Kim, and M. J. Yeo. 2021. "Estimation of air pollutant emissions from heavy industry sector in North Korea." *Particle and Aerosol Research (in Korean)* 17 (4): 133–148.

Li, J., H. Chen, X. Li, M. Wang, X. Zhang, J. Cao, F. Shen, Y. Wu, S. Xu, H. Fan, et al. 2019. "Differing toxicity of ambient particulate matter (PM) in global cities." *Atmospheric Environment* 212:305–315.

Lim, Y.-H., S. Kim, C. Han, H.-J. Bae, S.-C. Seo, and Y.-C. Hong. 2020. "Source country-specific burden on health due to high concentrations of PM2.5." *Environmental Research* 182:109085.

Liu, J., J. Li, and F. Yao. 2022. "Source-receptor relationship of transboundary particulate matter pollution between China, South Korea and Japan: Approaches, current understanding and limitations." *Critical Reviews in Environmental Science and Technology* 52 (21): 3896–3920.

Liu, S., J. Xing, S. Wang, D. Ding, L. Chen, and J. Hao. 2020. "Revealing the impacts of transboundary pollution on $PM_{2.5}$-related deaths in China." *Environment International* 134:105323.

Liu, T., G. He, and A. Lau. 2018. "Avoidance behavior against air pollution: evidence from online search indices for anti-$PM_{2.5}$ masks and air filters in Chinese cities." *Environmental Economics and Policy Studies* 20 (2): 325–363.

Lorenzoni, L., and F. Koechlin. 2017. "International comparisons of health prices and volumes: new findings." *Health Division.*

Luechinger, S. 2009. "Valuing air quality using the life satisfaction approach." *The Economic Journal* 119 (536): 482–515.

———. 2014. "Air pollution and infant mortality: a natural experiment from power plant desulfurization." *Journal of health economics* 37:219–231.

Manski, C. F., et al. 1997. "Monotone Treatment Response." *Econometrica* 65 (6): 1311–1334.

Mastromonaco, R. 2015. "Do environmental right-to-know laws affect markets? Capitalization of information in the toxic release inventory." *Journal of Environmental Economics and Management* 71:54–70.

Mellon, J. 2022. "Rain, Rain, Go Away: 192 Potential Exclusion-Restriction Violations for Studies Using Weather as an Instrumental Variable." *Available at SSRN 3715610.*

Min, J. 2019. "National survey on an awareness of air pollution." *Korean Weekly Economic Review* 833 (10): 1–12.

Mogstad, M., A. Santos, and A. Torgovitsky. 2018. "Using instrumental variables for inference about policy relevant treatment parameters." *Econometrica* 86 (5): 1589–1619.

Mogstad, M., and A. Torgovitsky. 2018. "Identification and extrapolation of causal effects with instrumental variables." *Annual Review of Economics* 10:577–613.

Mullins, J., and P. Bharadwaj. 2015. "Effects of short-term measures to curb air pollution: Evidence from Santiago, Chile." *American Journal of Agricultural Economics* 97 (4): 1107–1134.

Nam, K.-M., Y. Ou, E. Kim, and S. Zheng. 2022. "Air Pollution and Housing Values in Korea: A Hedonic Analysis with Long-range Transboundary Pollution as an Instrument." *Environmental and Resource Economics* 82 (2): 383–407.

National Research Council. 2010. *Global sources of local pollution: an assessment of long-range*
transport of key air pollutants to and from the United States. National Academies Press.

Neidell, M. 2009a. "Information, avoidance behavior, and health the effect of ozone on asthma hospitalizations." *Journal of Human Resources* 44 (2): 450–478.

———. 2009b. "Information, avoidance behavior, and health the effect of ozone on asthma hospitalizations." *Journal of Human Resources* 44 (2): 450–478.

———. 2010. "Air quality warnings and outdoor activities: evidence from Southern California using a regression discontinuity design." *Journal of Epidemiology & Community Health* 64 (10): 921–926.

Newey, W. K., and K. D. West. 1987. "A Simple, Positive Semi-Definite, Heteroskedasticity and Autocorrelation Consistent Covariance Matrix." *Econometrica* 55, no. 3 (May): 703. doi:10.2307/1913610.

NIER. 2018. *대기환경연보 2017 [Annual report of air quality in Korea 2017].* Technical report. National Institute of Environmental Research (NIER).

Noonan, D. S. 2014. "Smoggy with a Chance of Altruism: The Effects of Ozone Alerts on Outdoor Recreation and Driving in Atlanta." *Policy Studies Journal* 42 (1): 122–145.

Organization for Economic Cooperation and Development. 2018. *OECD Economic Surveys Korea 2018.* http://www.oecd.org/economy/surveys/Korea-2018-OECD-economic-survey-overview.pdf. Accessed: 2020-10-29.

Organization, W. H. 2021. *Review of evidence on health aspects of air pollution: REVIHAAP project: technical report.* Technical report. World Health Organization. Regional Office for Europe.

Ostro, B. D. 1987. "Air pollution and morbidity revisited: a specification test." *Journal of Environmental Economics and Management* 14 (1): 87–98.

Ostro, B., J. M. Sanchez, C. Aranda, and G. S. Eskeland. 1996. "Air pollution and mortality: results from a study of Santiago, Chile." *Journal of Exposure Analysis and Environmental Epidemiology* 6 (1): 97–114.

Othman, J., M. Sahani, M. Mahmud, and M. K. S. Ahmad. 2014. "Transboundary smoke haze pollution in Malaysia: Inpatient health impacts and economic valuation." *Environmental Pollution* 189:194–201.

Park, M., H. S. Joo, K. Lee, M. Jang, S. D. Kim, I. Kim, L. J. S. Borlaza, et al. 2018. "Differential toxicities of fine particulate matters from various sources." *Scientific Reports* 8, no. 1 (November): 17007. ISSN: 2045-2322. doi:10.1038/s41598-018-35398-0. https://doi.org/10.1038/s41598-018-35398-0.

Park, S., C. Song, M. Kim, S. Kwon, and K. Lee. 2004. "Study on size distribution of total aerosol and water-soluble ions during an Asian dust storm event at Jeju Island, Korea." *Environmental Monitoring and Assessment* 93 (1): 157–183.

Pérez, N., J. Pey, X. Querol, A. Alastuey, J. López, and M. Viana. 2008. "Partitioning of major and trace components in PM_{10}–$PM_{2.5}$–PM_1 at an urban site in Southern Europe." *Atmospheric environment* 42 (8): 1677–1691.

Perrino, C., S. Canepari, M. Catrambone, S. Dalla Torre, E. Rantica, and T. Sargolini. 2009. "Influence of natural events on the concentration and composition of atmospheric particulate matter." *Atmospheric Environment* 43 (31): 4766–4779.

Peters, R., N. Ee, J. Peters, A. Booth, I. Mudway, and K. J. Anstey. 2019. "Air pollution and dementia: a systematic review." *Journal of Alzheimer's Disease* 70 (s1): S145–S163.

Pope III, C. A., and D. W. Dockery. 1992. "Acute health effects of PM10 pollution on symptomatic and asymptomatic children." *American review of respiratory disease* 145 (5): 1123–1128.

Pope, C. A., and D. W. Dockery. 1999. "31 - Epidemiology of Particle Effects." In *Air Pollution and Health,* edited by S. T. Holgate, J. M. Samet, H. S. Koren, and R. L. Maynard, 673–705. London: Academic Press. ISBN: 978-0-12-352335-8. doi:https://doi.org/10.1016/B978-012352335-8/50106-X. https://www.sciencedirect.com/science/article/pii/B978012352335850106X.

Powdthavee, N., and A. J. Oswald. 2020. "Is there a link between air pollution and impaired memory? Evidence on 34,000 English citizens." *Ecological Economics* 169:106485.

Pullabhotla, H. K., and M. Souza. 2022. "Air pollution from agricultural fires increases hypertension risk." *Journal of Environmental Economics and Management:* 102723.

Randerson, J. T., Y. Chen, G. R. van der Werf, B. M. Rogers, and D. C. Morton. 2012. "Global burned area and biomass burning emissions from small fires." *Journal of Geophysical Research: Biogeosciences* 117 (G4). doi:https://doi.org/10.1029/2012JG002128.

Rémy, S., Z. Kipling, J. Flemming, O. Boucher, P. Nabat, M. Michou, A. Bozzo, M. Ades, V. Huijnen, A. Benedetti, et al. 2019. "Description and evaluation of the tropospheric aerosol scheme in the European Centre for Medium-Range Weather Forecasts (ECMWF) Integrated Forecasting System (IFS-AER, cycle 45R1)." *Geoscientific Model Development* 12 (11): 4627–4659.

RIHP. 2020. *주요국 의원급 의료기관 진찰료 [Medical examination fees in major countries].* Technical report. Research Institute for Healthcare Policy (RIHP).

RIHP. 2021. *제20대 대통령 선거 보건의료 분야 정책제안서 [The 20th presidential election - policy proposal for health care].* Technical report. Research Institute for Healthcare Policy (RHIP).

Rivera, N. M. 2021. "Air quality warnings and temporary driving bans: Evidence from air pollution, car trips, and mass-transit ridership in Santiago." *Journal of Environmental Economics and Management* 108:102454. ISSN: 0095-0696. doi:https://doi.org/10.1016/j.jeem.2021.102454. https://www.sciencedirect.com/science/article/pii/S0095069621000371.

Rocha, R., and A. A. Sant'Anna. 2022. "Winds of fire and smoke: Air pollution and health in the Brazilian Amazon." *World Development* 151:105722.

Roy, D., Y.-C. Seo, S. Kim, and J. Oh. 2019. "Human health risks assessment for airborne PM_{10}-bound metals in Seoul, Korea." *Environmental Science and Pollution Research* 26 (23): 24247–24261.

Ryu, Y.-H., and S.-K. Min. 2021. "Long-term evaluation of atmospheric composition reanalyses from CAMS, TCR-2, and MERRA-2 over South Korea: Insights into applications, implications, and limitations." *Atmospheric Environment* 246:118062.

Saberian, S., A. Heyes, and N. Rivers. 2017. "Alerts work! Air quality warnings and cycling." *Resource and Energy Economics* 49:165–185.

Sapkota, A., J. M. Symons, J. Kleissl, L. Wang, M. B. Parlange, J. Ondov, P. N. Breysse, G. B. Diette, P. A. Eggleston, and T. J. Buckley. 2005. "Impact of the 2002 Canadian forest fires on particulate matter air quality in Baltimore City." *Environmental Science and Technology* 39 (1): 24–32.

Schmid, O., and T. Stoeger. 2016. "Surface area is the biologically most effective dose metric for acute nanoparticle toxicity in the lung." Inhaled Particle Dosimetry, *Journal of Aerosol Science* 99:133–143. ISSN: 0021-8502. doi:https://doi.org/10.1016/j.jaerosci.2015.12.006.

Schwartz, J., and D. W. Dockery. 1992. "Particulate air pollution and daily mortality in Steubenville, Ohio." *American Journal of Epidemiology* 135 (1): 12–19.

Seagrave, J., J. D. McDonald, E. Bedrick, E. S. Edgerton, A. P. Gigliotti, J. J. Jansen, L. Ke, L. P. Naeher, S. K. Seilkop, M. Zheng, et al. 2006. "Lung toxicity of ambient particulate matter from southeastern U.S. sites with different contributing sources: relationships between composition and effects." *Environmental Health Perspectives* 114 (9): 1387–1393.

Sergi, B., I. Azevedo, S. J. Davis, and N. Z. Muller. 2020. "Regional and county flows of particulate matter damage in the US." *Environmental Research Letters* 15 (10): 104073.

Shapiro, M. A., and M. Yarime. 2021. "Effects of national affiliations and international collaboration on scientific findings: The case of transboundary air pollution in Northeast Asia." *Environmental Science and Policy* 118:71–85.

Sharma, D., and D. Mauzerall. 2022. "Analysis of Air Pollution Data in India between 2015 and 2019." *AEROSOL AND AIR QUALITY RESEARCH* 22 (2).

Shehab, M. A., and F. D. Pope. 2019. "Effects of short-term exposure to particulate matter air pollution on cognitive performance." *Scientific Reports* 9 (1): 1–10.

Smith, W., L. Pan, S. Honomichl, S. Chelpon, R. Ueyama, and L. Pfister. 2021. "Diagnostics of Convective Transport over the Tropical Western Pacific from Trajectory Analyses." *Journal of Geophysical Research: Atmospheres* 126 (17): e2020JD034341.

Strak, M., N. A. Janssen, K. J. Godri, I. Gosens, I. S. Mudway, F. R. Cassee, E. Lebret, F. J. Kelly, R. M. Harrison, B. Brunekreef, et al. 2012. "Respiratory health effects of airborne particulate matter: the role of particle size, composition, and oxidative potential—the RAPTES project." *Environmental Health Perspectives* 120 (8): 1183–1189.

Strak, M., M. Steenhof, K. J. Godri, I. Gosens, I. S. Mudway, F. R. Cassee, E. Lebret, B. Brunekreef, F. J. Kelly, R. M. Harrison, et al. 2011. "Variation in characteristics of ambient particulate matter at eight locations in the Netherlands–The RAPTES project." *Atmospheric Environment* 45 (26): 4442–4453.

Stunder, B. 2004. *Global Data Assimilation System (GDAS) 1° product.* `http://ready.arl.%20noaa.gov/gdas1.php`.

Tan Soo, J.-S. 2018. "Valuing air quality in Indonesia using households' locational choices." *Environmental and Resource Economics* 71 (3): 755–776.

Thurston, G. D., L. C. Chen, and M. Campen. 2022. "Particle toxicity's role in air pollution." *Science* 375 (6580): 506–506.

1992. RIO DECLARATION ON ENVIRONMENT AND DEVELOPMENT, June. Report of the United National Conference on Environment and Development. United Nations. Accessed May 1, 2020. `https://www.un.org/en/development/desa/population/migration/generalassembly/docs/globalcompact/A_CONF.151_26_Vol.I_Declaration.pdf`.

Wagstrom, K. M., S. N. Pandis, G. Yarwood, G. M. Wilson, and R. E. Morris. 2008. "Development and application of a computationally efficient particulate matter apportionment algorithm in a three-dimensional chemical transport model." *Atmospheric Environment* 42 (22): 5650–5659.

Ward, A. L. S., and T. K. Beatty. 2016. "Who responds to air quality alerts?" *Environmental and Resource Economics* 65 (2): 487–511.

Werf, G. R. van der, J. T. Randerson, L. Giglio, T. T. van Leeuwen, Y. Chen, B. M. Rogers, M. Mu, et al. 2017. "Global fire emissions estimates during 1997–2016." *Earth System Science Data* 9 (2): 697–720. doi:10.5194/essd-9-697-2017. https://essd.copernicus.org/articles/9/697/2017/.

World Health Organization. 2021. *WHO global air quality guidelines: particulate matter ($PM_{2.5}$ and PM_{10}), ozone, nitrogen dioxide, sulfur dioxide and carbon monoxide.* World Health Organization.

Wu, Y., T. Jin, W. He, L. Liu, H. Li, C. Liu, Y. Zhou, J. Hong, L. Cao, Y. Lu, et al. 2021. "Associations of fine particulate matter and constituents with pediatric emergency room visits for respiratory diseases in Shanghai, China." *International Journal of Hygiene and Environmental Health* 236:113805.

Xue, T., G. Geng, Y. Han, H. Wang, J. Li, H.-t. Li, Y. Zhou, and T. Zhu. 2021. "Open fire exposure increases the risk of pregnancy loss in South Asia." *Nature Communications* 12 (1): 3205.

Yang, J., and B. Zhang. 2018. "Air pollution and healthcare expenditure: Implication for the benefit of air pollution control in China." *Environment international* 120:443–455.

Yi, F., H. Ye, X. Wu, Y. Y. Zhang, and F. Jiang. 2020. "Self-aggravation effect of air pollution: evidence from residential electricity consumption in China." *Energy Economics* 86:104684.

Yoo, C. 2021. "(2nd LD) S. Korea suffocated by worst yellow dust storm in a decade." *Yonhap News Agency* (March 29). Accessed March 29, 2021. https://en.yna.co.kr/view/AEN20210329002952315.

Yuan, C.-S., C.-G. Lee, S.-H. Liu, J.-c. Chang, C. Yuan, and H.-Y. Yang. 2006. "Correlation of atmospheric visibility with chemical composition of Kaohsiung aerosols." *Atmospheric Research* 82 (3-4): 663–679.

Zabrocki, L., A. Alari, and T. Benmarhnia. 2022. "Improving the design stage of air pollution studies based on wind patterns." *Scientific Reports* 12 (1): 1–10.

Zhang, Q., X. Jiang, D. Tong, S. J. Davis, H. Zhao, G. Geng, T. Feng, B. Zheng, Z. Lu, D. G. Streets, et al. 2017. "Transboundary health impacts of transported global air pollution and international trade." *Nature* 543 (7647): 705–709.

Zheng, S., and M. E. Kahn. 2017. "A new era of pollution progress in urban China?" *Journal of Economic Perspectives* 31 (1): 71–92.

Zheng, S., J. Wang, C. Sun, X. Zhang, and M. E. Kahn. 2019. "Air pollution lowers Chinese urbanites' expressed happiness on social media." *Nature human behaviour* 3 (3): 237–243.

Zheng, S., X. Zhang, W. Sun, and C. Lin. 2019. "Air pollution and elite college graduates' job location choice: Evidence from China." *The Annals of Regional Science* 63 (2): 295–316.

Zou, E. Y. 2021. "Unwatched pollution: The effect of intermittent monitoring on air quality." *American Economic Review* 111 (7): 2101–26.

Appendix A

Supplementary Information for Chapter 1

A.1 Methods

Data Collection

Air pollutants

We obtained hourly data on ambient levels of PM_{10}, $PM_{2.5}$ (this is available only starting in 2015), ozone, sulfur dioxide, nitrogen dioxide, and carbon monoxide from the Air Korea portal (https://airkorea.or.kr/) administered by the Korea Environment Corporation (KECO), a South Korean government agency that manages air quality monitors (for a map of monitor locations and districts included in our sample see Extended Data Figure A1). Holding the set of monitors constant, we estimated exposure for all missing monitor–hours over our sample period by calculating the empirical CDF for the monitor with missing data and then selecting the quantile of this CDF equal to the inverse squared distance-weighted quantile of observations for the five nearest non-missing monitors. Daily values for each monitor are the mean of hourly values.

Observations of airborne heavy metals

KECO also manages the observations of airborne heavy metals used in our analysis of PM chemistry. We requested daily observations of these measures using the official information disclosure process through the South Korean information request portal (https://open.go.kr/); use of the data was granted on the condition that it

not be shared. KECO measures airborne heavy metals (lead and calcium) recorded by monitors of Air Pollution Monitoring Supersites every two hours. We aggregated those observations to daily average levels. We omitted readings from the Incheon supersite, located on Baekryeong Island, as it is far from any urban PM monitor.

Weather and atmospheric visibility

We collected hourly monitor-level readings for temperature, humidity, and precipitation using the Korea Meteorological Administration (KMA) portal. We then performed the same procedure for filling missing observations and assigning exposure to districts as detailed for pollutants above.

We also obtained measures of visibility (reported as visible distance) for the small set of reporting monitors in the KMA's automated synoptic observation system. We matched these hourly observations to those for the nearest monitors reporting levels of airborne heavy metals, applying a ceiling to all observations of 10 km to account for differences across stations in their censoring practices.

Health spending

Our health outcome of interest is the morbidity spending associated with outpatient and emergency visits due to respiratory disease. We were granted access to this data through a restricted-use agreement with the National Health Insurance Service (NHIS) data center, which manages the transaction information of South Korea's Social Health Care System. Our analysis uses a 10% (N $\approx$ 5 million) sample of insured individuals. The sampling was carried out by stratifying individuals by each pair of district and age group, the latter of which was based on five-year age groups (0 to 4, 5 to 9, and so on). Individuals who died before the end of our analysis period were excluded. We then filtered for records associated with respiratory disease (J-category illnesses according to the International Classification of Diseases, 10^{th} revision [ICD-10]) that occurred during the period 2005 to 2016. We then aggregated this individual expenditure information by date and district. To determine expenditure per capita, we used denominators reported by NHIS; to calculate total expenditure across South Korea, we linearly interpolate estimates of the district-level population between census years.

Some aspects of this data set are of note. First, health expenditures per capita include outpatient and emergency visits covering all the different levels of facilities in the South Korean healthcare system (public health centers, doctor's offices, clinics, hospitals, general hospitals, and tertiary general hospitals). We exclude costs incurred

from inpatient visits, as they require several layers of referrals and tend to involve more complex sequelae.

Second, our data set incorporates private copayments plus costs covered by the healthcare system, allowing us to gauge the impact of air pollution on total health costs.

Third, we only include districts with 'urban' air pollution monitors during the analysis period. KECO manages several types of air quality monitors, including "urban" and "rural" locations. We used urban monitors because they better represent the degree of air quality experienced by the population. Indeed, due to better representation, local government agencies use urban monitors to determine whether environmental standards are met.(NIER 2018) We also exclude districts where air quality monitors were installed too recently (2016 or later). This filtering process left us with 147 districts out of the 229 districts in South Korea, while still covering the entirety of 17 provinces and over 91% of the population (see Extended Data Figure A1).

Fourth, our data set excludes individuals who moved into or out of the districts we analyze during our data period. Moving can lead to discontinuous changes in district-level health expenditure, complicating interpretation of our results.

Decomposition of PM by source

The PM observations used in this analysis come from a network of monitors located throughout South Korea. We decompose the PM values reported by these monitors in two steps. First, we extract the portion of PM associated with dust and sea salt using a global reanalysis product that estimates surface concentrations. Second, we combine a probabilistic estimate of pollution transport with high-resolution estimates of emission rates to apportion the remaining PM among two sources: human activities (which we further subdivide into four originating jurisdictions: China, South Korea, North Korea, and "other") and wildfire. Finally, we assign these exposures to districts (second-level administrative units) in South Korea.

Dust and sea salt

In the first step in our source decomposition, we partition out dust and sea salt from total observed PM. We collect 3-hourly rasters of surface-level PM components from the European Centre for Medium-Range Weather Forecasts (ECMWF) Atmospheric Composition Reanalysis 4, or EAC4,(Inness et al. 2019) and calculate the inverse distance weighted mean of the nine nearest raster values of each EAC4 surface-level

PM component for each monitor–day. Following the weighting scheme used in the ECMWF Integrated Forecasting System (IFS-AER),(Rémy et al. 2019) we determine the portion of total PM that is attributable to mineral dust, which we rescale to match total PM values reported by each station.

In addition, we adjust for "Yellow Dust" days, as EAC4 is known to systematically underestimate this particular source of PM.(Ryu and Min 2021) Though these events are infrequent, they can produce daily average PM values in South Korea above 1000 $\mu g/m^3$ as large quantities of coarse dust are removed by aeolian erosion from the soil and rocks of the Mongolian plateau and are carried by strong winds across the Yellow Sea.[1] This adjustment is made only on days and in provinces when the Korea Meteorological Agency reported a Yellow Dust event, a determination made by visual inspection by trained meteorologists in conjunction with the output of a physical model of dust erosion.(Korea Meteorological Administration (KMA)) For these observations, if we estimate that PM that is not EAC4 dust is above its 90^{th} percentile for that monitor's weekday–month, all such PM above the monitor's weekday–month median value is attributed to Yellow Dust. Our main analysis treats EAC4 dust and this additional Yellow Dust component jointly. In addition, to account for misreporting, we also apply this adjustment to neighboring provinces or the same province on an adjacent day if its reported values are above its weekday-by-month 99^{th} percentile. This adjustment affects 2.3% of province–days. We note that this procedure follows from a similar approach developed to account for extreme $PM_{2.5}$ from wildfires in North America.(Burke et al. 2021)

We perform a similar procedure for sea salt by determining the portion of non-dust PM that is attributable to sea salt from EAC4 and scale that to match the non-dust PM value for each station.

PM from human activity and wildfire

The second step of our decomposition determines the contributions of human activities and wildfire to the portion of observed PM that remains after removing dust and sea salt. We first generate a large number of air parcel backtrajectories using a physical model of atmospheric dynamics, the Hybrid Single-Particle Lagrangian Integrated Trajectory (HYSPLIT) model,(Draxler and Hess 1998) and the GDAS1 global atmosphere reanalysis product.(Stunder 2004) These backtrajectories represent the paths taken by a hypothetical parcel of air traveling backwards in time

[1] Importantly, the meteorological conditions on these days are unusual and may also carry higher- or lower-than-usual quantities of PM from other sources, though we have no way of directly testing this.

from its observed destination, based on the timing and distribution of observed wind flows (e.g., Figure 1.1A). Note that wind flow in the atmosphere is well observed and tightly constrained in this mid-latitude region by its relationship to air temperature and pressure, both of which are also well observed.

We initialize backtrajectories at eight times of day (every 3 hours beginning at 2 a.m. local time) and eight heights (2, 4, 8, 16, 32, 64, 128, 256, and 512 meters) at each PM monitor on each day and track each parcel for 240 hours back in time (16.3 billion locations along 67.9 million paths). We define trajectories that pass twice the height of the planetary boundary layer as exiting the model and provide small vertical perturbations to particles that collide with the surface to keep them aloft. For each hour of each trajectory that arrives at a monitor on a specific day, this results in 16 parcel locations where emissions are potentially entrained in the air parcel before it arrives at its destination in South Korea. We rasterize these locations into a $0.1^\circ \times 0.1^\circ$ grid by counting the number of parcel instances that occur within each grid cell and smooth these estimated counts across space using a Gaussian kernel ($\sigma = 1$ pixel) to account for uncertainty in trajectories. Finally, we normalize the sum of each raster to one, creating a map that we interpret as the probability (denoted π) that each grid cell contributes material to that specific air parcel in that hour of its trajectory.

To estimate the quantity of emissions that are entrained in the air parcel from each location during a specific hour, we multiply these contribution-probability rasters by sector-specific PM emissions (denoted q) from the Emissions Database for Global Atmospheric Research (EDGAR) 5.0.(European Commission, Joint Research Centre (JRC)/Netherlands Environmental Assessment Agency (PBL) 2019) We rescale EDGAR values to account for hourly, weekly, seasonal, and secular variation in emissions intensity using a set of scalars for high-resolution temporal profiles.(Crippa et al. 2020) We follow the same procedure for 3-hourly Global Fire Emissions Database (GFED) 4.1s,(Werf et al. 2017; Randerson et al. 2012; Giglio, Randerson, and Werf 2013) where we use emissions rates based on estimated fuel type for burn fire location. HYSPLIT does not contain active chemistry, so we apply the simple approximation that non-methane volatile organic compounds (VOCs), sulfur dioxide, nitrogen oxides, and ammonia emissions estimated in EDGAR 5.0 are converted to an equivalent mass of PM.[2]

[2]Somewhat surprisingly, we find that our results are not sensitive to this assumption; this may be because the correlations between primary PM and NO_x, SO_2, NMVOC, and NH_3 emissions are very high. Assuming zero conversion into secondary aerosols changes our results by only a small margin. That said, seasonal variation in the conversion efficiency or rate may affect our results, but the direction of this adjustment is not known.

We model deposition, scavenging, and chemistry in a simplified framework that assumes net exponential decay. We empirically calibrate a separate decay rate (denoted r) for each quarter of the year—to account for seasonal differences in atmospheric moisture, temperature, and cloud physics—that maximizes the correlation between the observed values of non-dust and non-salt PM (in South Korea) and the values predicted by our trajectory model (exponential decay rates of 0.004, 0.008, 0.016, and 0.006, respectively, with maximum Pearson correlations for all seasons around 0.6). We note that the assumption of a constant decay rate/particle lifetime is a simplification made elsewhere, such as in a trajectory analysis over the western Pacific,(Smith et al. 2021) and the decay rates we recover (implying a half-life of particles around 24 hours) are similar to those suggested elsewhere in the literature, such as in the AMS/EPA Regulatory Model.(Air Quality Modeling Group, U.S. Environmental Protection Agency 2004) We then apply these rates to each parcel throughout its trajectory.

We separately track PM for each non-dust, non-salt origin j, scaling the predicted relative contributions of all origins to match the residual level of PM that arrives, and is observed, at monitor l at time t. Our estimate for the relative quantity of PM from origin j arriving at monitor l at time t is

$$\hat{p}_{ljt} = \sum_{\tau=0}^{T} \sum_{v \in j} \underbrace{\pi_{lvt\tau}}_{\substack{\text{Probability that} \\ \text{air mass from } v \text{ at } t-\tau \\ \text{arrives at } l \text{ at } t}} \cdot \underbrace{q_{v(t-\tau)}}_{\substack{\text{Emissions} \\ \text{from } v \text{ at } t-\tau}} \cdot \underbrace{(1-r)^{\tau}}_{\text{Decay factor}} \tag{A.1}$$

where $\pi_{lvt\tau}$ is the probability, estimated from HYSPLIT, that an air mass has arrived at location l at time t from pixel v in origin j at time $t-\tau$, $q_{v(t-\tau)}$ is a measure of actual emissions at location v and time $t-\tau$ (from EDGAR and GFED), and $(1-r)^{\tau}$ is the fraction of emissions that remain at arrival following deposition/decay/scavenging. To compute $\hat{p}_{ljt}$, we sum what remains of the emissions $q_{v(t-\tau)}$ over all locations v in origin j (e.g., over all grid cells in China) and over all emission times (i.e., for emissions that have traveled to our exposed population for 0 hours [$\tau = 0$], 1 hour [$\tau = 1$], 2 hours [$\tau = 2$], etc.).

Partitioning observed PM

The estimate $\hat{p}_{ljt}$ represents only the *relative* contribution of origin j to non-dust and non-salt PM observed at monitor l at time t. To apportion this PM to an origin, we begin with $\ddot{p}_{lt}$, the PM observed at l at time t that remains after accounting for

dust and sea salt using the method described above in "Dust and sea salt" (i.e., $\ddot{p}_{lt} \equiv p_{lt} - p_{lt,\text{dust}} - p_{lt,\text{sea salt}}$). This residual is apportioned proportionately as

$$p_{ljt} = \ddot{p}_{lt} \cdot \frac{\hat{p}_{ljt}}{\sum_j \hat{p}_{ljt}} \tag{A.2}$$

where p_{ljt} is the amount of observed PM at monitor l and time t from origin j, where j includes South Korea, North Korea, China, wildfires, and "other sources." The procedure above, in "Dust and sea salt," provides a similar value for $j \in \{\text{dust, sea salt}\}$. Figures 1.1D–E illustrate this partition. We then aggregate these seven estimates by district: for each district i, we interpolate based on values of p_{ljt}, calculating an inverse squared distance-weighted average to each district i's center of population (calculated using Meta's High Resolution Population Density Maps**??**). This procedure yields 600,119 observations, p_{ijt}, for all seven origins j.

Econometric analysis

The main text contains two separate econometric analyses. The first analysis validates our decomposition of PM by origin by evaluating how the contribution of PM from different origins affects the chemical and physical properties of PM observed at a small number of South Korean monitors that collect these data. The second analysis estimates the impact of PM from each origin on health costs in districts across South Korea.

Decomposing properties of PM mixtures by origin

We estimate the extent to which PM from each origin is associated with differences in the chemical and physical characteristics of the PM mixture that arrives at each destination. To do this, we empirically decompose the chemical and physical properties of PM (concentrations of lead and calcium, $PM_{2.5}$, and visibility) observed at a limited number of advanced monitors into contributions from each origin, based on the amount of PM that we attribute to origin j on each day t in districts containing these advanced monitors. The chemical or physical property c_{it} (e.g., lead concentration) observed in district i (treating the district's advanced monitor and the district as synonymous) on day t is an additive mixture of contributions from different origins

$$c_{it} = c_{i,\text{South Korea},t} + c_{i,\text{China},t} + \ldots + c_{i,\text{wildfire},t} + \epsilon_{it} \tag{A.3}$$

where c_{ijt} is the contribution from j that arrives at monitor i on day t and ϵ_{it} is unmodeled error. For these chemical or physical proprieties, the contribution from location j is the product of the total PM from origin j (p_{ijt}) and the change in c per additional unit of origin j PM (λ_{ij}; e.g., the change in ambient lead observed at location i for a given increase in PM from origin j). Specifically:

$$c_{it} = p_{i,\text{South Korea},t} \cdot \lambda_{i,\text{South Korea}} + p_{i,\text{China},t} \cdot \lambda_{i,\text{China}} + \ \ldots \ + p_{i,\text{wildfire},t} \cdot \lambda_{i,\text{wildfire}} + \epsilon_{it} \tag{A.4}$$

which we solve via multiple linear regression. Here, we allow λ to differ by location i precisely so we are able to test its consistency over space, but we assume it is stable over our sample period. To aid comparison, we present in Figure 1.2 the set of λ_{ij}'s as partial correlation coefficients. The specific construction of this figure is illustrated in Extended Data Figure A2: (1) Multiple correlation coefficients for all origins j but only a single destination site i (and a pair of chemical/physical variables) are plotted (Extended Data Figure A2A). (2) We repeat this process for all destinations i. Then, coefficients are regrouped based on their origin, pooling across destinations to define a convex hull for each origin (Extended Data Figure A2B). This allows us to assess patterns in the chemical/physical features of air that arrives at a set of destinations from each origin (Extended Data Figure A2C).

Estimating the health response to undifferentiated total PM

Our objective is to develop a statistical framework that can be used to directly measure the relationship between exposure to PM from a specific origin and changes in health costs. In prior analyses, researchers have focused on modeling the health effects of total PM without distinguishing between contributing origins. Thus, we first analyze the health response to undifferentiated PM as in the previous literature. Then, we extend this framework to include the impacts of PM from different origins.

Conceptually, our model for respiratory health costs, h_{it}, from undifferentiated PM occurring in district i on day t is:

$$h_{it} = \underbrace{\bar{D}(\mathbf{p}_{it},\, \bar{A}(\mathbf{p}_{it}))}_{\text{damage from PM}} + \underbrace{\bar{f}(\mathbf{Q}_{it},\, \mathbf{W}_{it},\, \bar{\boldsymbol{\zeta}}_{it},\, \bar{\theta}_t)}_{\text{other causes}} + \bar{e}_{it} \tag{A.5}$$

where $\bar{D}(\cdot)$ is the damage from PM ($\mathbf{p}$), accounting for avoidance ($\bar{A}$). Other patterns in health costs that can be netted out by covariates are captured in $\bar{f}(\cdot)$, including the effects of other pollutants ($\mathbf{Q}$), meteorological conditions ($\mathbf{W}$), and a rich set

of non-parametric fixed effects ($\bar{\boldsymbol{\zeta}}$) and trends ($\bar{\theta}$). We discuss each of these model elements below. Unmodeled variation in health spending is captured by $\bar{e}$. We use a bar above estimated model elements to denote that they describe components of the model for *undifferentiated PM*, in contrast to an alternative model that differentiates contributions by origin, in which bars are omitted (presented below). We discuss each of the arguments of Equation A.5 in turn and then describe how we estimate the model.

Total particulate matter The term $\mathbf{p}_{it}$ describes the levels of total PM daily from the time $t - L$ to t, where L is the number of daily lags over which impacts accrue. We set $L = 28$ days to ensure potential delayed health effects are accounted for. As discussed in the main text, delays sometimes occur because lower-level referrals are required to visit a specialty hospital in the South Korean healthcare system. Thus, $\mathbf{p}_{it} = (p_{it},\ \cdots,\ p_{i(t-28)})$.

Accounting for avoidance behavior $\bar{A}$ is a summary measure of avoidance behavior. As ambient PM increases, individuals may recognize higher levels of air pollution based on changes in atmospheric visibility or information provided by governments and take defensive action (e.g., wearing face masks) or avoid certain activities (e.g., by staying at home). These actions may then in turn reduce the average damages incurred per additional unit of PM(Neidell 2009b; Deschenes, Greenstone, and Shapiro 2017; Anderson, Hyun, and Lee 2022; Aguilar-Gomez et al. 2022; Carleton et al. 2022); thus, it is usually thought that $\frac{\partial \bar{A}}{\partial P} > 0$ and $\frac{\partial \bar{h}}{\partial \bar{A}} < 0$. We thus design a function for the net damages caused by PM ($\bar{D}$) capable of incorporating this potential mechanism. Conceptually, we assume health damages are generated by a process:

$$\bar{D}(\mathbf{p}_{it},\ \bar{A}(\mathbf{p}_{it})) = \sum_{k=0}^{28} \underbrace{\bar{g}_k(p_{i(t-k)})}_{\text{biological response}} \cdot \underbrace{(1 - \bar{A}_{t-k}(p_{i(t-k)}))}_{\text{attenuation from avoidance}} \tag{A.6}$$

where we have explicitly expanded the number of terms in the summation to account for the 28 lagged days of pollution exposure that might contribute to harm on day t. Here, $\bar{g}_k$ is the biological impact of $p_{i(t-k)}$ on the health response in the absence of avoidance, where k indexes the damage from sequential lags. $\bar{A}_{t-k}$ measures the level of avoidance triggered by the PM level at time $t - k$, and can take on a value between zero (no avoidance) and one (total avoidance), inclusive. Thus, the effects of $\bar{g}_k$ can be partially mitigated by avoidance behavior, captured by the multiplicative term $(1 - \bar{A}_{t-k})$ which drives damages to zero as $\bar{A}_{t-k} \to 1$. This expression for $\bar{D}$ describes, conceptually, how the data are assumed to be generated, however we do not

observe avoidance behavior directly and thus cannot rely on explicit measurements of avoidance in our estimation. To overcome this challenge, we draw on techniques developed in the study of climate change damages(S. Hsiang 2016; Carleton et al. 2022) and note that estimation can be simplified because avoidance behavior is an explicit response to the level of pollution; that is, $\bar{A}_{t-k}$ can be written as a function of $p_{i(t-k)}$ (i.e., pollution levels are a "sufficient statistic" for avoidance(Chetty 2009)). Thus, under the simplifying assumption that both $\bar{g}_k$ and $\bar{A}_k$ are approximately linear in $p_{i(t-k)}$, the expression for damages in Eq. A.6 reduces to a quadratic function with two parameters for each lag:

$$\bar{D}(\mathbf{p}_{it},\, \bar{A}(\mathbf{p}_{it})) = \sum_{k=0}^{28} \bar{\alpha}_k \cdot p_{i(t-k)} + \bar{\beta}_k \cdot p^2_{i(t-k)} \tag{A.7}$$

which can be directly estimated from data. Consequently, the shape of our response function is non-linear in pollution, consistent with prior analyses,(Deryugina et al. 2019) and this non-linearity embeds information about the degree of unobserved avoidance undertaken by individuals.

Covariates We also account for a matrix of potential confounding variables related to our health outcomes of interest and pollutant levels, which are included as covariates in our regression analysis. We account for the levels of other air pollutants (nitrogen dioxide, carbon monoxide, ozone, and sulfur dioxide), denoted by the matrix $\mathbf{Q}_{it} = (\mathbf{q}_{1it},\, \mathbf{q}_{2it},\, \mathbf{q}_{3it},\, \mathbf{q}_{4it})$, and meteorological conditions (temperature, humidity, and precipitation), denoted as $\mathbf{W}_{it} = (\mathbf{w}_{1it},\, \mathbf{w}_{2it},\, \mathbf{w}_{3it})$. Similar to our notation describing PM, these matrices include the contemporaneous and lagged values of each variable, capturing effects within the 28-day window for exposure that we are studying.

Non-parametric controls and trends To account for a wide variety of time-dependent and time-invariant unobserved determinants of both pollution levels and health spending,(Ostro 1987; Schwartz and Dockery 1992; Chay and Greenstone 2003; Ostro et al. 1996) we include district-by-year-by-month-by-weekday ($\bar{\boldsymbol{\zeta}}_{it}$) and holiday ($\bar{\theta}_t$) intercepts (also referred to as "fixed effects"(Greene 2003)), which absorb these groups' mean values. Our identification of the effect of PM on health relies on the ability of this adjustment to account for potentially confounding variations in both pollution and health outcomes that are correlated with the day of the week (e.g., weekdays and weekends), season (e.g., flu season from December to February), year (e.g., the outbreak of swine flu pandemic in 2009), or district (e.g.,

differences in industrial infrastructure, health system, demographics, and socioeconomic conditions). With this approach, we assess the relationship between PM and health outcomes by comparing only observations within the same weekday, month, year, and district group; in other words, our estimates describe how health outcomes change as a function of pollution by comparing outcomes on the set of, for example, non-holiday Mondays within March 2012 within a single district of South Korea.(Angrist and Pischke 2008)

Estimation Combining Eqs. A.5 and A.7 with model components described above, we empirically estimate how health costs respond to undifferentiated PM by solving the panel regression:

$$h_{it} = \underbrace{\sum_{k=0}^{28} \left[\bar{\alpha}_k \cdot p_{i(t-k)} + \bar{\beta}_k \cdot p_{i(t-k)}^2\right]}_{\bar{D}(\boldsymbol{p})} + \underbrace{\sum_{n=1}^{4} \bar{\boldsymbol{\gamma}}_n(\mathbf{q}_{nit}) + \sum_{m=1}^{3} \bar{\boldsymbol{\delta}}_m(\mathbf{w}_{mit}) + \bar{\boldsymbol{\zeta}}_{it} + \bar{\theta}_t}_{\bar{f}(\cdot)} + \bar{e}_{it} \tag{A.8}$$

where h_{it} is a health outcome of interest in district i in time t and $p_{i,t-k}$ is the level of the total undifferentiated PM in district i at time $t-k$. Other model variables are as described above. $\bar{\boldsymbol{\gamma}}_n$ and $\bar{\boldsymbol{\delta}}_n$ are flexible nonlinear functions of pollution and meteorological covariates, respectively, that account for the potentially nonlinear impact of these variables on health. For temperature, we use a cross-basis function that models the dose–response function as a three-knot natural cubic spline with knots placed at the 10^{th}, 50^{th}, and 90^{th} percentiles of the temperature distribution and with the lag–response function modeled as a piecewise zero-order spline with knots at lags 1, 2, 4, 7, and 14. For humidity and all non-PM pollutants, we adopt the same lag–response specification but choose an equally-spaced two-knot natural cubic spline for the dose–response function. For precipitation, we also adopt the same lag–response specification but adopt a zero-order spline dose–response function with knots spaced in logs throughout the range of historically observed of daily total precipitation (3.13, 11, 23, 38, 56, 78.5, 101.5, and 129 mm). This structure for the dose–lag–response specifications we adopt for our covariates are motivated by prior findings in the literature(Gasparrini et al. 2015; Carleton et al. 2022) and efficient computation for a high-dimensional model. We also include a rich set of district-by-year-by-month-by-weekday fixed effects described above and indicated by $\bar{\boldsymbol{\zeta}}$; $\bar{\theta}$ is a holiday fixed effect. The error term, $\bar{e}_{it}$, accounts for variation in the outcome not explained by PM and the other covariates. We cluster standard errors at the province level, which accounts for arbitrary forms of temporal auto-correlation in health outcomes within a province between all days in our sample, as well as arbitrary

spatial auto-correlation across all districts within a province.(Newey and West 1987; Conley 1999; S. M. Hsiang 2010)

Computing damages by origin assuming undifferentiated PM To compute partial damages for PM from specific origins using the undifferentiated PM model, we estimate Eq. A.8 and isolate the estimated terms in the damage component $\bar{D}(\cdot)$. We then compute the damages that would be experienced if the entire South Korean population were exposed to a constant specific PM level $\bar{\rho}$. We thus compute damages $\bar{D}(\boldsymbol{p} = \bar{\boldsymbol{\rho}})$ where the vector $\bar{\boldsymbol{\rho}}$ is defined such that all 29 elements (representing lags) are set to the same value—i.e., $\bar{\boldsymbol{\rho}} := (\bar{\rho}, ..., \bar{\rho})$. Fig. 1.3A illustrates the function $\bar{D}(\bar{\boldsymbol{\rho}})$ evaluated across different values of $\bar{\rho}$. We then compute the damages that would be attributed to a specific origin j by evaluating $\bar{D}(\cdot)$ at $\boldsymbol{p} = \bar{\boldsymbol{\rho}}_j$, the average level of PM originating from j that is incident on the South Korean population.

Estimating the health response to PM from different origins

Simultaneously estimating damages for PM from multiple origins (both transboundary and domestic) is the central contribution of this analysis. To do this, we extend the framework and approach described in Eqs. A.5-A.8 to differentiate impacts of PM from different origins, rather than estimating a undifferentiated pooled effect. Conceptually, when accounting for multiple PM sources, we continue to consider health impact that originate from PM damage and other factors:

$$h_{it} = D(\mathbf{P}_{it},\, A(\mathbf{P}_{it})) + f(\mathbf{Q}_{it},\, \mathbf{W}_{it},\, \boldsymbol{\zeta}_{it},\, \theta_t) + e_{it} \tag{A.9}$$

where terms correspond to analogs in Eq. A.5 but with the bar notation removed (to indicated that these are no longer from the undifferentiated model) and with one key substantive difference. In Eq. A.9, PM is represented by the matrix $\mathbf{P}_{it}$, which contains PM values from different origins observed in location i and time from $t-28$ to t, which contrasts with the vector of undifferentiated PM in Eq. A.5. $\mathbf{P}_{it}$ consists of seven vectors describing PM from each origin: South Korea, China, North Korea, dust, wildfire, sea salt, and other sources. Each of the seven vectors is composed of the PM values from their respective origin for the period from $t-28$ to t; hence, $\mathbf{P}_{it}$ is composed of 203 elements.

Accounting for avoidance with multiple PM sources Accounting for avoidance in a model with multiple sources of PM is more complex than in the undifferentiated PM model, since individuals may exhibit a different avoidance response to each type of PM and each type of avoidance can alter the health response to PM

from each origin. Individuals likely respond differently to PM from different origins because they have different chemical and physical properties (e.g., they may smell different or alter visibility in a distinct way). However, it is likely that the total level of PM that is incident on a population, from all sources, also affects their avoidance behavior.

Thus, we adjust the approach in Eq. A.6 to allow for these possible different avoidance responses, one for PM from each origin and for total PM. Further, each type of avoidance can alter the health response for PM from each origin. Replacing the terms that include the undifferentiated PM with those that include the PM levels from heterogeneous origins and adding avoidance terms yields:

$$D(\mathbf{P}_{it},\, A(\mathbf{P}_{it})) = \sum_{k=0}^{28} \underbrace{\left(\sum_{j=1}^{7} g_{jk}(p_{ij(t-k)}) \right)}_{\text{biological response}} \cdot \left(1 - \underbrace{A_{0k}(p_{i(t-k)})}_{\text{total PM avoidance}} - \underbrace{\sum_{j=1}^{7} A_{jk}(p_{ij(t-k)})}_{\text{origin-specific avoidance}} \right) \tag{A.10}$$

In this differentiated framework, there are seven g_{jk} for each lag k, corresponding to the biological responses from the seven origins indexed by j. The second set of parentheses contains multiple avoidance terms. A_0 is similar to $\bar{A}$ in Eq. A.6 in the sense that it captures the degree of avoidance behavior triggered by the total level of the undifferentiated PM. This is important because government agencies provide information on the total level of PM ($p_{i(t-k)} = \sum_{j=1}^{7} p_{ij(t-k)}$) and distribute advisory information based on it. In the case of South Korea, ambient air quality is classified by PM level into four categories: good (0–30 µg/m^3), moderate (31–80 µg/m^3), unhealthy (81–150 µg/m^3), and very unhealthy (151–600 µg/m^3), and air pollution advisories and alerts are issued based on the hourly PM level in extreme cases.(Anderson, Hyun, and Lee 2022) Avoidance via this channel is reflected in the term $A_{0k}(p_{i(t-k)})$.

Eq. A.10 also accounts for the impact of any form of avoidance specifically associated with each origin, since the the extent of induced avoidance likely differs for PM from each origin. For example, as demonstrated in Fig. 1.2, the physical properites of PM differ across origins, resulting in different degrees of salience and coresponding defensive behaviors. For example, sea salt, wildfire smoke, and industrial-origin PM have different optical qualities and thus likely induce different responses. This potential heterogeneity is reflected by independent and separate functions A_{jk} for each PM origin j. As a result, an increase of $p_{ij(t-k)}$ induces the avoidance behavior through both a component of avoidance that is origin-specific (A_{jk}) and also a component

that reflects total PM (A_{0k}).

Expansion of the product in Eq. A.10 yields numerous terms. Some terms are a function of PM from a single origin (e.g., $g_{jk}(p_{ij(t-k)})$ and $g_{jk}(p_{ij(t-k)}) \cdot A_j(p_{ij(t-k)})$). In addition, there are nonlinear cross-terms that describe interactions between PM from differing origins (e.g., $g_{jk}(p_{ij(t-k)}) \cdot A_0(p_{i(t-k)})$ and $g_{jk}(p_{ij(t-k)}) \cdot A_{j'}(p_{ij'(t-k)})$, $j \neq j'$). Thus, under the parsimonious assumption that g_{jk} and A_j are each approximately linear (similar to the approach for undifferentiated PM) expansion of Eq. A.10 yields a model that reduces to containing first and second-order terms for PM from each origin (similar to Eq. A.7) as well as second-order terms that interact PM from different origins ($p_{ij(t-k)} \cdot p_{ij'(t-k)}$). Both sets of terms appear in the estimating equation below.

Estimation Combining Eqs. A.9–A.10, expanding and simplifying the expression, and including the non-parametric trends and controls contained in $f(\cdot)$ from Eq. A.8 yields our complete preferred model specification:

$$h_{it} = \underbrace{\sum_{j=1}^{7}\sum_{k=0}^{28}\left(\alpha_{jk} \cdot p_{ij(t-k)} + \beta_{jk} \cdot p_{ij(t-k)}^2\right) + \sum_{j=1}^{7}\sum_{j' \neq j}\sum_{k=0}^{28} \gamma_{jj'k} \cdot p_{ij(t-k)} \cdot p_{ij'(t-k)}}_{D(\mathbf{P}_{it})} + \underbrace{\sum_{n=1}^{4} \boldsymbol{\gamma}_n(\mathbf{q}_{nit}) + \sum_{m=1}^{3} \boldsymbol{\delta}_m(\mathbf{w}_{mit}) + \boldsymbol{\zeta}_{it} + \theta_t}_{f(\cdot)} + e_{it} \tag{A.11}$$

where h_{it} is health costs and all terms correspond to their analogs in Eq. A.8. Bar notation is removed to indicate where estimated values for parameters will differ from values in the undifferentiated model in Eq. A.8 (since the model is estimated jointly, many parameters will be affected by allowing the effect of PM to be differentiated by origin, even if the specification for these terms does not change).

Analogous to the derivation of Eq. A.7 for undifferentiated PM, $\alpha_{jk} \cdot p_{ij(t-k)}$ and $\beta_{jk} \cdot p_{ij(t-k)}^2$ terms in the first summation correspond to the estimated values that represent $g_{jk}(p_{ij(t-k)}) \cdot \left(1 - A_{0k}(p_{ij(t-k)}) - A_{jk}(p_{ij(t-k)})\right)$ in Eq. A.10. However, there are now seven terms per lag, reflecting the seven origins (j) of differentiated PM. Consistent with the model for undifferentiated PM, there are 28 lags. The second summation of Eq. A.11 contains many cross-terms that interact PM from different origins (j and $j' \neq j$). Each $\gamma_{jj'k}$ corresponds to values for $g_{jk}(p_{ij(t-k)}) \cdot$

$\big(A_{0k}(p_{ij'(t-k)}) + A_{j'k}(p_{ij'(t-k)})\big)$ terms in Eq. A.10. Here, negative coefficient estimates would imply that the impact of PM from j on h_{it} is partially mitigated by avoidance behavior in response from simultaneously incident PM from j'. Other variables are the same as in Eq. A.8.

Computing partial damages by origin To compute partial damage for PM from specific origins accounting for different simultaneous health impacts for each, we estimate parameters in Eq. A.11 and isolate $D(\mathbf{P}_{it})$, the component describing heath damages from simultaneous incidence of PM from multiple different origins. We then estimate what health impacts would be if incident PM from a single origin were ρ and incidence from all other origins were zero. This approach is analogous to the calculations presented for the undifferentiated PM model, however in that case it was not necessary to be explicit about the level of PM from j' when calculating impacts from j; that said, the implicit assumption is identical, enabling a comparison between the two sets of results in Fig. 1.3.

Specifically, to compute partial damages from origin j, we compute $D(\mathbf{P}_{it} = \boldsymbol{\varrho}_j)$ where we define $\boldsymbol{\varrho}_j := (\mathbf{0}, \cdots, \mathbf{0}, \boldsymbol{\rho}_j, \mathbf{0}, \cdots, \mathbf{0})$ and $\boldsymbol{\rho}_j := (\rho_j, \cdots, \rho_j)'$. Thus, we set all 29 terms describing incidence from j to have the constant value ρ_j (i.e., $\mathbf{p}_{ijt} = \boldsymbol{\rho}_j$) and all elements in other vectors describing PM from non-j origins are set at zero (i.e., $\mathbf{p}_{ij't} = \mathbf{0}$, $\forall\ j' \neq j$). We then vary the value of ρ_j for each j independently to trace out a partial damage function for that origin. Fig. 1.3B presents $D(\boldsymbol{\varrho}_j)$ for the top four origins that contribute the most to the observed total PM in South Korea.

Damages from mixtures of PM To compute damages from mixtures of PM from different sources we use an approach that is similar to computing partial damages by origin, but we relax the assumption that PM from all non-j origins is zero. Instead, we continuously vary the quantity of PM incident from two different origins at a time and compute the resulting health damages, setting incidence from other origins to zero. Our calculation of the differentiated PM health damage function $D(\mathbf{P}_{it})$ enables us to compute damages from arbitrary mixtures of origin-specific PM, however we restrict our presentation to two origins at a time for interpretability, since it is visually complex to present more dimensions simultaneously. Nonetheless, in our calculations of total health burden (described below), we compute impacts from observed mixtures of PM from all seven origins simultaneously.

Specifically, we estimate Eq. A.11 and compute damages $D(\mathbf{P}_{it} = \boldsymbol{\varrho}_{jj'})$ where we define $\boldsymbol{\varrho}_{jj'} := (\mathbf{0}, \cdots, \mathbf{0}, \boldsymbol{\rho}_j, \mathbf{0}, \cdots, \mathbf{0}, \boldsymbol{\rho}_{j'}\mathbf{0}, \cdots, \mathbf{0})$, where the j^{th} vector is $\boldsymbol{\rho}_j = (\rho_j, \cdots, \rho_j)$ (i.e., $\mathbf{p}_{ijt} = \boldsymbol{\rho}_j$) and the j'^{th} vector is $\boldsymbol{\rho}_{j'} = (\rho_{j'}, \cdots, \rho_{j'})$ (i.e., $\mathbf{p}_{ij't} = \boldsymbol{\rho}_{j'}$). All other vectors are set at zero (i.e., $\mathbf{p}_{ij''t} = \mathbf{0}$, $\forall j'' \notin \{j, j'\}$). We compute the value

for $D(\cdot)$ while continuously varying values for ρ_j and $\rho_{j'}$ to generate surfaces that describe damages from mixtures of PM from these two different origins.

Fig. 1.4 illustrates the surface of health responses that result from different mixtures of PM from distinct origins. For example, in the left panel of Fig. 1.4, we demonstrate the healthcare expenditure response to the mixtures of PM from South Korea and that from China, the first and second largest contributing origins to PM observed in South Korea, while setting PM from the other origins at zero. Fig. 1.4 visualizes the curvature of the surface $D(\boldsymbol{\varrho}_{jj'})$ with contours ("iso-damage" curves) on the $\rho_j \times \rho_{j'}$ plane. Each contour traces the combinations of $(\rho_j, \rho_{j'})$ that results in a fixed quantity of health expenditure.

Substitutability of components in a PM mixture We evaluate the behavior of health damages as a PM mixture is incrementally altered by considering the "substitutability" of PM constituents in the mixture. The slope of each contour in Fig. 1.4 enables us to evaluate the degree of substitutability for PM from the two origins in the mixture, given a specific baseline level of PM incidence from each $(\rho_j, \rho_{j'})$. Substitutability is the degree to which PM from origin j would need to be reduced in order to offset the health damage resulting from an incremental increase in PM from origin j'. Note that due to the of the nonlinear structure of the damage surface $D(\cdot)$, the substitutability of PM from each origin is a function of the PM load.

Substitutability is equal to the slope of a contour associated with health expenditure G in Fig. 1.4 (or a similar surface). The slope $\frac{\mathrm{d}\rho_j}{\mathrm{d}\rho_{j'}} = -\left(\frac{\partial D(\boldsymbol{\varrho}_{jj'})}{\partial \rho_{j'}}\right) / \left(\frac{\partial D(\boldsymbol{\varrho}_{jj'})}{\partial \rho_j}\right)$ will be -1 if a one-unit increase (decrease) in PM from origin j could be substituted with a one-unit decrease (increase) in PM from origin j' with no change in the health response (holding PM from other origins at zero). A steeper or more negative slope would imply that the health impact of one unit of PM from the origin on the x-axis (PM from origin j) is larger than the impact of one unit of PM on the y-axis (PM from origin j') since a one-unit increase (decrease) of PM from origin j necessitates a larger decrease (increase) of PM from origin j' to achieve the same health response. For example, in the left panel of Fig. 1.4, across the contour corresponding to one million USD, the slope is approximately -2.6, implying that exposure to one additional $\mu g/m^3$ of PM from China has the same incremental impact on health costs in South Korea as exposure to an additional 2.6 $\mu g/m^3$ of PM from South Korea.

Estimation of total PM-specific health damages by origin We use our empirical measurements of PM-specific damages to estimate the total health costs experienced by the South Korean population due to PM emissions from each origin.

We do this by computing health costs due to actual incidence of PM by origin (estimated by partitioning observed PM, described above) relative to the health costs that would be expected if emissions from a single origin j were eliminated. This approach holds the emissions of all non-j at their observed level in both cases, so all that is changed is the PM from j. For example, we compute health costs in South Korea with all origins contributing PM and with contributions of PM from China shut off—with the difference representing the net health impact of PM from China. Specifying the emissions of all non-j origins in both scenarios is important because $D(\cdot)$ is nonlinear in PM from all origins. We believe this approach provides the most accurate estimate for the overall total impact that individual origins have on health in South Korea.

To estimate total harm by origin, we estimate Eq. A.11 and compute damages $D(\cdot)$ for our study period in two scenarios: one with PM equal to actual incidence ($\mathbf{P}_{it}$) and a counterfactual scenario with emissions from origin j set to zero ($\mathbf{P}^0_{ijt}$). The difference in damage between these two is the harm traceable to PM from origin j. Specifically, we compute

$$\widehat{\text{total damage}}_j = \sum_{i \in \mathbf{I}} \sum_{t \in \mathbf{T}} \phi_{it} \cdot \left[D(\mathbf{P}_{it}) - D(\mathbf{P}^0_{ijt}) \right] \tag{A.12}$$

where $\mathbf{P}_{it}$ is the matrix of PM values that are actually incident on poulations (the same values used in estimation) and $\mathbf{P}^0_{ijt}$ is the same, except that the PM values corresponding to origin j are set at zero (i.e., $\mathbf{p}_{ijt} = (p_{ijt}, \cdots, p_{ij(t-28)}) = \mathbf{0}$). For example, for the origin with index $j = 1$, $\mathbf{P}^0_{i1t} = (\mathbf{0}, \mathbf{p}_{i2t}, \cdots, \mathbf{p}_{i7t})$. Therefore, the difference $D(\mathbf{P}_{it}) - D(\mathbf{P}^0_{ijt})$ is the average per capita damages in district i on day t attributable to origin j. This value is then scaled by ϕ_{it}, the population in district i at time t, and aggregated across days $t \in \mathbf{T}$ and regions $i \in \mathbf{I}$. The bounds of aggregation vary, with values in Fig. 1.5A–C aggregating over specific years (and all districts) and Fig. 1.5D–F aggregating across districts within a province (and all years). Table 1.1 aggregates across all districts and all years in the sample.

Extended Data

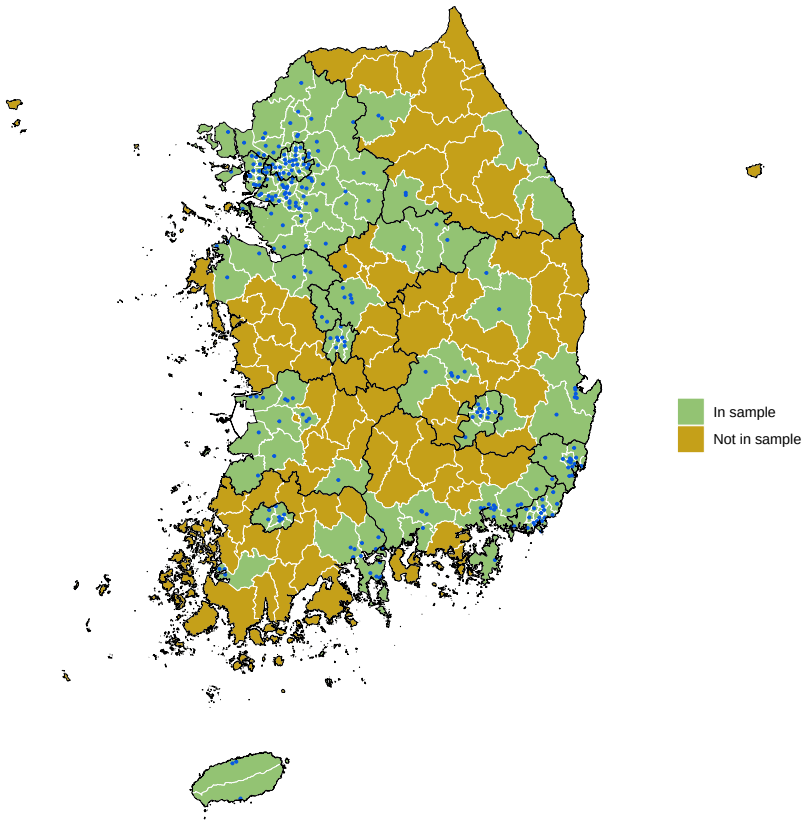

Figure A1: **Boundaries of districts and provinces; locations of air pollution monitors**

Notes: Districts in our main model (those meeting minimum data length and monitor coverage requirements) are shown in green. Borders between districts within a province are shown in white, and borders between provinces are shown in black. Pollution monitors used in the main analysis are shown as blue points.

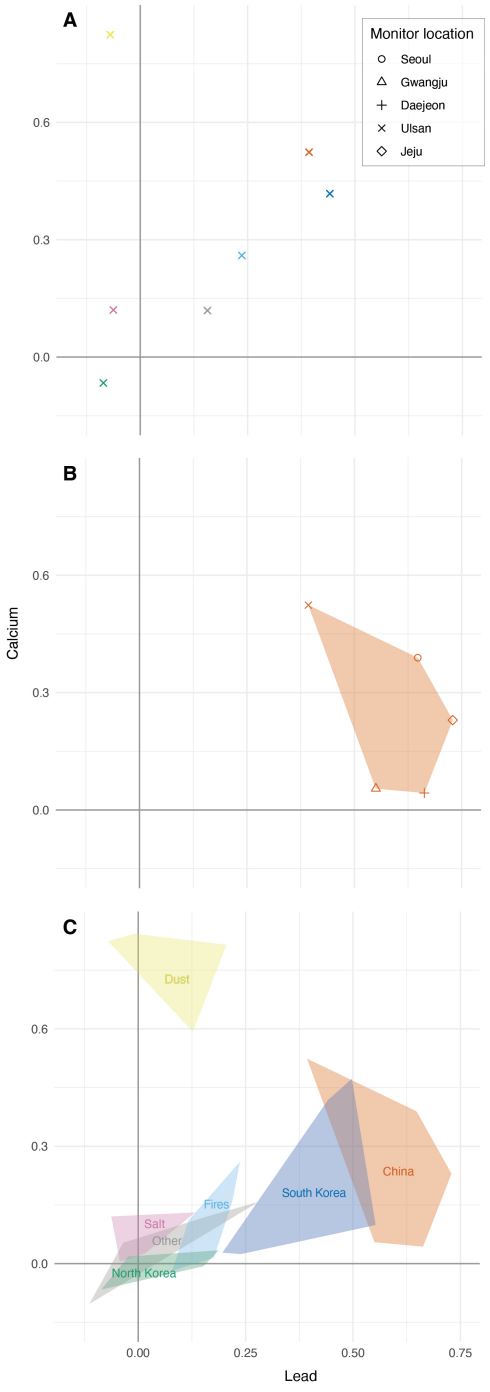

Figure A2: **Extended Explanation of Figure 1.2**

Notes: (A) Partial correlations between PM of each origin and the concentrations of atmospheric lead (x-axis) and calcium (y-axis) using only data from the chemistry monitor in Ulsan. (B) Partial correlations between PM from a single origin (China) and atmospheric lead (x-axis) and calcium (y-axis) using data from all five chemistry monitors; a convex hull is drawn around these points to aid pattern recognition. (C) depicts these convex hulls for PM of each origin and is the form shown in Figure 1.2.

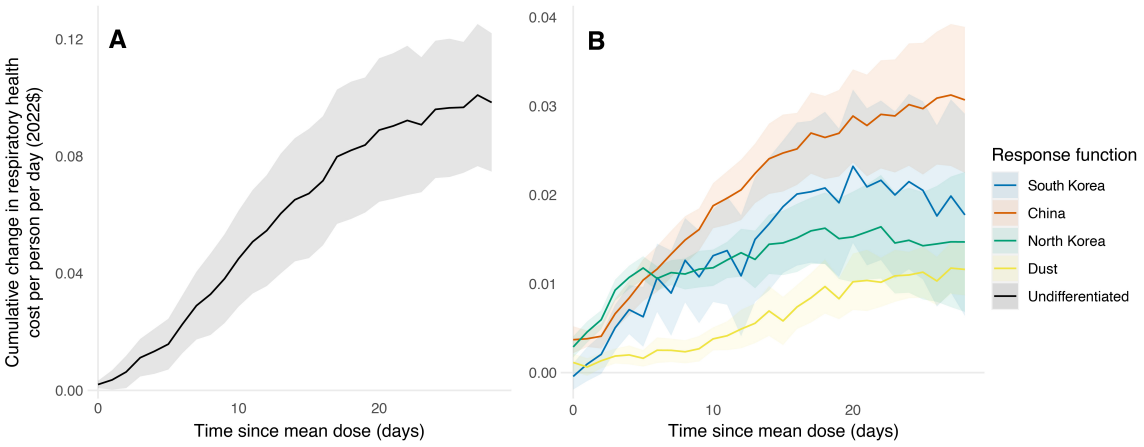

Figure A3: **Lag–response relationships.**

Notes: (A) The undifferentiated lag–response relationship, calculated with levels of all sources at their mean values (is shown only for comparison and is not used in our calculations for the attribution of respiratory health spending to PM origins). For full model specification, see Methods. (B) The cumulative lag–response relationships for PM by origin.

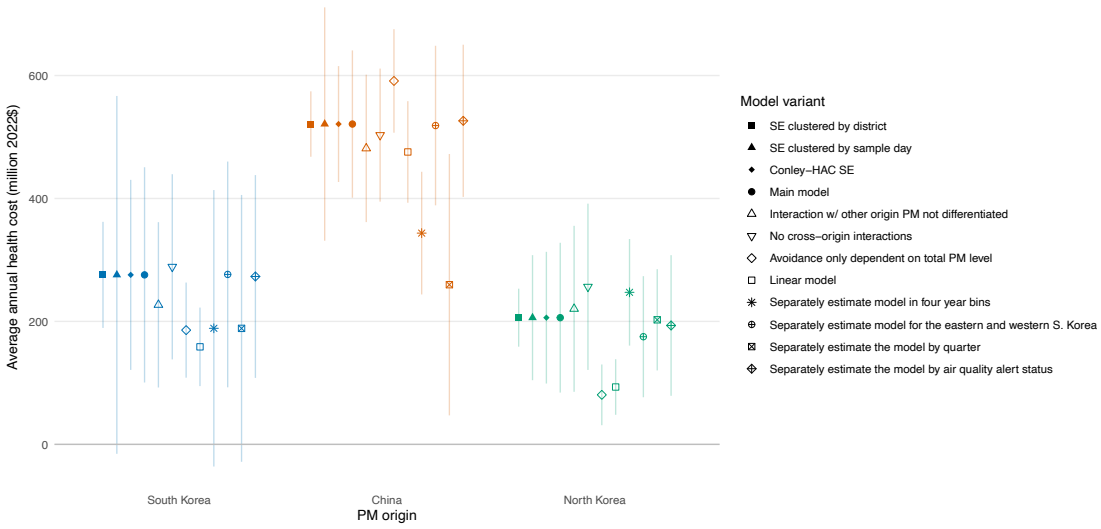

Figure A4: **Model robustness checks.**

Notes: For ease of comparison, the model is estimated using alternate specifications and model results are combined with estimated exposures to determine differences in average annual attributed health costs by origin. Line ranges indicate 95% confidence intervals. Results for the main model, which follows Eq. A.11 with standard errors clustered at the province level, are shown fourth from the left. The three estimates to the left of the main estimates show sensitivity to changing the method used for calculating standard errors: for the first set of estimates, standard errors are clustered at the district level; for the second set of estimates, standard errors are clustered at the day level; for the third set, standard errors are calculated using a spatial heteroskedasticity and autocorrelation robust (Conley-HAC) method.(Conley 1999) Estimates 5 through 8 present variants of Eq. A.11, but with a modified functional form that is progressively less flexible: for the fifth set of estimates, the model includes linear and quadratic terms for each origin of PM and interactions between each origin of PM and the total quantity of PM from every other origin (interactions with other PM are not differentiated); for the sixth set of estimates, the model includes only linear and quadratic terms for PM of each origin (no cross-origin interactions); for the seventh set, the model includes only a linear term for each origin of PM and an interaction of that term with the total level of PM (the curvature of each origin's dose–response function is dependent only on the total level of ambient PM); for the eighth set, the model includes only a linear term for each origin of PM. Estimates 9 through 12 separately estimate Eq. A.11 by four year bins, for the eastern and western half of South Korea, for each quarter of the calendar year, and for days when air quality alerts were and were not issued, respectively.

Appendix B

Supplementary Information for Chapter 2

Table B1: Percentage of Wind Direction by Province

Province	C	N	NNE	NE	ENE	E	ESE	SE	SSE	S	SSW	SW	WSW	W	WNW	NW	NNW
Seoul	16.3	4.5	3.3	5.2	9.1	4.6	3.2	1.2	1.9	2.9	8.6	6.8	4.2	7.6	8.1	7.4	5.1
Busan	7.2	6.2	8.4	9.2	6.1	4.4	2.2	4.1	2.2	4.3	6.3	5.2	3.5	7.7	8.7	8	6.3
Daegu	16.7	7.7	6	4.5	1.8	4	5.7	2.4	2.3	6.9	2.7	3.4	5.6	7.5	6.2	8.4	8.2
Incheon	32.4	3.1	1.1	1.7	1.8	5.9	6.2	3.9	2.5	2.5	2.8	2.9	4.5	11.3	9.3	3.9	4.2
Gwangju	22.5	4.8	6.6	4	4.1	2.6	2.4	2.8	13.1	8.5	3.4	1.9	2	3	4.4	7.9	6.1
Daejeon	54	4.7	2.7	0.8	1.5	1.9	2.9	2	2.4	2.9	3.6	4.7	3.1	2.6	2	3.1	5.3
Ulsan	14.2	7.7	5.7	8	4.3	3.1	3.5	2.6	1.2	1.6	4.7	6.8	8.7	4.6	5.8	7.8	9.8
Gyeonggi-do	43	4.3	3.1	3.5	4	3.3	2.9	1.7	2.3	3.2	4.7	4.3	3.1	5.5	4.4	3.5	3.2
Gangwon-do	54	5.9	2.7	1.2	1.1	1.7	2.4	0.9	1.1	2.3	2.9	5.7	3.7	6.5	1.7	3.6	2.8
Chungcheongbuk-do	68.2	3.5	2.5	0.3	0.9	1.9	1.6	1.8	1.3	1.7	2.5	1.4	1	3.8	2.7	3	1.7
Chungcheongnam-do	25	7.9	2.3	3	3.6	4	3.8	3.1	2.4	7	11.1	5.4	1.2	2.2	4.4	8	5.6
Jeollabuk-do	51.4	6.9	3.3	3.3	4.1	4	3.8	1.3	2	3.5	1.6	1.4	1.5	1.6	2.7	3.1	4.6
Jeollanam-do	32.8	9.4	3.6	4.6	5.1	4	2.1	3.9	3.9	2.5	1.8	1.7	1.4	1.8	5.6	10.4	5.2
Gyeongsangbuk-do	53.7	4	2.5	1.8	2.2	3.2	1.4	0.5	0.5	3	2.3	1.3	0.6	5.4	5.3	8.8	3.5
Gyeongsangnam-do	53.7	7.5	2.6	2.8	4.9	2.5	3.7	2.4	1.9	2.1	1.5	2.2	0.3	0.5	1.9	4.9	4.7
Jeju	6.2	12.1	8.8	5.2	5	6.6	4.6	1.9	2.8	6.9	4	3.4	1.1	1.2	2.2	9.9	18.1

Appendix C

Supplementary Information for Chapter 3

C.1 Generalization of Theoretical Framework

For ease of exposition we present a model in which average daily PM is the running variable, but in our application the running variable is the maximum 2-hour minimum PM level (over one day). Here we show that our model's conclusions hold if the running variable is an arbitrary function of daily PM.

Suppose that individuals base their behavior on daily mean PM, $\overline{pm}$, while the running variable is a different function of daily pm, $f(pm)$. The RD estimand then compares days on which $f(pm)$ is just above the alert threshold ($f(pm) \downarrow c$) to those on which it is just below the alert threshold ($f(pm) \uparrow c$).

Specify individual beliefs as

$$\overline{pm}_i = \begin{cases} pm^{avg} & \text{if} \quad f(pm) = f(pm) \uparrow c \\ pm^{hi} & \text{if} \quad f(pm) = f(pm) \downarrow c \end{cases}$$

where pm^{avg} represents average daily mean PM conditional on $f(pm)$ being below the threshold c and pm^{hi} represents average daily mean PM conditional on $f(pm)$ being above the threshold c. Let pm^c be average daily mean PM conditional on $f(pm) = c$. For our bounding exercise we assume that $pm^{hi} \approx pm^c$, or at least that $|pm^{hi} - pm^c| << |pm^{avg} - pm^c|$. This representation is a reasonable approximation of our actual PM data. For example, in our PM2.5 data, $pm^{avg} = 22.7$, $pm^{hi} = 66.7$, and $pm^c = 57.5$. Thus pm^{hi} is much closer to pm^c than pm^{avg} is. More generally, the approximation only needs to be sufficiently accurate that the alerts do not cause individuals to behave *less* optimally than they would absent the alert's information.

Individuals maximize utility by choosing activity levels $a_i = \text{argmax}_a \, U_i(a, \overline{pm}_i)$. Then

$$U_i = \begin{cases} U_i(a_i(pm^{avg}), pm^c) & \text{if} \quad f(pm) = f(pm) \uparrow c \\ U_i(a_i(pm^{hi}), pm^c) & \text{if} \quad f(pm) = f(pm) \downarrow c \end{cases}$$

An individual's private change in utility from PM crossing the alert threshold is

$$\Delta \, U_i = U_i(a_i(pm^{hi}), pm^c) - U_i(a_i(pm^{avg}), pm^c) = \\ [b_i(a_i(pm^{hi})) - b_i(a_i(pm^{avg}))] - s_i^{pvt}[p_s(a_i(pm^{hi}), pm^c) - p_s(a_i(pm^{avg}), pm^c)].$$

Naturally $\Delta \, U_i \geq 0$ since $pm^{hi} \approx pm^c$ and $a_i = \text{argmax}_a \, U_i(a, pm_i)$ — i.e. more accurate PM information can only (weakly) increase the individual's utility — but

accurately quantifying ΔU_i is challenging even with good data on s_i^{pvt}. This challenge arises because it is difficult to estimate $b_i(a_i)$, the benefits of different activities (and thus the costs of avoidance behaviors); a_i may be high dimensional, and researchers rarely have data on all, or even most, elements of a_i.

C.2 Additional Data Notes

Procedure for Calculating Running Variable: To be consistent with the particulate pollution alert system, we first calculate the 2-hour-minimum of particulate matter ($PM_{dh}^{2h\ min}$) in hour h on day d. Next, we obtain a daily maximum of 2-hour-minimum PM measures in each hour and subtract the alert thresholds (c), where $c = 150$ in case of PM10 and $c = 90$ (or 75 since March 27th of 2018) in case of PM2.5. These transformations generate the daily running variables (rv_d). Last, we utilize the running variables rounded to the nearest integer. The process may be summarized as follows:

1. $PM_{dh}^{2h\ min} = \min_h\{PM_{d(h-1)}, PM_{dh}\} \quad (d : date,\ h : hour)$
2. $PM_{d}^{2h\ min\ max} = \max_d\{PM_{dh}^{2h\ min}\}$
3. $rv_d = PM_{d}^{2h\ min\ max} - c$
4. Rounding rv_d to the nearest integer

As expected, our running variable has a tight correlation with PM10 and PM2.5, respectively. It is thus reasonable to believe the running variable captures the relationship between particulate pollution and health expenditures in the main regression. Nevertheless, we also control for different combinations of air quality variables as a robustness check (Appendix Table C12).

Cost Evaluation of Air Pollution Alert System: To determine alert system costs, we first searched for reports about environmental expenditures from the seven major cities in our study. We identified a category entitled "Air Pollution Management System - Public Management Cost." Among the items listed under this category, we selected the ones related to the air pollution alert system (Appendix Table C15). We considered not only directly related items, such as the cost of issuing alerts via SMS, but also broadly related items, such as the management cost of air pollution monitors. Appendix Table C16 presents the total costs of the alert system for each city.

C.3 Additional Robustness Checks

Manipulation Test: In other contexts researchers have found evidence that pollution measurements are manipulated to remain below certain thresholds. While the officials charged with determining alerts in our context face no obvious incentives to manipulate PM measurements, we nevertheless check to see whether there is any "missing" density of the running variable above the RD threshold. Appendix Figures C1 and C2 plot the distribution of the daily and hourly running variables, respectively. In both graphs, we see no unusual decrease in the density of observations above the threshold. In addition, we test for discontinuities in the density of the running variable at the RD threshold using the procedure in Cattaneo, Jansson, and Ma (2018). We fail to reject the null hypothesis of continuity in the density of the running variable (2016 to 2017) for bandwidths of 16, 20, and 24 units ($p = 0.43,\ 0.49,$ and 0.6 respectively) and the running variable (2017 to 2018) for bandwidths of 16, 20, and 24 units ($p = 0.46,\ 0.14,$ and 0.1 respectively).

Control Continuity: Our main control variables are weather variables. We test the continuity of the two weather variables in our model, temperature and precipitation, at the RD threshold. Appendix Figure C6 shows the average temperature and precipitation per district and day-of-the-sample plotted against the running variable, which lies in the interval $[-40, 40]$. There is no visual evidence of a discontinuity in either weather variable at the RD threshold.

Asymmetry in the Thresholds for Alert Issuance and Cancellation: Following the issuance of an alert, the running variable generally needs to drop substantially below the RD threshold before the alert gets canceled. To test the sensitivity of our results to this asymmetry in the issuance and cancellation of alerts, we consider two sample restrictions. First, we trim the sample to exclude alert days following the first day of an air quality alert and report parameter estimates obtained from the main specification. Alternatively, we drop out alert days on which the running variable is below zero. The results of these exercises, reported in Appendix Table C10, suggest that our estimates are not sensitive to the asymmetry in the issuance and cancellation thresholds.

No Treatment During Nighttime Hours: It seems unlikely that most individuals modify their behavior in response to an air quality alert issued during nighttime hours. As a robustness check, we estimate FRD regressions when dropping district-

days on which alerts were issued between 6 AM and 9 PM or between 8 AM and 8 PM. The results, reported in Appendix Table C10, are of similar magnitude to the estimates from our base model.

Alternative RD Specifications: Appendix Table C11 reports estimates from alternative RD specifications that control for a quadratic of the running variable. The health expenditure effects are of similar magnitude and statistical significance as our main results. We also check robustness to specifications in which we control for a quadratic in temperature or in which we control for year and month fixed effects instead of year-by-month fixed effects. Both sets of results are qualitatively similar to our main estimates.

Addition of Different Air Quality Variables We interpret our results as representing benefits of avoidance behavior. If the alerts had a direct effect on pollution levels, however, then our results would represent a combination of the benefits of avoidance behavior and lower ambient pollution levels. Appendix Table C5 demonstrates that there is no discontinuous change in ambient PM levels at the RD threshold. As an extra check we estimate specifications, reported in Appendix Table C12 that control for PM10, PM2.5, both PM measures, or the AQI. The addition of these air-quality controls has virtually no impact on our RD estimates.

Different Standard Error Clusters: The panel nature of our data is atypical for a RD design. We thus consider the impacts of different clustering choices for the standard errors. Appendix Table C13 reports the standard errors clustered at different combinations of spatial and time units. All coefficients that were significant in Tables 3.4 and 3.5 remain significant across all clustering choices.

Spillover Effects: Our RD estimates could be attenuated if alerts affect health spending in adjacent regions. To address this concern, we estimate the impact of PM alerts in the nearest alert region to region r on the outcome variables in region r. Appendix Table C14 demonstrates that the RD estimates are not statistically significant across all three age groups, suggesting an absence of spillover effects of the alerts to other regions.

Falsification Test: As the final robustness check, we estimate effects at alternative "placebo" RD thresholds. Specifically, we construct alternative running variables by

subtracting 20, 30, or 50 units from PM10 and PM2.5 concentration. All of the estimates for alternative running variables are statistically insignificant (Appendix Table C14), as would be expected if our research design is valid.

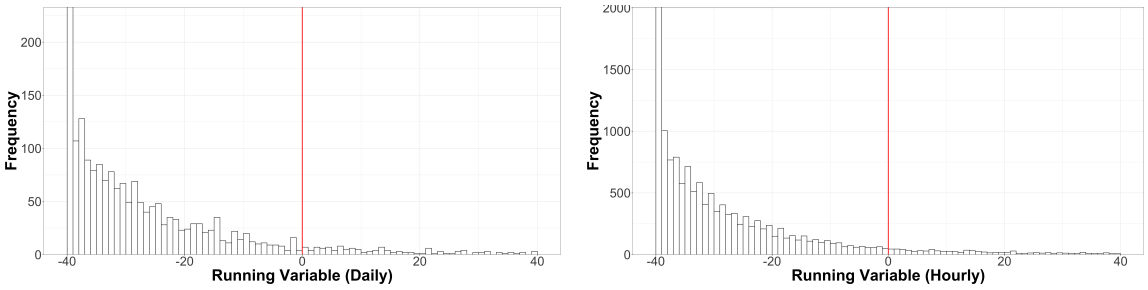

Figure C1: Histogram of running variable (2016–2017)

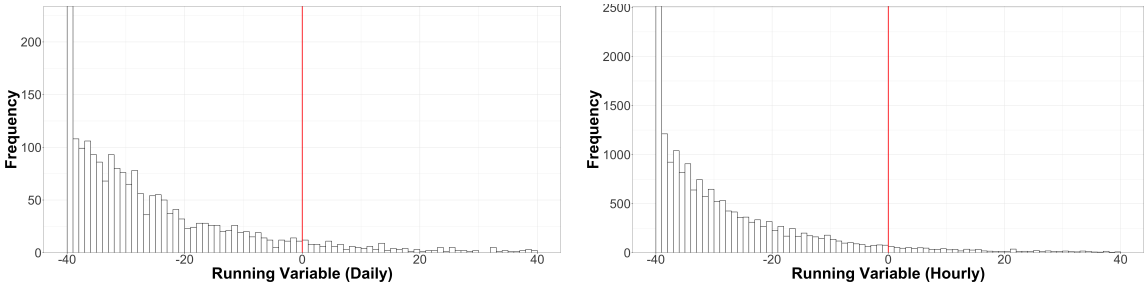

Figure C2: Histogram of Running Variable (2017–2018)

Notes: The red line denotes the RD threshold of zero.

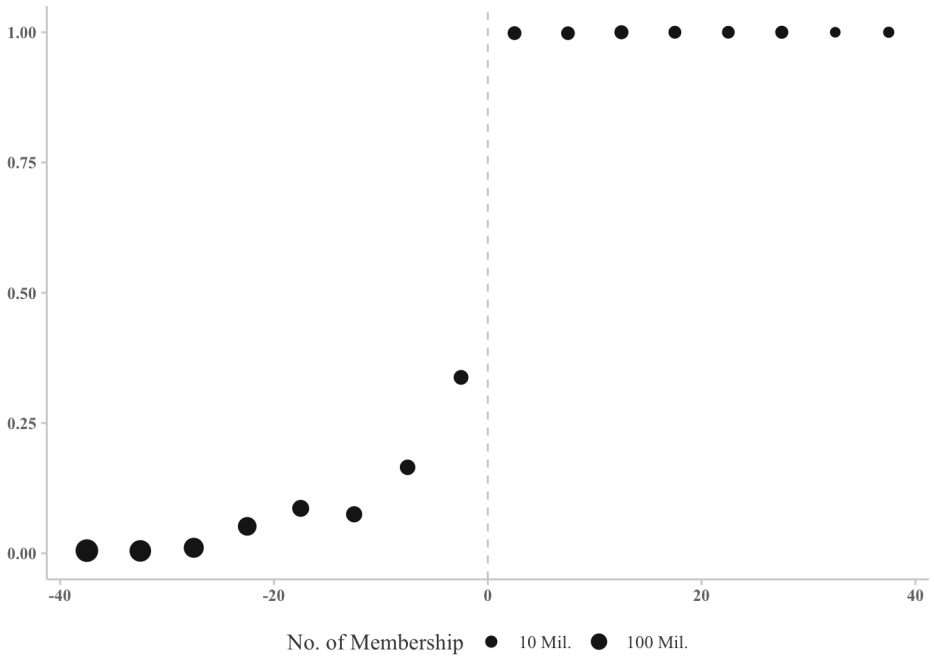

Figure C3: Treatment Discontinuity (2017−2018)

Notes: Each point represents the population-weighted average of observations in a given bin, the width of which is five. The y-axis indicates the average probability of a particulate matter advisory. The x-axis indicates the value of the running variable (a threshold-normalized function of PM).

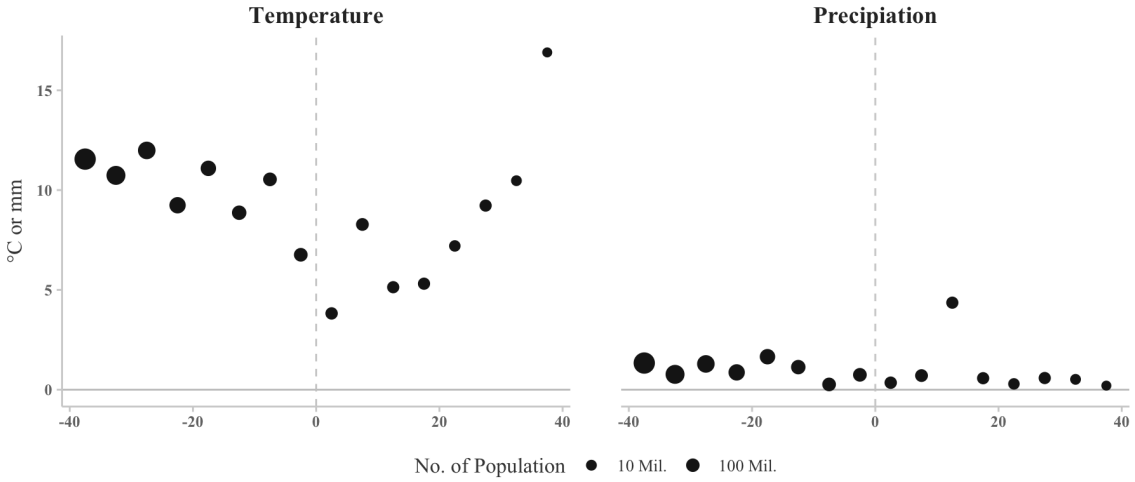

Figure C4: Continuity of Weather Control Variables (2016−2017)

Notes: Each point represents the population-weighted average of observations in a given bin, the width of which is five. The y-axis indicates the average temperature or rainfall. The x-axis indicates the value of the running variable (a threshold-normalized function of PM).

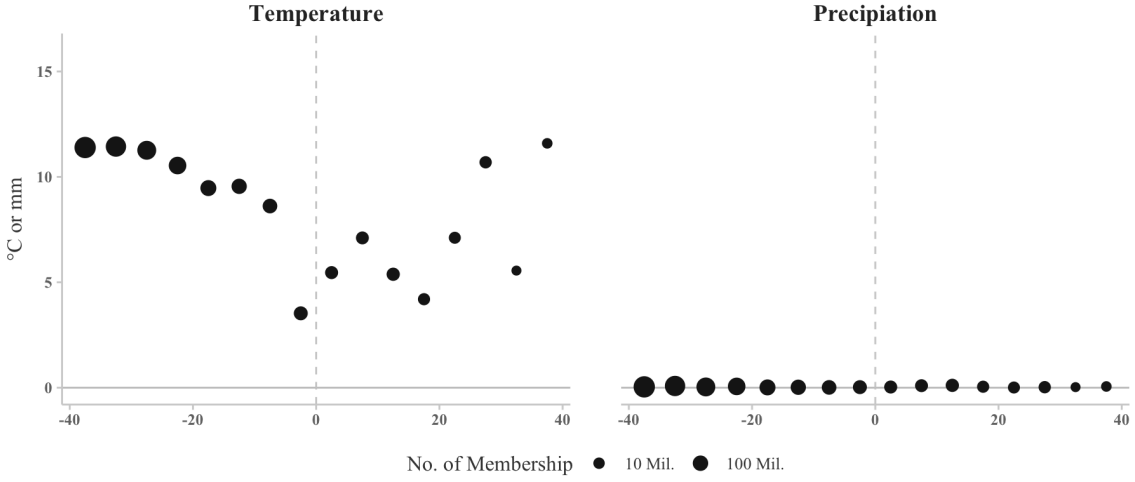

Figure C5: Continuity of Weather Control Variables (2017−2018)

Notes: Each point represents the population-weighted average of observations in a given bin, the width of which is five. The y-axis indicates the average temperature or rainfall. The x-axis indicates the value of the running variable (a threshold-normalized function of PM).

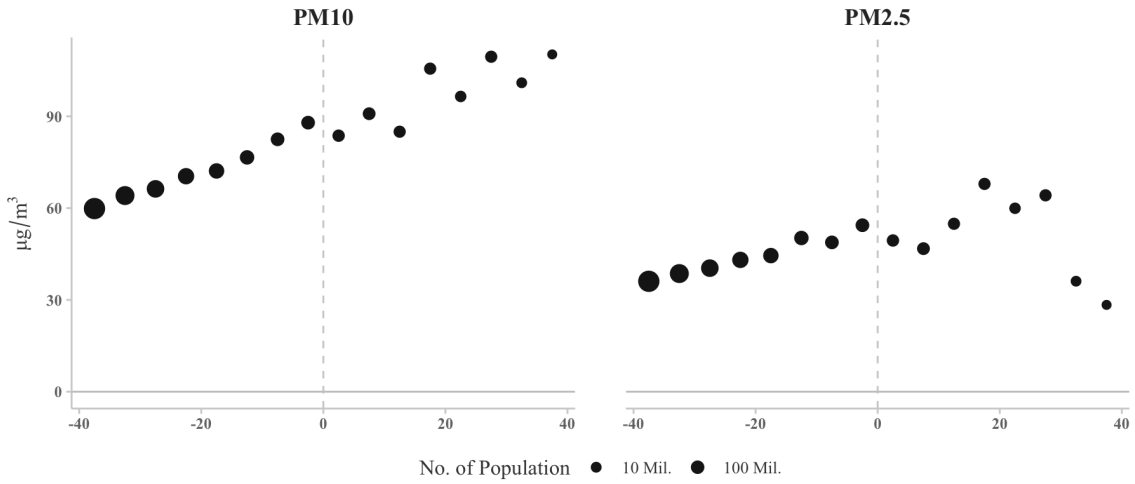

Figure C6: Continuity of PM variables (2016−2017)

Notes: Each point represents the population-weighted average of observations in a given bin, the width of which is five. The y-axis indicates the weighted average level of daily PM10 or PM2.5 The x-axis indicates the value of the running variable (a threshold-normalized function of PM).

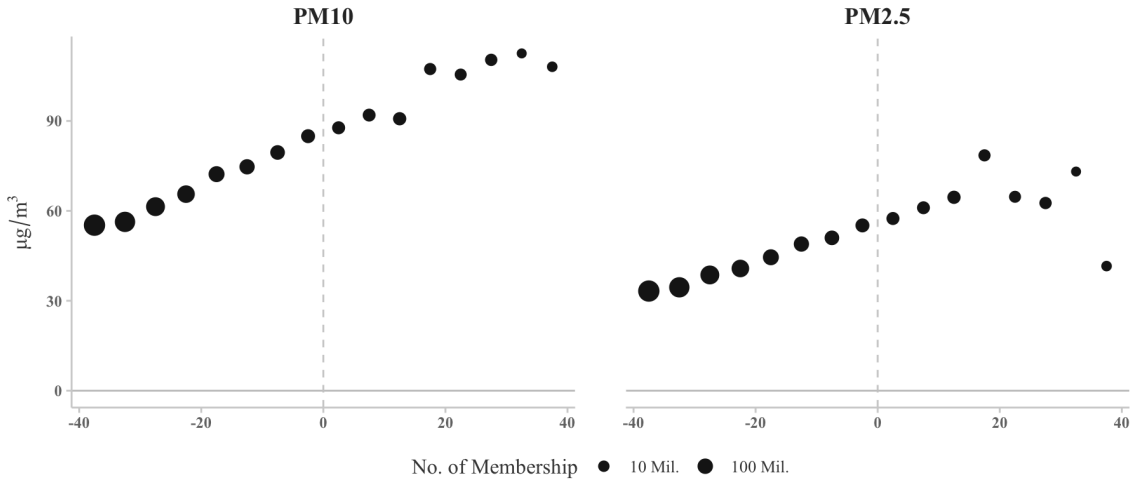

Figure C7: Continuity of PM variables (2017−2018)

Notes: Each point represents the population-weighted average of observations in a given bin, the width of which is five. The y-axis indicates the weighted average level of daily PM10 or PM2.5. The x-axis indicates the value of the running variable (a threshold-normalized function of PM).

Table C1: Examples of Alert Systems in the World

Alert Policies	Country	Regions Covered	Estimated Population Covered (mil.)	Related Links
4-tier Alert System	China	All	1,387.2	LINK
Particulate Matter Alerts	South Korea	All	51.7	LINK
EnviroFlash	US	Many	193.8	LINK
Public Weather Alerts	Canada	Ontario	14.6	LINK
Air quality alerts	Australia	New South Wales	8.2	LINK
Sistema de Monitoreo Atmosférico	Mexico	Mexico City	8.8	LINK
Haze Alerts	Singapore	All	5.6	LINK
Pollution Alerts	UK	All	66.7	LINK

Notes: This list includes examples of prominent air-quality alert systems worldwide, but it is not comprehensive. The Chinese 4-tier Alert system coverage was calculated by summing the populations of the second-tier administrative units in which air pollution monitors are installed. EnviroFlash coverage was calculated based on the population in counties where the US EPA manages air pollution monitors. All links were checked on 20 September 2021.

Table C2: Summary Statistics

Treatment & Covariates	Full Sample				Bandwidth = 40			
	Mean	SD	Min	Max	Mean	SD	Min	Max
Alert	0.04	0.2	0	1	0.1	0.3	0	1
PM10 ($\mu g/m^3$)	42.1	22.3	3.0	253.9	65.8	20.2	14.9	160.1
PM2.5 ($\mu g/m^3$)	23.6	13.9	1.1	123.9	41.0	14.7	6.6	123.9
Temperature (°C)	13.5	10.2	-17.3	34.4	10.5	8.5	-9.6	34.4
Precipitation(mm)	0.1	0.5	0	13.1	0.1	0.2	0	3.8

Notes: The number of district-day observations is 53,290 (73 districts, 760 days, 2017−2018) and 11,324 for the full sample and the sample based on a bandwidth of 40, respectively.

Table C3: Types of Medical Institutions in South Korea

Levels of Institutions	Types of Institutions	Description
Tertiary	Tertiary General Hospitals	· The Minister of Health and Welfare may designate a general hospital providing highly specialized medical services for treating serious diseases as a tertiary hospital among general hospitals.
Secondary	General Hospitals	· A general hospital shall have at least 100 beds.
	Hospitals	· Hospitals shall have at least 30 beds or beds for long-term care.
Primary	Public Health Centers	· Publicly owned regional healthcare institutions
	Clinic	· A medical institution in which a doctor, dentist, or oriental medical doctor provides medical services primarily to outpatients

Sources: Korea Law Translation Center, Korea Legislation Research Institute https://elaw.klri.re.kr/kor_service/lawView.do?hseq=53532&lang=ENG, accessed on Sep 15, 2021

Notes: Source link provides additional details on the definitions of each institution type.

Table C4: Out-of-pocket Payments for Outpatient Visits in the South Korean Healthcare System

Type of Institutions	Cases	Out-of-pocket Payments
Tertiary Hospitals	Normal Patients	· 100% of consultation fee + 40% of remaining medical expenses · (Pregnant Women) 40% of total medical expenses · (Age $<$ 1) 20% of total medical expenses
General Hospitals	Urban Areas	· 50% of total medical expenses · (Pregnant Women) 40% of total medical expenses · (Age $<$ 1) 20% of total medical expenses
	Rural Areas	· 45% of total medical expenses · (Pregnant Women) 40% of total medical expenses · (Age $<$ 1) 20% of total medical expenses
Hospitals	Urban Areas	· 40% of total medical expenses · (Pregnant Women) 20% of total medical expenses · (Age $<$ 1) 10% of total medical expenses
	Rural Areas	· 35% of total medical expenses · (Pregnant Women) 40% of total medical expenses · (Age $<$ 1) 20% of total medical expenses
Clinics	Age $\geq$ 65	· ₩1,500 when total medical expenses $\leq$ ₩15,000 · 10% when total medical expenses $>$ ₩15,000 & $\leq$ ₩20,000 · 20% when total medical expenses $>$ ₩20,000 & $\leq$ ₩25,000 · 30% when total medical expenses $>$ ₩25,000
	Age $<$ 65	· 30% of total medical expenses · (Pregnant Women) 10% of total medical expenses · (Age $<$ 1) 5% of total medical expenses
Public Health Centers	Age $\geq$ 6	· 30% when total medical expenses $>$ ₩12,000 · ₩500−₩2,200 depending on cases when total medical expenses $\leq$ ₩12,000
	Age $<$ 6	· 21% when total medical expenses $>$ ₩12,000 · ₩500−₩2,200 depending on cases when total medical expenses $\leq$ ₩12,000

Sources: Health Insurance Review and Assessment Service (HIRA) of South Korea https://www.hira.or.kr/dummy.do?pgmid=HIRAA030056020110 (in Korean), accessed on Sep 10, 2021

Notes: ₩ indicates Korean Won (KRW). 10,000 KRW is equivalent to approximately 8.7 USD. While this table shows general out-of-pocket payment ratios, it does not describe every specific case that could result in different ratios of out-of-pocket payments. For more details, refer to source link above.

Table C5: FRD Results using Particulate Matter as Dependent Variables

	Bandwidths		
Dependent Variable	16	20	24
PM10	0.331	1.685	4.190
	(4.989)	(4.112)	(3.362)
PM2.5	-3.613	-4.738	-4.098
	(4.363)	(4.692)	(4.590)

Notes: This table reports results from six 2SLS local-linear regressions. The dependent variable in all regressions is PM10 or PM2.5, measured in cents $\mu g/m^3$, and the independent variable of interest is an advisory indicator. All regressions control for the running variable, an interaction between the running variable and the indicator for the running variable being above the RD threshold, temperature, precipitation, and year-by-month and day-of-week fixed effects. The level of observation is the district by day, and observations are population weighted. Parentheses contain standard errors clustered by the day of sample. The bandwidth varies across columns as noted.

Table C6: Optimal Bandwidth

Dependent Variable	Optimal Bandwidth
Resp. (All)	18.321
Resp. (Adults)	19.293
Resp. (Older Adults)	20.526
Resp. (Minors)	17.135
Cardio. (All)	21.084
Cardio. (Adults)	21.354
Cardio. (Older Adults)	20.611
Cardio. (Minors)	17.726
Credit (All)	24.776
Credit (Restaurant)	24.222
Credit (Fashion)	20.906
Credit (Travel)	24.586
Resp. (All, 3-Day Rolling Sum)	17.088
Resp. (Adults, 3-Day Rolling Sum)	18.185
Resp. (Older Adults, 3-Day Rolling Sum)	22.185
Resp. (Minors, 3-Day Rolling Sum)	17.466
Cardio. (All, 3-Day Rolling Sum)	28.363
Cardio. (Adults, 3-Day Rolling Sum)	24.260
Cardio. (Older Adults, 3-Day Rolling Sum)	34.249
Cardio. (Minors, 3-Day Rolling Sum)	18.898
Credit (All, 3-Day Rolling Sum)	23.583
Credit (Restaurant, 3-Day Rolling Sum)	23.752
Credit (Fashion, 3-Day Rolling Sum	19.515
Credit (Travel, 3-Day Rolling Sum)	24.673

Notes: This table reports "optimal" bandwidths for different dependent variables, computed using methods from calonico2014robust, calonico2015rdrobust.

Table C7: RD Results for Respiratory Diseases, With Visits to Tertiary General Hospitals

	Age Groups			
	Minors (0-19)	Adults (20-64)	Older Adults (65+)	All
Reduced form				
$\mathbb{1}(RV >= 0)$	−8.804	−2.260	−2.532	−3.446
	(2.344)	(1.385)	(1.655)	(1.426)
	[2.887]	[1.381]	[1.866]	[1.505]
RV	−0.086	−0.045	0.011	−0.044
	(0.145)	(0.044)	(0.064)	(0.057)
	[0.142]	[0.045]	[0.072]	[0.058]
RV $\cdot \mathbb{1}(RV >= 0)$	0.627	0.218	0.173	0.270
	(0.166)	(0.112)	(0.131)	(0.109)
	[0.227]	[0.079]	[0.114]	[0.088]
2SLS				
$\mathbb{1}(RV >= 0)$	−14.062	−3.639	−4.095	−5.543
	(4.662)	(2.184)	(2.696)	(2.367)
	[5.484]	[2.134]	[2.829]	[2.450]
RV	0.020	−0.018	0.021	−0.003
	(0.204)	(0.063)	(0.084)	(0.084)
	[0.170]	[0.055]	[0.086]	[0.071]
RV $\cdot \mathbb{1}(RV >= 0)$	0.581	0.208	0.162	0.254
	(0.237)	(0.110)	(0.127)	(0.118)
	[0.297]	[0.079]	[0.110]	[0.104]
Adjusted R^2	0.839	0.866	0.796	0.897
N	2,530			

Notes: This table reports results from four reduced-form local-linear regressions (top panel) and four 2SLS local-linear regressions (bottom panel). The dependent variable in all regressions is respiratory disease expenditures for the relevant age group, *including visits to tertiary general hospitals* and measured in cents per capita (11.5 KRW = 0.01 USD). The independent variable of interest in the reduced-form (2SLS) regressions is an indicator for the running variable being above the RD threshold (advisory indicator). All regressions control for the running variable, an interaction between the running variable and the indicator for the running variable being above the RD threshold, temperature, precipitation, and year-by-month and day-of-week fixed effects. The level of observation is the district by day, and observations are population weighted. Parentheses (square brackets) contain standard errors clustered by the running variable (day of sample). The bandwidth is set to 20 in all regressions.

Table C8: RD Results for Cardiovascular Diseases, With Visits to Tertiary General Hospitals

	Age Groups			
	Minors (0-19)	Adults (20-64)	Older Adults (65+)	All
Reduced form				
$\mathbb{1}(RV >= 0)$	−0.096	−1.877	−5.992	−2.133
	(0.054)	(0.527)	(2.133)	(0.618)
	[0.062]	[0.509]	[2.421]	[0.681]
RV	0.005	0.059	0.216	0.065
	(0.003)	(0.025)	(0.100)	(0.025)
	[0.003]	[0.021]	[0.118]	[0.028]
RV $\cdot \mathbb{1}(RV >= 0)$	−0.003	0.012	−0.032	0.014
	(0.007)	(0.038)	(0.155)	(0.042)
	[0.008]	[0.039]	[0.214]	[0.052]
2SLS				
$\mathbb{1}(RV >= 0)$	−0.153	−3.022	−9.691	−3.431
	(0.095)	(1.024)	(3.930)	(1.168)
	[0.113]	[0.789]	[3.786]	[1.073]
RV	0.006	0.082	0.291	0.091
	(0.006)	(0.082)	(0.102)	(0.033)
	[0.004]	[0.025]	[0.129]	[0.033]
RV $\cdot \mathbb{1}(RV >= 0)$	0.003	0.003	−0.058	0.005
	(0.007)	(0.044)	(0.147)	(0.041)
	[0.007]	[0.045]	[0.227]	[0.057]
Adjusted R^2	0.022	0.799	0.854	0.874
N	2,530			

Notes: This table reports results from four reduced-form local-linear regressions (top panel) and four 2SLS local-linear regressions (bottom panel). The dependent variable in all regressions is cardiovascular disease expenditures for the relevant age group, *including visits to tertiary general hospitals* and measured in cents per capita (11.5 KRW = 0.01 USD). The independent variable of interest in the reduced-form (2SLS) regressions is an indicator for the running variable being above the RD threshold (advisory indicator). All regressions control for the running variable, an interaction between the running variable and the indicator for the running variable being above the RD threshold, temperature, precipitation, and year-by-month and day-of-week fixed effects. The level of observation is the district by day, and observations are population weighted. Parentheses (square brackets) contain standard errors clustered by the running variable (day of sample). The bandwidth is set to 20 in all regressions.

Table C9: Analysis of Dynamic Effects with Different Bandwidths

	Age Groups			
Respiratory Illness	Minors (0-19)	Adults (20-64)	Older Adults (65+)	All
Sample Modification				
Bandwidth: 16	−32.087	−10.266	−11.953	−14.688
	(10.967)	(4.058)	(5.892)	(5.065)
Bandwidth: 20	−38.220	−10.703	−12.977	−16.125
	(13.769)	(4.662)	(6.624)	(5.935)
Bandwidth: 24	−32.998	−7.851	−8.139	−12.693
	(13.702)	(4.715)	(6.878)	(5.882)
Cardiovascular Illness				
Sample Modification				
Bandwidth: 16	−0.146	−4.796	−25.911	−7.034
	(0.089)	(1.682)	(12.085)	(2.533)
Bandwidth: 20	−0.064	−5.279	−30.388	−8.042
	(0.075)	(1.993)	(12.987)	(3.057)
Bandwidth: 24	0.007	−3.785	−26.687	−6.718
	(0.076)	(2.059)	(12.366)	(3.081)
N	Bandwidth 16: 1,857 Bandwidth 20: 2,530 Bandwidth 24: 3,380			

Notes: This table reports results from 24 2SLS local-linear regressions with varying bandwidths (16, 20, or 24). The dependent variable in all regressions is three-day respiratory or cardiovascular disease expenditures (from day t to day $t+2$) for the relevant age group, measured in cents per capita (11.5 KRW = 0.01 USD), and the independent variable of interest is an advisory indicator. All regressions control for the running variable, an interaction between the running variable and the indicator for the running variable being above the RD threshold, temperature, precipitation, and year-by-month and day-of-week fixed effects. The level of observation is the district by day, and observations are population weighted. Parentheses contain standard errors clustered by day of sample.

Table C10: Robustness Check - Exclusion of Later Alert Days and Removal of Early/Late Alerts

	Age Groups			
Respiratory Illness	Minors (0-19)	Adults (20-64)	Older Adults (65+)	All
Sample Modification				
Without Later Alert Days	−13.622	−1.563	−1.229	−3.579
	(6.692)	(1.290)	(1.396)	(2.006)
Without Later Alert Days of RV < 0	−13.213	−3.412	−3.812	−5.219
	(4.678)	(1.855)	(2.432)	(2.174)
Without 9PM−6AM	−16.274	−4.093	−4.687	−6.320
	(6.248)	(2.268)	(2.996)	(2.675)
Without 8PM−8AM	−17.759	−4.428	−5.113	−6.856
	(6.908)	(2.451)	(3.281)	(2.918)
Cardiovascular Illness				
Sample Modification				
Without Later Alert Days	−0.025	−2.056	−8.425	−2.237
	(0.045)	(0.746)	(3.484)	(0.896)
Without Later Alert Days of RV< 0	−0.036	−2.387	−8.204	−2.723
	(0.030)	(0.619)	(2.897)	(0.815)
Without 9PM−6AM	−0.043	−3.064	−10.502	−3.533
	(0.038)	(0.834)	(4.012)	(1.091)
Without 8PM−8AM	−0.047	−3.315	−11.457	−3.833
	(0.041)	(0.924)	(4.495)	(1.218)

Notes: This table reports results from 32 2SLS local-linear regressions. The dependent variable in all regressions is respiratory or cardiovascular disease expenditures for the relevant age group, measured in cents per capita (11.5 KRW = 0.01 USD), and the independent variable of interest is an advisory indicator. All regressions control for the running variable, an interaction between the running variable and the indicator for the running variable being above the RD threshold, temperature, precipitation, and year-by-month and day-of-week fixed effects. The level of observation is the district by day, and observations are population weighted. Parentheses contain standard errors clustered by day of sample. The bandwidth is set to 20 in all regressions. In each panel, the first excludes alert days following the first day of an air quality alert, and the second row excludes alert days on which the running variable falls below zero. The third row excludes days on which the alert was cancelled before 6 am or triggered after 9 pm, while the fourth row excludes days on which the alert was cancelled before 8 am or triggered after 8 pm.

Table C11: FRD Coefficients with Different Specifications

	Age Groups			
Respiratory Illness	Minors (0-19)	Adults (20-64)	Older Adults (65+)	All
Specification Modification				
Quadratic RV	−18.220	−7.586	−7.718	−9.607
	(11.167)	(3.221)	(4.404)	(4.337)
Quadratic Temperature	−15.611	−4.064	−4.569	−6.167
	(5.710)	(2.105)	(2.808)	(2.499)
Alternative Time FE	−14.502	−2.982	−3.274	−5.045
	(5.698)	(2.152)	(2.858)	(2.495)
1-Day-Before Holiday FE	−13.414	−1.881	−1.765	−3.907
	(5.771)	(1.410)	(1.862)	(1.958)
Cardiovascular Illness				
Specification Modification				
Quadratic RV	−0.028	−4.611	−14.329	−5.138
	(0.074)	(1.487)	(6.994)	(1.714)
Quadratic Temperature	−0.039	−2.702	−9.022	−3.126
	(0.035)	(0.776)	(3.607)	(1.020)
Alternative Time FE	−0.041	−2.650	−9.286	−3.128
	(0.034)	(0.760)	(3.561)	(0.983)
1-Day-Before Holiday FE	−0.040	−2.697	−11.887	−3.342
	(0.038)	(0.888)	(4.558)	(1.182)

Notes: This table reports results from 24 2SLS local-linear regressions. The dependent variable in all regressions is respiratory or cardiovascular disease expenditures for the relevant age group, measured in cents per capita (11.5 KRW = 0.01 USD), and the independent variable of interest is an advisory indicator. All regressions control for the running variable, an interaction between the running variable and the indicator for the running variable being above the RD threshold, temperature, precipitation, and year-by-month and day-of-week fixed effects. The first, second, and third rows in each panel add controls for a quadratic in the running variable, a quadratic in temperature, and year and month fixed effects (instead of year-by-month fixed effects) respectively. The level of observation is the district by day, and observations are population weighted. Parentheses contain standard errors clustered by the day of sample. The bandwidth is set to 20 in all regressions.

Table C12: Robustness Check - Addition of Air Pollution Covariates

	Age Groups			
	Minors (0-19)	Adults (20-64)	Older Adults (65+)	All
Respiratory Illness				
Added Covariates				
PM10	−14.665	−3.294	−3.860	−5.379
	(5.249)	(1.912)	(2.507)	(2.253)
PM2.5	−14.232	−3.558	−4.033	−5.486
	(5.117)	(1.970)	(2.536)	(2.274)
PM10 & PM2.5	−14.531	−3.296	−3.849	−5.353
	(5.100)	(1.902)	(2.491)	(2.230)
AQI	−14.626	−3.489	−3.863	−5.510
	(5.462)	(1.933)	(2.589)	(2.300)
Cardiovascular Illness				
Added Covariates				
PM10	−0.036	−2.654	−8.957	−3.076
	(0.037)	(0.733)	(3.537)	(0.948)
PM2.5	−0.045	−2.790	−9.510	−3.174
	(0.035)	(0.733)	(3.529)	(0.945)
PM10 & PM2.5	−0.037	−2.663	−8.995	−3.076
	(0.036)	(0.731)	(3.545)	(0.942)
AQI	−0.027	−2.760	−8.890	−3.080
	(0.038)	(0.755)	(3.502)	(0.956)

Notes: This table reports results from 32 2SLS local-linear regressions. The dependent variable in all regressions is respiratory or cardiovascular disease expenditures for the relevant age group, measured in cents per capita (11.5 KRW = 0.01 USD), and the independent variable of interest is an advisory indicator. All regressions control for the running variable, an interaction between the running variable and the indicator for the running variable being above the RD threshold, temperature, precipitation, and year-by-month and day-of-week fixed effects. The first, second, third, and fourth rows in each panel add controls for PM10, PM2.5, both PM10 and PM2.5, and the AQI, respectively (averaged across the day). The level of observation is the district by day, and observations are population weighted. Parentheses contain standard errors clustered by day of sample. The bandwidth is set to 20 in all regressions.

Table C13: Robustness Check - Standard Errors with Different Clusters

	Age Groups			
Respiratory Illness	Minors (0-19)	Adults (20-64)	Older Adults (65+)	All
FRD Coefficient	−15.033	−3.777	−4.303	−5.829
Clustering Level				
Province by Day of Week	(5.345)	(1.568)	(1.953)	(1.938)
Province by Day of Sample	(6.114)	(2.140)	(2.621)	(2.524)
Region by Day of Week	(5.217)	(1.497)	(1.929)	(1.880)
Region by Day of Sample	(6.081)	(2.110)	(2.592)	(2.490)
District by Day of Week	(1.828)	(0.645)	(1.171)	(0.751)
District	(2.077)	(0.886)	(1.010)	(1.014)
Cardiovascular Illness				
FRD Coefficient	−0.040	−2.828	−9.641	−3.259
Clustering Level				
Province by Day of Week	(0.042)	(0.954)	(4.199)	(1.253)
Province by Day of Sample	(0.038)	(0.834)	(3.742)	(1.033)
Region by Day of Week	(0.042)	(0.923)	(3.966)	(1.209)
Region by Day of Sample	(0.038)	(0.813)	(3.607)	(1.001)
District by Day of Week	(0.039)	(0.462)	(2.645)	(0.569)
District	(0.036)	(0.518)	(2.336)	(0.540)

Notes: This table reports different standard errors for eight 2SLS local-linear regressions. The dependent variable in all regressions is respiratory or cardiovascular disease expenditures for the relevant age group, measured in cents per capita (11.5 KRW = 0.01 USD), and the independent variable of interest is an advisory indicator. All regressions control for the running variable, an interaction between the running variable and the indicator for the running variable being above the RD threshold, temperature, precipitation, and year-by-month and day-of-week fixed effects. The level of observation is the district by day, and observations are population weighted. In each panel parentheses contain standard errors clustered by province by day-of-week (second row), province by day-of-sample (third row), region by day-of-week (fourth row), region by day-of-sample (fifth row), district by day-of-week (sixth row), and district (seventh row). The bandwidth is set to 20 in all regressions.

Table C14: Robustness Check - Spillover Effect and Falsification Tests

	Age Groups			
Respiratory Illness	Minors (0-19)	Adults (20-64)	Older Adults (65+)	All
Specification Modification				
Spillover	−0.029	0.217	0.453	0.147
	(4.658)	(1.180)	(1.778)	(1.743)
Falsification (−20)	0.381	0.296	0.832	0.334
	(1.528)	(0.478)	(0.792)	(0.634)
Falsification (−30)	1.424	0.036	−0.186	0.286
	(1.023)	(0.333)	(0.520)	(0.430)
Falsification (−50)	−0.658	−0.335	−0.391	−0.400
	(0.715)	(0.232)	(0.358)	(0.310)
Cardiovascular Illness				
Specification Modification				
Spillover	0.029	0.295	−1.054	0.074
	(0.023)	(0.809)	(4.547)	(1.067)
Falsification (−20)	0.007	−0.062	−0.458	−0.037
	(0.025)	(0.340)	(1.951)	(0.461)
Falsification (−30)	−0.046	−0.072	−0.923	−0.206
	(0.017)	(0.257)	(1.656)	(0.380)
Falsification (−50)	−0.014	0.102	1.226	0.197
	(0.009)	(0.131)	(0.821)	(0.193)

Notes: This table reports results from 32 2SLS local-linear regressions. The dependent variable in all regressions is respiratory or cardiovascular disease expenditures for the relevant age group, measured in cents per capita (11.5 KRW = 0.01 USD), and the independent variable of interest is an advisory indicator, which is shifted either geographically or generated by shifting the running variable by a constant. In each panel, the first row shifts the advisory indicator to correspond to an advisory in the nearest alert region to region i. The second, third, and fourth rows use an advisory indicator that is generated after shifting the running variable downwards by 20, 30, or 50 units respectively. All regressions control for the running variable, an interaction between the running variable and the indicator for the running variable being above the RD threshold, temperature, precipitation, and year-by-month and day-of-week fixed effects. The level of observation is the district by day, and observations are population weighted. Parentheses contain standard errors clustered by day of sample. The bandwidth is set to 20 in all regressions.

Table C15: List of Budget Items Related to Alert System

City	Item
Gwangju	Air Pollution Monitor - Electricity Cost
Gwangju	Line Rental for Air Quality Warning System
Gwangju	Air Pollution Monitor Management Cost (General)
Gwangju	Air Pollution Monitor - Automatic Control System
Gwangju	Air Pollution Monitor Alert System
Daejeon	Advertisement - Electronic Board Fee
Daejeon	Line Rental for Air Pollution Management System
Daejeon	Air Pollution Management System - Maintenance Cost
Daejeon	Air Pollution Management System - Establishment Cost
Daejeon	Air Pollution Monitor - Installation Cost
Daegu	Line Rental for Air Quality Warning System
Daegu	Air Pollution Alert System - Maintenance Cost
Busan	Air Pollution Monitor - Maintenance Cost
Busan	Air Pollution Monitor Data Collecting Machine - Maintenance Cost
Busan	Air Pollution Monitor - Battery Change
Busan	Indoor Air Quality Monitor - Maintenance Cost
Busan	Indoor Air Quality Monitor Data Collecting Machine - Maintenance Cost
Busan	Air Pollution Alert System - Maintenance Cost
Busan	Sampling & Analysis Equipment - Maintenance Cost
Busan	Air Pollution Monitor - Maintenance Cost
Busan	Indoor Air Quality Monitor - Maintenance Cost
Busan	Air Pollution Monitor - Electronic Board Maintenance Cost
Seoul	Air Pollution Information System - Office Management Cost
Seoul	Air Pollution Information System - Maintenance Cost
Seoul	Air Pollution Information System - SMS Service
Seoul	Air Quality Modeling System Construction
Seoul	Air Quality Evaluation Program Development
Seoul	Air Quality Real-Time Information Provision System Construction
Seoul	Air Pollution Information System - IT Development
Seoul	Ambient Air Quality Situation Room Construction
Seoul	Ambient Air Quality Information Service Infrastructure
Seoul	Air Quality Information System - Supervision
Seoul	Air Pollution Information System - IT Solution & Planning Development
Ulsan	Advertisement - Electronic Board Fee
Ulsan	Air Pollution Monitor - Electricity Cost
Ulsan	Line Rental for Air Pollution Monitor
Ulsan	Ambient Air Quality Situation Room - Maintenance Cost
Ulsan	Air Pollution Monitor - Outsourcing Maintenance Cost
Ulsan	Air Pollution Monitor Equipment - Maintenance Cost
Ulsan	Air Pollution Monitor - Maintenance Cost
Ulsan	Environmental Measurement Equipment Inspection Cost
Ulsan	Air Pollution Monitor - Battery Change
Incheon	Air Pollution Monitoring - Public Cost
Incheon	Air Pollution Monitoring - Equipment Maintenance Cost
Incheon	Environmental Measurement Equipment Inspection Cost
Incheon	Air Pollution Monitor - Movement Cost
Incheon	Air Pollution Monitor - Outsourcing Maintenance Cost
Incheon	Environment Automatic Monitoring System - Outsourcing Maintenance Cost
Incheon	Air Pollution Monitor Network Establishment

Notes: Each row reports an item related to the alert system in each city.

Table C16: Costs of the Air Pollution Alert System Management

City	Cost [USD, 2017]	Cost [USD, 2018]
Gwangju	190,751	192,317
Daejeon	151,530	190,887
Daegu	293,925	309,012
Busan	375,257	471,538
Seoul	187,879	634,157
Ulsan	329,588	464,695
Incheon	485,627	571,334
Toal	2,014,558	2,833,940

Notes: Each row reports the system management cost of air quality alerts in the seven major cities in the sample.